FINAL TECHNICAL REPORT

Guidelines for Regional Liquefaction Hazard Mapping

by:

Laurie G. Baise

and

Jennifer A. Lenz

Department of Civil and Environmental Engineering
Tufts University
113 Anderson Hall, Medford, MA 02155
phone: 617-627-2211 fax: 617-627-3994
email: laurie.baise@tufts.edu
webpage: http://ase.tufts.edu/cee/faculty/baise/bio.asp

U.S. Geological Survey
National Earthquake Hazard Reduction Program
Award No. 05HQGR0103

August 31, 2006

Research supported by the U.S. Geological Survey (USGS), Department of the Interior, under USGS award number 05HQGR0103. The views and conclusions contained in this document are those of the authors and should not be interpreted as necessarily representing the official policies, either expressed or implied, of the U.S. Government.

ABSTRACT

Guidelines for regional liquefaction hazard mapping

Laurie G. Baise
and
Jennifer A. Lenz

Department of Civil and Environmental Engineering, Tufts University, 113 Anderson Hall, Medford, MA 02155; phone: 617-627-2211; fax: 617-627-3994; email: laurie.baise@tufts.edu

Program Element I: National and Regional earthquake hazards assessments

U.S. Geological Survey
National Earthquake Hazard Reduction Program
Award No. 05HQGR0103

August 31, 2006

This project was a one-year study to develop guidelines for incorporating geotechnical data in regional liquefaction hazard mapping projects. Regional liquefaction hazard mapping projects have been completed for many projects around the United States and each project has used a slightly different methodology. Many of the early projects relied solely on surficial geology to assess liquefaction susceptibility. The current trend is to include geotechnical boring data along with the surficial geology when characterizing the liquefaction susceptibility. One of the challenges in completing these projects is deciding how to combine surficial geology information, which is on a regional scale and geotechnical boring information, which is on a site-specific scale. This report sets out a common methodology for evaluating the geotechnical data associated with liquefaction hazard. The proposed method relies on the Simplified Procedure for liquefaction potential at the sample scale and the liquefaction potential index (LPI) at the profile scale. At the regional scale, statistical, probabilistic, and geostatistical methods are used to characterize the variability of liquefaction potential within and across geologic units. We use the outlined methods to reevaluate datasets acquired from nine liquefaction hazard mapping projects. The primary issues were: 1) the importance of an accurate and appropriate ground water table, 2) the effect of soil type restrictions (I_c), 3) the effect of geotechnical data type, and 4) the population and spatial variability of LPI over geologic units. Depending on the regional conditions, either groundwater or soil type can play a major role on determining the liquefiability of soils. The choice of standard penetration (SPT), cone penetration test (CPT) or shear wave velocity (V_s) data and the inherent spatial variability of liquefaction potential were issues at all investigated sites. We find that if densely spaced CPT or V_s data are collected, the data generally exhibit spatial correlation which can be used with geostatistics to interpolate between measurement locations. The spatial correlation for CPT and V_s was observed with correlation distances on the order of several kilometers. In contrast, standard penetration test (SPT) LPI values typically show high variability and no spatial correlation (except at one site). When spatial correlation does not exist, population estimates of liquefaction potential using statistics illustrated with box-plots or probability through cumulative distributions are appropriate. By

estimating the variability of liquefaction potential both across a geologic unit and across an area, we are better able to provide a useful estimate of liquefaction hazard.

TABLE OF CONTENTS

1.0 INTRODUCTION 1

2.0 DATA 2

2.1 Oakland, CA 2

2.2 St. Louis, IL 4

2.3 San Bernardino Valley, CA 4

2.4 Shelby County, TN 5

2.5 San Francisco and Southern San Francisco Bay Area, CA 6

2.6 San Fernando Valley, CA 6

2.7 Salt Lake City, UT 6

2.8 Evansville area, IN 7

2.9 Boston, MA 7

3.0 GEOTECHNICAL DATA ANALYSIS 8

3.1 Liquefaction Potential for CPT 8

3.2 Liquefaction Potential for SPT 8

3.3 Liquefaction Potential for V_s 9

3.4 Liquefaction Potential Index 9

3.5 Probability of Liquefaction 10

3.6 Statistical and Probabilistic Analysis 11

3.7 Geostatistical Analysis 12

4.0 CHALLENGES FOR REGIONAL LIQUEFACTION HAZARD MAPPING WITH GEOTECHNICAL DATA 13

4.1 Choice of Data (SPT, CPT, V_s) 13

4.2 Soil type and I_c Issues 15

4.3 Earthquake load 16

4.4 Groundwater 17

4.5 Liquefaction Analysis 17

4.6 Criteria for liquefaction zoning 19

4.7 Regional variability of liquefaction potential 21

5.0 CONCLUSIONS 25

6.0 PUBLICATIONS AND CONFERENCE PRESENTATIONS ORIGINATING FROM THIS RESEARCH 26

7.0 REFERENCES 26

LIST OF TABLES

Table 1. Projects and data reviewed
Table 2. Percent increase in LPI values between 10 – 20 m
Table 3. Liquefaction potential classifications
Table 4. Coefficient of variation by geologic unit in Oakland, CA
Table 5. LPI values with varied depths of integration for CPT and SPT in Oakland, CA
Table 6. Cumulative frequency distributions by geologic unit in Salt Lake City, UT

LIST OF FIGURES

Figure 1. Location map for 10 sites reviewed
Figure 2. Distribution plot examples
Figure 3. Typical exponential semivariogram diagram
Figure 4. Profiles of CPT, SPT and V_s data in the Oakland, CA area
Figure 5. LPI distributions of SPT, CPT and V_s data by geologic unit in Oakland, CA
Figure 6. LPI distributions grouped by liquefaction susceptibility
Figure 7. CPT-based LPI map using different I_c values for the Oakland, CA area
Figure 8. USGS 2% PE for 50 years PSHA map for Shelby County, TN
Figure 9. SPT-based LPI map using different groundwater levels for Shelby County, TN
Figure 10. Example of LPI integration techniques for an SPT profile
Figure 11. CPT profile comparing factor of safety and probability of liquefaction values
Figure 12. LPI distributions for SPT data in the Southern San Francisco Bay region
Figure 13. LPI distributions by geologic unit
Figure 14. Semivariograms
Figure 15. LPI distributions and semivariograms for a subregion of Salt Lake City, UT
Figure 16. Ordinary kriging results for CPT and V_s LPI in Oakland, CA
Figure 17. Ordinary kriging results for CPT-based LPI using lower I_c cutoff in Oakland, CA
Figure 18. Ordinary kriging results for Qds geologic unit in Oakland, CA
Figure 19. Ordinary kriging results for SPT-based LPI in Salt Lake City, UT

LIST OF APPENDICIES

Appendix A. Oakland, CA
Appendix B. Salt Lake City, UT

Appendix C. San Bernardino, CA
Appendix D. Evansville, IN
Appendix E. Southern San Francisco Bay, CA
Appendix F. San Fernando, CA
Appendix G. Shelby County, TN
Appendix H. St. Louis, IL
Appendix I. San Francisco, CA

1.0 INTRODUCTION

This project is a one-year study to develop guidelines for incorporating geotechnical data in regional liquefaction hazard mapping projects. Regional liquefaction hazard mapping projects have been completed for many (>20 NEHRP funded) projects around the United States and each project has used a slightly different methodology. Many of the first projects relied solely on surficial geology to assess liquefaction hazard. The current trend is to include geotechnical boring data along with the surficial geology when characterizing the liquefaction susceptibility. One of the challenges in completing these projects is deciding how to combine surficial geology information, which is on a regional scale and geotechnical information, which is on a site-specific scale.

Three recent studies have attempted to address this issue using statistical methods (Baise et al. 2006; Holzer et al. 2006; Rix and Romero-Hudock 2006). The Holzer et al. (2006) and Rix and Romero-Hudock (2006) studies use the same methodology where the liquefaction hazard is assessed using probabilities derived from cumulative frequency distributions of the liquefaction potential index. Baise et al. (2006) explores using statistical distributions to determine the variability of liquefaction hazard in a region and to address sampling density combined with geostatistical interpolation to address spatial variability of liquefaction hazard. A common issue raised by Holzer et al. (2006) and Rix and Romero-Hudock (2006) is the assumption of statistical homogeneity within geologic units. In order to apply statistical methods to develop distributions of liquefaction hazard across a geologic unit, one must assume that the geologic unit is statistically homogeneous. The study by Baise et al. (2006) demonstrates how geostatistical analysis can be used first to determine if geologic units are statistically homogenous and second, if homogeneity is not found (i.e. spatial correlation exists), geostatistical methods can be used to interpolate the liquefaction hazard across geologic units, thereby identifying liquefiable zones within geologic units.

This report presents a methodology which incorporates statistical and geostatistical analyses to evaluate liquefaction hazard from geotechnical data for regional mapping. The proposed methodology expressly includes characterization of inherent geologic/geotechnical variability. We provide guidelines on geotechnical data collection and analysis for regional liquefaction mapping projects. Statistical and geostatistical analyses are used to characterize sample distributions both by geologic unit and across broad areas in order to assess overall variability. More accurate, detailed maps of liquefaction hazard that account for inherent geologic variability will considerably improve the assessment of liquefaction hazards and allow communities to better plan and mitigate the effects of liquefaction on the built environment.

Specifically, this project addresses the issues of 1) combining geologic and geotechnical data for regional liquefaction hazard mapping and 2) incorporating spatial variability of liquefaction hazard into a regional map. The project reevaluates 10 regional liquefaction hazard mapping projects to develop guidelines for including geotechnical based liquefaction hazard in regional maps and providing an assessment of spatial variability within mapped units. The 10 projects are from a variety of regions and use multiple forms of data. All projects use geologic data in the form of surficial geology. In addition, eight projects use standard penetration test (SPT) data to inform the liquefaction hazard, while four projects use cone penetration test (CPT) data, and one uses shear wave velocity (V_s). Most of the projects analyze the geotechnical data in terms of the

Seed and Idriss simplified procedure (Seed and Idriss 1971) as updated and modified for SPT (Youd et al. 2001), CPT (Robertson and Wride 1998; Youd et al. 2001), and V_s (Andrus and Stokoe II 2000; Youd et al. 2001). This report tries to summarize each of the previous mapping projects and to identify common challenges and trends associated with using geotechnical data for liquefaction hazard mapping projects. Common challenges in regional liquefaction hazard studies include: 1) choice of data type (SPT, CPT, V_s), 2) soil type, 3) estimating earthquake load, 4) estimating groundwater, 5) assumptions and methods used in liquefaction potential analysis, 6) criteria for mapping, and 7) spatial variability.

2.0 DATA

In this section, we present the various methods previous researchers have used to produce liquefaction hazard maps for ten sites, focusing specifically on how each study incorporated regional geologic and hydrologic information with site-specific geotechnical information. In subsequent sections, we will evaluate the assembled datasets using a common methodology to evaluate the liquefaction potential derived from geotechnical data and the resulting mapped hazard. As much as possible for our analysis, we use the same geologic, hydrologic and geotechnical data as are used in the previously completed liquefaction hazard maps. Of course, it is not always feasible to locate or use these data or maps, so we include information on where our data diverges from the previously used data. The ten projects discussed herein are shown on a map of the United States in Figure 1. Table 1 includes a list of the projects and the data we used to review the liquefaction potential, and summary figures for each project are assembled in the appendicies.

2.1 Oakland, CA

The area along the eastern shore of San Francisco Bay in the greater Oakland, California area has been investigated through many research efforts to determine liquefiable areas and compare with previously observed liquefaction surface effects. Holzer et al. (2006) produced a regional liquefaction hazard map of the area using 202 seismic CPT profiles compiled for the Open-File Report 02-296 (Holzer et al. 2002) and the data and figures are available at http://quake.usgs.gov/prepare/cpt/. A generalized map of the surficial geology by Helley and Graymer (1997) was modified for this study. At most CPT sounding locations, the depth to groundwater was measured directly within the CPT open hole and supplemented with additional water levels reported in borings logs collected by the California Geological Survey (CGS). Therefore, the resulting hazard map was based on average current or modern water levels. Holzer et al. (2006) calculated the liquefaction potential based on M6.6 and M7.1 earthquake scenarios from the Hayward fault located west of the site. Using the attenuation relation equation from Boore et al. (1997), they estimated the peak ground accelerations (PGA) for the two earthquake magnitudes to be 0.4 and 0.5g, respectively, across the site. To determine the liquefaction hazard, they used cumulative frequency distributions of the LPI for each surficial geologic unit and subunit. They proposed that for any surficial geologic unit the percent area predicted to have liquefaction surface effects during a given design earthquake can be estimated from the cumulative frequency distributions at LPI $\geq$ 5. Using this method they assigned a specific probability of liquefaction for a given geologic unit. To use this method they assumed that each surficial geologic unit and subunit were statistically homogenous.

Knudsen et al. (2000) produced a preliminary liquefaction susceptibility and quaternary geology map for the Central San Francisco Bay region in California and the map images and databases are available in the USGS Open-File Report 00-444 and at http://pubs.usgs.gov/of/2000/of00-444/. This map covers the greater Oakland area as well as San Francisco and parts of southern San Francisco Bay which will be discussed later in this report. Knudsen et al. (2000) used the borehole database developed by the CGS Seismic Hazard Mapping Program (SHMP) which is available on the SHMP website at http://gmw.consrv.ca.gov/shmp/. Groundwater estimates were interpolated from the CGS boring database along with hydrologic information from other government agencies as well as some current field measurements. The researchers determined the liquefaction susceptibility for each geologic unit using a criteria matrix that included historical liquefaction surface effects, geologic conditions, typical depth to groundwater and geotechnical analyses of borings. They based the quantitative evaluation of SPT on Tinsley et al. (1985) and assumed the potential earthquake hazard was constant across the site and then determined the necessary PGA to trigger liquefaction for each geologic unit. Using these criteria they produced a liquefaction susceptibility map by giving a liquefaction susceptibility category (Very High to Very Low) to each geologic unit.

An additional interpretation of the surficial geology and the liquefiable areas in the San Francisco Bay area was completed by the California Geologic Survey as part of the SHMP. The CGS determined the zones of liquefaction for portions of San Francisco Bay and southern California. The CGS used the SHMP borehole database as well as the CPT profiles from the USGS (Holzer et al. 2002) for this area. The groundwater is based on the depth to water information from the borehole database as well as historical high groundwater maps to determine the most conservative groundwater level. This study determined the PGA and earthquake magnitude values from the deaggragated 10% PE for 50 years PSHA (Petersen et al. 1996) on spatially uniform alluvium conditions. The PGA and magnitude measurements were completed on a grid with 5 km spacing. The CGS methodology for determining liquefaction zones used criteria developed by the Seismic Hazards Mapping Act Advisory Committee as described by the California Department of Conservation, Division of Mines and Geology (2000). This method combines geologic and hydrologic mapping, past liquefaction surface effects, and geotechnical analyses. For the geotechnical analysis, the CGS determines the minimum Factor of Safety (FS) for each boring location and then considers the slope of the layer, adjacent free faces, and thickness and depth of the potentially liquefiable soil to determine the liquefaction potential of the layer. The liquefaction map from the CGS only delineates the areas underlain by potentially liquefiable sediment and does not provide a susceptibility category or probability for liquefaction.

The geotechnical data we used for the Oakland, California area includes the CGS borehole database and the seismic CPT database from Holzer et al. (2002). From the seismic CPT database, we also interpreted layered shear-wave velocity models using algorithms developed by Thompson et al. (2007). We use the surficial geologic map from Knudsen et al. (2000), which seemed to be the most detailed electronic map files available at the time for the entire San Francisco Bay area. The CGS liquefaction studies based their geology on Knudsen et al. (2000), while Holzer et al. (2006) used an older geologic map of the area. Depth to groundwater was measured directly in the CPT open hole and used for the CPT liquefaction calculations. We interpolated the groundwater values for the CPT profiles that did not report water levels. We

used the depth to water measurements from the CGS borehole database for the SPT-based liquefaction calculations. To determine the earthquake load, we interpolated the 2002 National Probabilistic Seismic Hazard Assessment (PSHA) maps (Frankel et al. 2002) 10% PE in 50 years assuming a constant site coefficient of Class D (stiff soil). Using the deaggragation from the 10% PE in 50 years, we assumed an earthquake magnitude of M6.8 for the area, which is the earthquake with the maximum contribution to the PSHA.

2.2 St. Louis, IL

Pearce and Baldwin (2005) produced a map of the relative liquefaction susceptibility of the St. Louis, Missouri and Illinois area based on Quaternary geologic maps, subsurface borings, groundwater levels and a quantitative analysis of the liquefaction susceptibility based on SPT. This study used SPT data from over 200 boreholes collected from the Illinois State Geological Survey (ISGS) and the Missouri Department of Transportation along with other various environmental investigation projects. For the area of the study within Illinois, the Quaternary geologic maps were from the ISGS (Grimley and Lepley 2001a; Grimley and Lepley 2001b; Grimley et al. 2001; Phillips 1999; Phillips et al. 2001), and for the portions within Missouri, the geologic maps were completed during this study. For Illinois, they based the groundwater levels on the potentiometric surface map from Kohlhase (1987), and for Missouri, they used groundwater levels from the USGS National Water Database, the Missouri GSRAD digital information base, and boring log information. This study used a design earthquake of M7.5, which is based on estimates of the magnitudes of the historic large earthquakes in the area. Using this earthquake scenario, they estimated the PGA to be up to 0.3g, and used three PGA scenarios of 0.1g, 0.2g and 0.3g. To calculate the liquefaction susceptibility they produced plots of the recorded SPT $(N_1)_{60}$ versus the expected cyclic stress ratio (CSR) at each PGA for the major surficial geologic units. From these plots they compared the liquefaction threshold curve from the Simplified Procedure to the plotted ($(N_1)_{60}$, CSR) pairs to estimate a PGA trigger for liquefaction in each surficial geologic unit. To determine liquefaction susceptibility, this study combined geologic and groundwater conditions with an estimated PGA trigger to assign a liquefaction susceptibility class to each geologic unit.

For St. Louis, our area of study includes the portions of St. Louis in Illinois as well as additional parts of Madison County, Illinois. We attained our geotechnical and groundwater data from the ISGS borehole database (http://www.isgs.uiuc.edu/wwdb/index.htm). For the borings which did not include groundwater information, we interpolated the depth to water at these locations. The quadrangle maps of the quaternary geology used by Pearce and Baldwin (2005) were not available electronically, instead we use an electronic version of the Illinois Quaternary geology by Lineback (1979). We applied a constant PGA of 0.2 g and a M7.5 design earthquake for our LPI calculations. As discussed in Pearce and Baldwin (2005), the spatial locations provided in the ISGS boring database are in some cases only based on the Township, Range and Section of the boring. There are some profiles that plot at the same location, in these instances, we chose the deepest boring to continue liquefaction calculations. But, because of the uncertainty in the spatial location of some of the borings, we chose not to evaluate the spatial correlation of the database.

2.3 San Bernardino Valley, CA

Matti and Carson (1991) completed a report on the liquefaction susceptibility of the alluvial sediments in the San Bernardino Valley in southern California. This report used a combination of

site-specific SPT data along with regional geologic and hydrologic conditions. As part of this study, they updated the surficial geology maps for the purposes of liquefaction evaluation. The groundwater conditions were from Carson and Matti (1986) and were based on measurements from the California Department of Water Resources. This study collected borehole data from 138 sites in the area. The researchers elected to look at the major earthquake scenario for each of the three major faults in the area (the San Andreas, San Jacinto and Cucamonga faults), and used attenuation relations to determine the likely PGA values for each of the three events at each boring location. For the SPT, they determined if the sample is likely to liquefy using the Simplified Procedure for the three earthquake scenarios over a range of groundwater levels. From this they determined a liquefaction susceptibility rating based on the ratio of susceptible to unsusceptible SPT for each combination of geologic unit, sediment type, groundwater interval and earthquake scenario. This report produced three regional liquefaction susceptibility maps for each of the three likely major earthquakes in the area.

In the San Bernardino Valley, we compared the CPT dataset collected by the USGS Western Earthquake Hazards Team (available at http://quake.usgs.gov/prepare/cpt/) to the liquefaction susceptibility categories from Matti and Carson (1991). We compiled the groundwater data from both the CPT logs and the USGS National Water Database and interpolated groundwater levels for the CPT profiles that did not have reported levels. Instead of calculating a deterministic PGA from the three major faults in the area, we estimated the PGA by interpolating the 2002 PSHA 2%PE for 50 years (Frankel et al. 2002) and applied a constant site coefficient for stiff soil. Additionally, we assumed an earthquake magnitude of M7.6, which is the earthquake with the maximum contribution to the PSHA deaggragation for the region. For the surficial geology of the area, we used the preliminary geology map of the San Bernardino 30' x 60' quadrangle from the USGS Open-File Report 2003-293 (Morton and Miller 2003).

2.4 Shelby County, TN

Rix and Romero-Hudock (2006) prepared liquefaction hazard maps for Memphis, Tennessee and parts of Shelby County using both SPT and CPT data. The data is comprised of 623 SPT profiles (Ng et al. 1989; Hwang et al. 1999) and 18 CPT profiles at 5 sites (Liao et al. 2001; 2002). They used geologic maps from the USGS 7.5-minute quadrangle series from Northwest Memphis, Northeast Memphis, Southeast Memphis, Southwest Memphis, Ellendale and Germantown (Broughton and Van Arsdale 2004; Cox 2004; Moore and Diehl 2004a; Moore and Diehl 2004b; Van Arsdale 2004a; Van Arsdale 2004b). For the geotechnical analysis, they calculated an LPI value for each CPT and SPT profile using PGA values from 0.1 – 0.5g and earthquake magnitudes M6.0 – 8.0. Because of the limited CPT data, they supplemented the CPT data with stochastically simulated profiles for each geologic unit using an autocorrelation function and a conditional probability density function to generate simulated tip resistance (q_t) and sleeve friction (f_s) profiles, respectively. They then calculated the probability of having an LPI > 5 or LPI > 15 for each geologic unit over the range of PGA and magnitude values using the SPT data and the actual and simulated CPT profiles. They assigned each geologic unit a probability of exceeding an LPI value of 5 or 15, corresponding to moderate and major liquefaction, based on SPT or CPT values for a given earthquake scenario. According to Holzer et al. (2006), these values can be interpreted as the probability that liquefaction will occur within a geologic unit for a particular seismic event. To assign a single probability value to each geologic unit, Rix and Romero-Hudock (2006) combined the SPT and CPT probabilities by weighting the SPT data by

two-thirds and the actual CPT data by one-third. Using the single probability values for each geologic unit, they produced liquefaction hazard maps for the area for both moderate and major liquefaction events using M7.7 and M6.2 earthquake scenarios. These maps are available at http://earthquake.usgs.gov/regional/ceus/.

For Shelby County, Tennessee, we used the borehole database from Hwang et al. (1999) for our geotechnical and groundwater data. For the borings that did not include groundwater information, we used an interpolated value. To calculate the LPI values for our comparison, we used a constant PGA of 0.4g from a M7.5 earthquake and did not calculate the entire range of PGA and magnitude values as was done in Rix and Romero-Hudock (2006).

2.5 San Francisco and Southern San Francisco Bay Area, CA

The City of San Francisco and southern San Francisco Bay area both have two liquefaction susceptibility maps: Open-File Report 00-444 and the CGS liquefaction zone maps, both of which are previously described under the Oakland, CA liquefaction hazard mapping project. The CGS liquefaction zone maps use the same methodologies and data as in the Oakland area, except that there was no CPT data collected for this area.

We used geotechnical and groundwater data from the CGS borehole database, along with the surficial geology map from Knudsen et al. (2000) for these areas. For a PGA estimate, we interpolated the 10% PE in 50 years PSHA map (Frankel et al. 2002) assuming a constant site coefficient of Class D (stiff soil). For both areas, we assumed a M7.9 design earthquake, which is the maximum magnitude earthquake used by the CGS for this area.

2.6 San Fernando Valley, CA

The CGS also produced liquefaction zone maps in the southern California area as part of the SHMP. For the San Fernando, CA area, the CGS updated the surficial geology maps for this study based on the maps by Hitchcock and Wills (1998; 2000). The geotechnical data includes over 850 borings collected from previous investigations from both private and government projects. They determined that the highest historical groundwater levels for the area occurred in 1944 and digitized the groundwater values from the California State Water Rights Board Report (1962) for a conservative estimate of groundwater conditions. The CGS used the same methodologies as in San Francisco Bay area for estimating the PGA, evaluating the geotechnical data for liquefaction potential, and determining the liquefaction susceptibility.

The geotechnical and groundwater data we used for the San Fernando Valley are from the CGS borehole database. If no groundwater level was given for a site, the depth to water was interpolated from the boring logs. Therefore, the groundwater levels used are current levels and not the maximum historical levels as were used in the CGS liquefaction zone map. We estimated the PGA from the 10% PE in 50 years PSHA (Frankel et al. 2002) assuming a constant site coefficient of Class D (stiff soil). We used a M6.5 design earthquake for this site, which is the earthquake with the maximum contribution to the PSHA.

2.7 Salt Lake City, UT

A literature search for previously completed liquefaction maps for the Salt Lake City area only produced a single liquefaction potential map produced by the Utah Geological Survey (Anderson

et al. 1994). No information was found on how these maps were produced. We used a database of both SPT and CPT profiles compiled by the Utah Liquefaction Advisory Group (http://www.civil.utah.edu/~bartlett/ulag.html) for the Salt Lake City region. For the borings and CPT profiles that did not include groundwater data, we interpolated the depth to water measurements from the boring database. The surficial geology is from the Utah Geological Survey geologic map of the Salt Lake City 30' x 60' quadrangle (Map#: 190DM), which was digitized from Bryant (1990). For the PGA, we used the 2% PE in 50 years PSHA with a constant Class D site coefficient. For this site, we assumed a M6.8 design earthquake based on the deaggragation of the PSHA.

2.8 Evansville area, IN

The USGS completed an extensive CPT database for the Evansville area in parts of Indiana and Kentucky and can be downloaded from http://quake.usgs.gov/prepare/cpt/data/, but at the time of this report no liquefaction susceptibility maps have been produced for the area. The surficial geology came from two separate maps for Indiana and Kentucky. For Indiana, we used the Indiana Geological Survey Miscellaneous Map #49 digitized from Gray (1989), and we used the USGS preliminary integrated geologic map databases for Kentucky (Nicholson et al. 2005), and can be downloaded at http://pubs.usgs.gov/of/2005/1324. A majority of the CPT profiles did not have groundwater information, so we interpolated the groundwater data from the CPT depth to water measurements and the Indiana Department of Natural Resources Wells database. We used PGA values from the 2% PE in 50 years PSHA with a Class D site factor, and estimated a M7.7 design earthquake from the deaggragation.

2.9 Boston, MA

Baise and Brankman (2004) completed liquefaction hazard maps for eight USGS 7.5 minute quadrangles that included the downtown Boston area and surrounding communities. To develop these maps, existing surficial geologic maps were augmented with field reconnaissance mapping to provide a base for assessing the properties of the geologic units. A database of 2963 borings was compiled to provide data on the subsurface properties of the geologic units. However, since the liquefaction hazard was focused in the artificial fill unit, the majority of borings were located in regions of artificially filled land near downtown Boston and did not span other geologic units. Therefore, the liquefaction hazard maps were primarily based on surficial geology liquefaction susceptibility with the exception of the artificial fill, which was evaluated using SPT based liquefaction hazard statistics (Brankman and Baise 2006). The liquefaction calculations used the Youd et al. (Youd et al. 2001) updated Simplified Procedure to determine PGA trigger levels.

From a subset of the Boston study data, Baise et al. (2006) used statistics to address issues of sampling density for liquefaction hazard mapping and geostatistics to evaluate spatial variability of liquefaction within a single mapped unit – artificial fill overlying alluvial deposits. The statistical analysis demonstrated the effect of small sample size on liquefaction hazard estimates derived from geotechnical data. The liquefaction potential was evaluated for three soil layers beneath and including the artificial fill. The artificial fill layer exhibited moderate spatial correlation and probability of liquefaction values were interpolated across the unit to determine zones of potentially liquefiable material.

Because the Boston data set only provided SPT for the artificial fill and Baise et al. (2006) presented a statistical and geostatistical analysis of that dataset, we did not reanalyze the dataset herein.

3.0 GEOTECHNICAL DATA ANALYSIS

In order to compare the projects discussed above, we reevaluate the geotechnical data using a common methodology, which is presented below. The liquefaction potential analysis is based on the Seed-Idriss Simplified Procedure. We recommend the presented methodology for calculating liquefaction potential using CPT, SPT, and V_s. In addition, we include the methodology for calculating the probability of liquefaction which is gaining acceptance and will likely be the preferred method in the future. We include the geostatistical analysis methodology that we are recommending for evaluating spatial variability and, when appropriate, for interpolating between data points.

3.1 Liquefaction Potential for CPT

We calculate the cyclic stress ratio (*CSR*) for each profile using the Simplified Procedure proposed by Seed and Idriss (1971):

$$CSR = 0.65\left(\frac{a_{\max}}{g}\right)\left(\frac{\sigma_{vo}}{\sigma'_{vo}}\right)r_d$$

where a_{max} is the peak horizontal acceleration, g is the acceleration of gravity, σ_{vo} and σ'_{vo} are the total and effective overburden stresses and r_d is the stress reduction coefficient as given by (2001).

To determine the soil types that are considered non-liquefiable, we estimate the grain characteristics, I_c, and the normalized tip resistance, q_{c1N}, directly from the CPT profile as given in Robertson and Wride (1998). Using a correction factor based on the I_c and the q_{c1N}, we calculate an equivalent clean sand normalized CPT tip resistance, $(q_{c1N})_{cs}$, (Robertson and Wride 1998). We assume for this study that if the soils have an $I_c > 2.6$, then they are likely to be too clay or silt-rich to liquefy. However, it is recommended by Youd et al. (2001) that soils with an $I_c > 2.4$ should be sampled and tested to confirm the soil type and the liquefiability. We determine the cyclic resistance ratio (*CRR*) along the CPT profile using the clean sand normalized tip resistance as recommended by Robertson and Wride (1998).

3.2 Liquefaction Potential for SPT

For the SPT, we calculate the *CSR* for each reported blow count using the same equations and assumptions as discussed for the CPT. We correct the blow counts using the recommendations from Youd et al. (2001) along with the overburden stress correction factor from Kayen et al. (1992). In order to correct for the effect of fine grained soils, we use fines content to determine the equivalent clean sand corrected blow count (Youd et al. 2001). The fines content for each sample was either reported in the borehole data as the percent fines passing the #200 sieve or estimated based on the lithology. We then approximate the *CRR* using the clean-sand normalized blow counts as recommended in Youd et al. (2001).

3.3 Liquefaction Potential for V_s

Shear-wave velocities were measured in the Oakland, CA area using a seismic cone penetrometer by Holzer et al. (2002). The tip of the cone was equipped with a seismometer and recorded the shear-waves travel time from a strike plate at the ground surface at approximately 2 m depth increments. From the shear-wave travel time data we interpret a layered velocity model for each site using automated algorithms written in the open-source statistical language and environment *R* (R Development Core Team 2006). Thompson et al. (2007) developed the automated algorithms to calculate the shear-wave velocity profile based on Boore (2003). To account for the overburden pressure, we use the following equation (Kayen et al. 1992):

$$V_{s1} = V_s\left(\frac{P_a}{\sigma'_{v0}}\right)^{0.25}$$

where V_{s1} is the overburden-stress corrected shear wave velocity, P_a is the atmospheric pressure and σ'_{v0} is the initial effective vertical stress in the same units as P_a. Assuming that the soils are Holocene in age, we determine the CRR using (2000):

$$CRR = a\left(\frac{V_{s1}}{100}\right)^2 + b\left(\frac{1}{V_{s1}^* - V_{s1}} - \frac{1}{V_{s1}^*}\right)$$

where V_{s1}^* is the limiting upper value of V_{s1} for liquefaction and a and b are curve fitting parameters, which are 0.022 and 2.8, respectively. V_{s1}^* depends on the average percent fines content (FC) of the layer and is calculated as follows:

V_{s1}^* = 215 m/s for FC ≤ 5%

V_{s1}^* = 215 m/s – 0.5*(FC – 5) for FC > 5% and FC < 35%

V_{s1}^* = 200 m/s for FC ≥ 35%

If V_{s1} is greater than V_{s1}^*, the soil layer is assumed to not be liquefiable. Along each profile, we determine the liquefiable soils using the CPT-based grain characteristic, I_c. We use the CSR values from the CPT profiles and the V_s -based CRR values to determine a factor of safety against liquefaction.

3.4 Liquefaction Potential Index

The liquefaction potential index (LPI) is a measure of the effects of liquefaction based on the severity of liquefaction and the depth and width of the liquefiable zones. The LPI is evaluated for the top 20 meters of a soil profile. Because many of the CPT, SPT and V_s profiles do not reach a maximum depth of 20 meters, we discard the profiles that are less than 10 meters in depth. In order to determine whether profiles with depths between 10 and 20 m could be included in the analysis, we took all profiles of 20 m depth or greater and calculated the LPI increase for the lower 10 m of the profile. Table 2 presents the percent of profiles that show an increase in the LPI of more than 2 and 5 between 10 and 20 m. For the 12 data sets that we reevaluated, we determined that, on average, 21% of the sites showed a moderate increase (>2) in the LPI value and 7% of the sites showed a significant increase (>5) between 10-20 m.

The factor of safety (*FS*) against liquefaction is given as:

$$FS = \left(\frac{CRR_{7.5}}{CSR}\right) \cdot MSF \cdot K_\sigma$$

where *CSR* is the calculated cyclic stress ratio generated by the design earthquake, $CRR_{7.5}$ is the cyclic resistance ratio for magnitude 7.5 earthquake, *MSF* is the magnitude scaling factor and K_σ is the correction for high overburden pressure. For this study, we use the revised *MSF* from (2001). Hynes and Olson (1999) derived the K_σ correction factor to be:

$$K_\sigma = (\sigma'_{v0} / P_a)^{(f-1)}$$

where *f* is a function of site conditions. Youd et al. (2001) recommend *f* values between 0.6 – 0.8, depending on the relatively density. We assume a conservative estimate for *f* of 0.8.

The LPI, based on the method by Iwasaki et al. (1982), is defined as:

$$LPI = \int_0^{20} F_L \cdot w(z) \cdot dz$$

where $w(z) = 10 - 0.5z$ (z = depth in meters) and dz is the differential increment of depth. We use the liquefaction potential categories proposed by Sonmez (2003) which defined F_L as:

$$F_L = 0 \text{ for } FS \geq 1.2$$

$$F_L = 1 - FS \text{ for } FS < 0.95$$

$$F_L = 2 \times 10^6 e^{-18.427 \cdot FS} \text{ for } 1.2 > FS > 0.95$$

For the SPT, we use the lithology classifications for each borehole to remove layers which we would expect to be too clay or silt-rich to liquefy. We evaluate the non-liquefiable soil layers based on recommendations from Andrews and Martin (2000). If the recommendation stated that further testing was required, we continue the evaluation of the liquefaction potential of the sample.

Since the CPT and V_s profiles are continuous, we use a discretized form of the LPI given by Luna and Frost (Luna and Frost 1998):

$$LPI = \sum_{i=1}^{NL} w_i F_{Li} H_i$$

where w_i and F_{Li} are determined, as discussed previously for the SPT, for each layer, H_i is the thickness of the discretized layer and *NL* is the number of tests in a profile. H_i is determined by the sample frequency of the CPT. We use the liquefaction potential classifications proposed by Sonmez (2003)as shown in Table 3.

3.5 Probability of Liquefaction

Probabilistic correlations for liquefaction triggering (P_L) using Bayesian-updating have been developed for the SPT (Cetin et al. 2004) and CPT (Moss et al. 2006). For the CPT, we normalize the tip resistance using the iterative process discussed in Moss et al. (2006). We calculate the P_L for the entire CPT profile as given by Moss et al. (2006):

$$P_L = \Phi\left(-\frac{\left(q_{c,1}^{1.045} + q_{c,1}(0.110 \cdot R_f) + c(1 + 0.850 \cdot R_f) - 7.177 \cdot \ln(CSR) - 0.848 \cdot \ln(M_w) - 0.002 \cdot \ln(\sigma_v') - 20.923\right)}{1.632}\right)$$

where $q_{c,1}$ is the normalized tip resistance, R_f is the friction ratio, *CSR* is the cyclic stress ratio, M_w is the moment magnitude of design earthquake, σ_v' is vertical effective stress, and Φ is the standard cumulative normal distribution. For SPT, we calculate the P_L using Cetin et al. (2004):

$$P_L = \Phi\left(-\frac{\left(N_{1,60}\cdot(1+0.004\cdot FC)-13.32\cdot\ln(CSR)-29.53\cdot\ln(M_w)-3.70\cdot\ln\left(\frac{\sigma_v'}{P_a}\right)+0.05\cdot FC+16.85\right)}{2.70}\right)$$

where $N_{1,60}$ is the standardized blow count value and FC is the percent fines content. We typically do not present P_L calculations at the sites we reevaluate in part because we chose to use the LPI and an equivalent criteria does not currently exist for the P_L.

3.6 Statistical and Probabilistic Analysis

The liquefaction potentials (LPI) determined from geotechnical data are associated with point data. In order to extrapolate point data over the two-dimensional map surface, we have to assume that the liquefaction potential is a statistically homogeneous population (Baise et al. 2006; Holzer et al. 2006; Rix and Romero-Hudock 2006). If the assumption of statistical homogeneity holds, then each LPI represents a single realization from the parent population. When the LPI values are pooled by geologic unit, the results can be viewed using histograms, box-plots, or cumulative frequency plots (see Figure 2). Each plot presents the same information but in a different form. Figure 2 compares LPI populations for two distinct geologic units in St. Louis.

The histograms are useful for determining if the population follows a standard distribution (normal, lognormal, binomial, exponential, etc.). From the histogram shown in Figure 2, the LPI values most closely follow an exponential distribution. Baise et al. (2006) used histograms to characterize liquefaction susceptibility in Boston, MA. The box-plots summarize distribution characteristics (mean, median, quartiles, and outliers) and provide a useful means of comparison between populations. We use box-plots to compare population distributions between geologic units, CPT/SPT/ V_s populations, age, and mapped hazard category (see Figure 2 and appendicies).

The cumulative frequency plots are used by Holzer et al. (2006) and Rix and Romero-Hudock (2006) to assign probability values to geologic units from the pooled populations. The resulting probability values are usually given in terms of a probability of exceeding a LPI threshold, generally 5 (moderate liquefaction) or 15 (major liquefaction) as recommended by Iwasaki et al. (1982). Toprak and Holzer (2003) recommended the LPI thresholds of 5 and 12 from an analysis of LPI and surface manifestations of liquefaction during the 1989 Loma Prieta earthquake and the 2003 San Simeon earthquake. The probability values can be interpreted as either 1) probability of exceeding the LPI threshold at a point or 2) probable surface area within the geologic unit to exceed the LPI threshold. Holzer et al. (2006) recommends the first interpretation.

We recommend using all three methods to understand the distribution of LPI within pooled samples. As discussed in Baise et al. (2006), small populations of geotechnical data will not be able to accurately characterize the parent population within a geologic unit; therefore, probability estimates resulting from small samples are likely inaccurate and should be balanced with other available information (surficial geology, groundwater, etc.) As discussed in the next section, we also recommend testing the statistical homogeneity assumption using geostatistical methods to

confirm that the geologic unit represents a single population rather than a population exhibiting significant spatial correlation of LPI values (and therefore high and low probability zones).

3.7 Geostatistical Analysis

If we presume that a spatial structure exists, such that LPI values are not random and that closely spaced observations will be more similar than those farther apart, then geostatistics can be used for spatial predictions (Goovaerts 1997). In order to test the assumption of spatial structure, we can use the empirical semivariogram. We completed the geostatistical analysis using the geoR package in the statistical software R (Ribeiro Jr. and Diggle 2001). Using the LPI values from the geotechnical data, we estimate the empirical semivariogram, $\gamma(h)$, of n samples with N pairs separated at a distance of h using the following equation:

$$\gamma(h) = \frac{1}{2N}\sum_{i=1}^{N}[z(s_{i+h}) - z(s_i)]^2$$

where z is the sampled parameter, and s is the spatial location. The empirical semivariogram can be interpreted in terms of the spatial correlation of the dataset. A flat empirical semivariogram is fit by a pure nugget model and is indicative of no spatial correlation. When a data set does not have spatial correlation, the statistical homogeneity assumption is met and the best estimate of liquefaction potential is the population estimate. This methodology applied to geotechnical data for liquefaction potential assessment is discussed in Baise et al. (2006).

If the empirical semivariogram shows a positive slope from zero distance and then reaches some plateau, we typically fit an exponential model semivariogram with nugget variance:

$$\tilde{\gamma}(h) = \omega\left[1 - \exp\left(-\frac{h}{a}\right)\right] + \tau$$

The nugget, denoted as τ, is the variance at zero distance. The range, calculated as $3a$, is the distance at which the semivariogram levels off and beyond which the semivariance is constant. The sill, calculated as $\omega+\tau$, is the constant semivariance beyond the range. Figure 3 shows a typical semivariogram with the parameters labeled. The sill characterizes the population variance, the range indicates the distance over which samples show some correlation, and the nugget provides information on the short-scale variability.

If on the other hand, the empirical semivariogram shows a positive slope from zero distance but does not reach a plateau, a linear semivariogram model is more suitable:

$$\tilde{\gamma}(h) = \varphi(h) + \tau$$

where φ is the slope of the linear model and τ is the nugget. A linear variogram, in this case, indicates that the data are not sufficient in density or coverage to characterize the "true" spatial model, since we assume the semivariogram of the LPI follows an exponential model. The linear model, however, can still be used to model the observed spatial correlation.

The model parameters are solved by minimizing the weighted least-square error (Cressie 1985) in the form:

$$LOSS(\theta) = \sum_k N_k\left(\frac{\tilde{\gamma}_k - \gamma_k(\theta)}{\gamma_k(\theta)}\right)^2$$

where θ is the vector containing the model parameters, k is a counter corresponding to the bins.

When the semivariogram provides evidence for spatial correlation (i.e. data can be fit by either an exponential or linear model), the data can appropriately be interpolated. Using The estimate at an unsampled location, $\tilde{z}$, is the weighted sum of the surrounding samples:

$$\tilde{z} = \sum_{i=1}^{n} w_i z_i$$

where n is the number of measurements, and w is the set of weights. The variance of each predicted value, $\tilde{\sigma}_k^2$, is calculated from the equation:

$$\tilde{\sigma}_k^2 = \tilde{\sigma}^2 - \left(\sum_{i=1}^{n} w_i \tilde{C}_{i0} + \mu \right)$$

where:

$$\tilde{C}_{i0} = \sum_{j=1}^{n} w_j \tilde{C}_{ij} + \mu$$

and $\tilde{C}_{ij}$ is the model covariance matrix and μ is the Lagrange multiplier. the above equations, we can use ordinary kriging to produce an interpolated map where each interpolated value is a weighted average of neighboring points and includes a measure of estimate variance. The background on geostatistics can be found in Goovaerts (1997). The estimate variance can be used to indicate when the kriged value is a better estimate (lower variance) than the population estimate.

4.0 CHALLENGES FOR REGIONAL LIQUEFACTION HAZARD MAPPING WITH GEOTECHNICAL DATA

We reevaluated the geotechnical data associated with 9 of the 10 projects using the above mentioned methodology. The 10th project (Boston, MA) had originally been analyzed by the authors using similar methodology and therefore was not reevaluated. The summary figures for each project are shown in the appendicies. Several common challenges arose and will be discussed and illustrated below with appropriate figures.

4.1 Choice of Data (SPT, CPT, V_s)

Liquefaction hazard maps typically include SPT, CPT or V_s data to determine liquefaction potential at single locations in the subsurface. Each of the three data types have pros and cons, which should be considered prior to planning a liquefaction hazard mapping program. For the nine sites we reviewed, seven had SPT data, four had CPT data and one site had V_s data. Liquefaction evaluation using SPT, CPT and V_s has often been compared (Andrus et al. 2004; Juang et al. 2002).

Advocates for SPT cite the large SPT databases for developing liquefaction correlations and the capability for direct sampling of the soil to determine soil type, fines content and other parameters (Cetin et al. 2004; Youd et al. 2001). SPT are also readily available, and many of the projects we reviewed compiled boring logs to complete the geotechnical analysis. Although SPT profiles are abundant, many times the information is incomplete, such as type of equipment used, hammer energy, soil classification, fines content and other information necessary for liquefaction calculations. The researcher is then required to either disregard the SPT profile, which may lead to limited data for an area, or make assumptions, which can lead to uncertainties. Additionally,

SPT usually do not provide a continuous profile and thin layers can be missed. The test is not automated and is subject to human discretion, which can lead to the test being unreliable.

Advocates for the CPT praise the automated nature of the test which defines a continuous subsurface profile at fine intervals (typically 5 cm) with high repeatability (Robertson 2004). The CPT does not provide actual soil samples and, while CPT has been correlated to soil behavior (Robertson and Wride 1998), there may be inconsistencies. V_s profiles are also used to determine liquefaction potential, and some researchers promote V_s because shear-wave velocity and liquefaction resistance are influenced by similar factors such as void ratio, relative density, and cementation (Andrus and Stokoe II 2000). The issues with using V_s for liquefaction evaluation are that no samples are typically collected and thin layers of low velocity soils may not be detected.

To compare the repeatability of the SPT and CPTu (CPT with pore pressure measurements), Jeffries and Davies (1993) performed replicate trials of both and found that the CPTu is five times more precise than SPT. Juang et al. (2002) compared CPT and SPT based liquefaction potential using probability-based methods and found that different factor of safety limits should be applied to CPT and SPT in order to achieve the same probability of liquefaction. Andrus et al. (2004) constructed relationships between penetration resistance from the SPT and CPT and V_s using the CRR curves for each method. Both of studies determined that CPT-based liquefaction evaluation is the least conservative of the three.

For the liquefaction hazard maps we reviewed, the Oakland, CA area had data for all three geotechnical tests including 123 borings, 195 CPT profiles and 192 V_s profiles (see Appendix A for figures showing data locations). A direct comparison between SPT, CPT and V_s at the same location would be ideal, but the SPT data are not co-located with the CPT/ V_s. We compare a set of profiles that are in the afbm (artificial fill over San Francisco Bay Mud) geologic unit that are about 230 meters apart. The profiles at these locations for the CPT, SPT and V_s are shown in Figure 4. The V_s relies on stratigraphic information from the CPT. The stratigraphy is relatively consistent for the CPT and SPT with 2-3 m of sands and gravels (fill), over about 2 m of silts and clays, over 6-8 m of sands and silty sands. The V_s profile shows two layers, the top layer is a low-velocity layer indicating a soft clay or silt and the bottom layer indicates a stiffer potentially sand layer. It should be noted that the CPT stratigraphy tends towards silts and clays whereas the SPT stratigraphy tends towards gravel; however, because of the separation distance, we cannot conclude if this is a bias of the I_c-based soil types for the CPT or the result of natural spatial variation in the geologic deposit.

The factor of safety against liquefaction are also plotted in Figure 4 for all three methods and all identify potentially liquefiable material between 2-6 m, above and below the silt/clay layer. The primary difference between the methods is that the CPT also shows an additional liquefiable layer between 9-11 m, which is missed in both the SPT and V_s data. The LPI for these locations are 12.7 for the CPT, 7.6 for the SPT, and 13.6 for the V_s. The discrepancy between the LPI values for the three methods is common for this site and Figure 5 shows the distribution of LPI values for a subunit in the afbm, which is typically mapped as having a high to very high liquefaction potential. The median LPI values for each population indicate that CPT-based LPI is the most conservative method, while SPT LPI median value is the least conservative. Using the

cumulative frequency and an LPI threshold of 5 to evaluate probability of liquefaction, the three datasets would result in three estimates for the afbm unit (SPT - 44%, V_s - 63%, and CPT - 76%). The SPT-based LPI distribution has the largest range and is the most skewed (more zeros and more extreme LPI values (LPI > 30)). Each method shows a large range of LPI values from non-liquefiable to very high liquefaction potential although the V_s LPI distribution has the smallest spread. The disparity in distributions may be a result of varying levels of certainty in the test (spread), differences in liquefaction analysis (bias), how soil type is determined for each method (bias), or to spatial variability within the unit (sampling bias). The coefficient of variation (COV) can be used to provide a normalized indication of population width. Table 4 shows the COVs for each geologic unit in Oakland, CA using each data type. The CPT populations consistently have lower COVs then the SPT, as would be expected due to the automated nature of the test. The V_s COVs are relatively large or undefined as a result of the low LPI mean values.

Figure 6 shows each dataset for Oakland, CA and how it compares with the liquefaction susceptibility characterizations in the Knudsen et al. (2000) geologic maps. To evaluate the I_c issue for the CPT dataset, we plot the LPI distributions parsed by liquefaction susceptibility criteria using two I_c cutoff values (2.6 and 2.4, see discussion below) as seen in the top two plots of Figure 6. The CPT-based LPI values with a 2.6 cutoff value have high median and mean LPI values in the medium and low categories. However, when the 2.4 cutoff value is used, the CPT-based LPI distributions are lower and are more consistent with the published hazard maps, but the medium and low categories still show a large range of LPI values. The SPT-based LPI distributions (lower left plot) do not show a clear difference between the Very High, High and Medium categories, but the highest LPI values do fall in the Very High susceptibility category. The V_s data provide the most consistent estimate with the Knudsen et al. (2000) susceptibility categories with almost all of the very high LPI values in the Very High category.

The plots of LPI distributions pooled by susceptibility category and pooled by geologic unit illustrate differences in the populations (SPT, CPT, and V_s); however, they do not tell use which type of geotechnical data provides the most accurate estimate of liquefaction induced surface effects. For example, the consistency of the Vs LPI values with the susceptibility categories either indicates that V_s is a better indicator of liquefaction potential than either SPT or CPT or that V_s LPI is more consistent with geologic characterizations of liquefaction susceptibility and the observed SPT and/or CPT distributions are more representative of the population behavior. Further research should determine which data type is the most accurate estimator of liquefaction potential and surface effects.

4.2 Soil type and I_c Issues

The CPT is often criticized for evaluating liquefaction potential because of the difficulty in soil classification in the absence of a soil sample. Robertson and Wride (1998) used extensive field data to develop the CPT soil behavior type index, I_c, that has been correlated to both estimated soil type and fines content. For liquefaction calculations, Youd et al. (2001) recommend sampling all soils with an I_c between 2.4 and 2.6 (silty sand to sandy silt) to confirm soil type. For our LPI calculations, we assume that a soil can liquefy if the $I_c < 2.6$, and as a result may over predict the liquefaction potential. For liquefaction mapping in the Oakland area, Holzer et al. (2006) primarily relied on I_c-based soil classifications, but confirmed some soil types that had

I_c values near 2.6. They found that some soils were misclassified, particularly in strongly weathered Pleistocene alluvial fan deposits, and actually had clay content indicating the soil was non-liquefiable. Figure 7 compares the LPI results for two scenarios: 1) assuming that the soil is liquefiable with $I_c < 2.6$ and 2) assuming that the soil is liquefiable with $I_c < 2.4$. The dot size corresponds to the difference in LPI categories for the two assumptions. As discussed in Holzer et al. (2006), the Pleistocene alluvial fan deposits (Qf, Qpf) were most affected by this assumption (i.e. $2.4<I_c<2.6$) where the difference can result in the LPI category decreasing by as many as three categories. The mapped Qhf unit (which overlies Pleistocene alluvial fan deposits) also showed significant change in LPI as a result of the I_c cutoff. As seen in Figure 6, the $I_c < 2.4$ cutoff appears to better match the published liquefaction hazard maps. The CPT LPI results using the higher I_c cutoff are therefore conservatively biased and result in high liquefaction potential assigned to geologic units that are not expected to liquefy. In these cases when I_c values are between 2.4 and 2.6, the best practice is to collect samples in the area. Otherwise, one must make the conservative assumption (as we do here) and use $I_c <2.6$ as the liquefiability cutoff value.

Recently, the evaluation of liquefaction susceptibility of fine-grained soils has been under scrutiny after soils that would have been classified as non-liquefiable under the Chinese Criteria were observed to liquefy during the 1994 Northridge, 1999 Kocaeli and 1999 Chi-Chi earthquakes. Based on both field sampling and soil testing, Bray and Sancio (Bray and Sancio 2006) recommend, instead of the Chinese Criteria, using the ratio of water content to liquid limit and plasticity index to determine the liquefaction susceptibility of fine-grained soils. Their results show that young, shallow silts and clayey silts with low plasticity at high water content to liquid limit ratios can liquefy, which is contrary to the previous state-of-the-practice for liquefaction evaluation of fine-grained soils. Therefore, in regions where these soils exist, further sampling and testing of soils is recommended. We suspect that on-going and future research will help direct liquefaction susceptibility in fine-grained soils.

4.3 Earthquake load

Liquefaction evaluation is also dependent on the expected ground shaking hazard which can be estimated using either deterministic or probabilistic methods, or by calculating a PGA trigger level for liquefaction. The deterministic seismic hazard analysis (DSHA) includes choosing a particular earthquake of a certain size at a specified location. The probabilistic seismic hazard analysis (PSHA) methodology identifies the earthquake sources in the area and incorporates uncertainties in source size, location and interval of occurrence. The PGA liquefaction threshold (trigger) method interprets the CSR at a range of PGA values and compares these values to the Simplified Procedure threshold curves for liquefaction. During our review of liquefaction hazard maps, we find that Holzer et al. (2006) and Matti and Carson (1991) use a deterministic evaluation of the PGA and earthquake magnitude, Pearce and Baldwin (2005) and Knudsen et al. (2000) use liquefaction trigger levels and Rix and Romero-Hudock (2006) and the California Geologic Survey use probabilistic methods. Matti and Carson (1991) advocated the use of a deterministic estimate of the earthquake potential for the San Bernardino, CA area because they concluded there is a high likelihood that an earthquake will occur in the near future, based on the faulting-recurrence interval and lack of large historic earthquakes, and a probabilistic approach would underestimate the earthquake potential. The California Geological Survey (CGS) Seismic Hazard Mapping Act Advisory Committee (2004) recommends the use of the PSHA 10%

probability of exceedance over a 50-year period for determining liquefaction opportunity. Figure 8 shows the results of the peak acceleration with 2% probability of exceedance in 50 years from the USGS PSHA analysis for the Memphis area showing the variability of earthquake load over a region. The predicted peak acceleration ranges from 0.5 to 0.7 g. Both deterministic methods relying on attenuation relations and PSHA methods provide variable maps of PGA. We recommend using one of these methods to capture the variability of seismic demand.

4.4 Groundwater

Groundwater levels play a major role in determining liquefaction susceptibility of an area. In our review, we find that groundwater levels are typically taken from boring logs and other groundwater databases over a range of years to find the historical high groundwater levels that are then extrapolated across the area. However, in the Oakland, CA area Holzer et al. (2006) uses current groundwater levels from CPT and borings logs, and Rix and Romero-Hudock (2006) reviewed current groundwater levels for the Shelby County, TN area and then set an average groundwater level for the project area. We find that in some areas, liquefaction susceptibility depended primarily on the groundwater levels instead of the geologic unit. For example, the San Bernardino region shows strong dependence on groundwater level. In this area, the soils were generally loose enough to liquefy but only saturated in a small region (see Appendix C for figures). To show the affect groundwater can have on liquefaction potential, we present in Figure 9 the change in LPI category between a current groundwater level and an average groundwater level of 6 m for the Shelby County, TN area. Approximately 22% of the borings changed to a different LPI category, and the calculated LPI values varied by as much as 3 LPI categories in some cases. Care should be taken to determine the historical high groundwater levels of the area for a conservative estimate of the liquefiability of the area.

4.5 Liquefaction Analysis

Almost every report we reviewed uses the Simplified Procedure (Seed and Idriss 1971) to evaluate the factor of safety against liquefaction, but each report uses a different methodology to estimate the potential for liquefaction-induced deformations. Pearce and Baldwin (2005) do not calculate FS values, but instead calculate $(N_1)_{60}$ and CSR pairs from the SPT in saturated granular soils and plot with liquefaction threshold curves to estimate the PGA trigger for each surficial deposit. Matti and Carson (1991) in San Bernardino, CA area combined each FS value into populations based on geologic unit, groundwater depth and distance to a major fault and found the percentage of liquefiable tests to determine liquefaction susceptibility ratings. For the San Francisco Bay area, Knudsen et al. (2000) based their quantitative evaluation of liquefaction on Tinsley et al. (1985) who proposed that liquefaction susceptibility of a geologic unit can be categorized based on if the deposit is expected to liquefy for either a M6.5 or 8.0 event. The ratio of SPT with high susceptibility to the total SPT in a geologic unit within a groundwater interval was evaluated to determine the potential for liquefaction surface effects. The CGS simply calculates the minimum FS value for each boring as well as considering the depth, thickness, slope and presence of free faces for the susceptible layer.

The LPI, developed by Iwasaki et al. (1982), explicitly evaluates the depth and thickness by integrating liquefaction potential to a depth of 20 m within a soil profile and provides an estimate of liquefaction-related surface damage at a boring location. Both Holzer et al. (2006) and Rix and Romero-Hudock (2006) use the LPI to predict liquefaction deformations. The LPI is

integrated over 20 m, but many times the SPT or CPT profiles do not reach this depth and there is no consensus how to address this problem. Table 5 shows the number of tests available for SPT and CPT at the Oakland site when using different minimum depths. In Oakland, only 66 out 210 CPT profiles and 45 out of 218 SPT profiles reach 20 m whereas 195 CPTs and 123 SPT profiles reach 10 m. Rix and Romero-Hudock (2006) address this issue by only using SPT profiles that are greater than 15 m in depth and then extending the last measured blowcount value to 20 m to complete the profile. For their work, they determined that this results in a slightly conservative LPI since N-values typically increase with depth. We determine that there is little significant increase in LPI for the CPT and SPT profiles between 10-20 m at the Oakland site; however, the result would be different for a site with a deeper ground water table (>10 m). Table 5 also presents the mean, median, and maximum LPI values for the Oakland site using only the profiles (66 CPT and 45 SPT) that reach 20 m for the four cases: 1) using upper 10 m, 2) using upper 15 m, 3) using upper 20 m, and 4) extrapolating the 15 m value to 20 m. For these populations, the mean varied from 6.7 to 8.0 for the CPT and 3.6 to 5.7 for the SPT and median values varied by 4.3 to 6.0 for the CPT and 0 to 0.03 for the SPT. The LPI_{15} extrapolated best matched the statistics of the LPI_{20}.

Another issue that is not often addressed by researchers, is how the LPI is integrated over a soil column and correlated with lithology information, especially for SPT values that are not continuous. We perform linear interpolation between samples, but only for the lithologies classified as liquefiable, and if there is only one SPT for a soil layer, we assume that the SPT applies to the entire layer. A second option is to interpolate between points regardless of soil layer (but using the soil layers to determine liquefiability). And a third option is to divide each profile into sublayers around each sample and apply the sample value uniformly to the sublayer. Figure 10 illustrates each integration scheme for calculating SPT-based LPI values for an example profile. The difference in the calculated LPI values for each method with this boring was insignificant with less than a 0.5% change, however other borings may show more significant changes. The SPT borings in the Salt Lake City dataset often have wide sample spacing (~10 ft) which can lead to large LPI values as a result of extrapolating a single low FS value over a large length of the profile. We have attributed the difference in SPT and CPT LPI distributions in Salt Lake City to this possible cause (see Appendix B for figures).

Recently, researchers have developed probabilistic correlations for liquefaction triggering (P_L) using Bayesian-updating, which incorporate parameter and model uncertainty for liquefaction triggering, for the SPT (Cetin et al. 2004), CPT (Moss et al. 2006), and V_s (Kayen, R.E. et al. in preparation). Probability of liquefaction methods have been around since Liao et al. (1988), but have not gained widespread use. The current Bayesian-based methods may be more readily adopted. Cetin et al. (2004) advocates the P_L-based liquefaction assessment because of the reduced uncertainty and addresses other issues such as magnitude weighting factors, fines content adjustments and overburden stress corrections explicitly in the P_L calculation. However, there is currently no corollary to determine the potential for liquefaction-related surface damage from a profile of P_L values. Figure 11 shows both Factor of Safety and P_L calculated from a CPT profile in Oakland. The profile is in the Holocene alluvium with a water depth of 5.6 m. The calculated LPI is 8.6. In this profile, there are three potential critical layers (7 m, 10 m, and 18 m depth). The challenge with P_L values will be to determine an appropriate LPI equivalent

calculation and criteria to link P_L values with surface manifestations of liquefaction, or to define reasonable criteria for identifying a critical layer and associated probability of liquefaction.

4.6 Criteria for liquefaction zoning

Regional liquefaction hazard maps are typically produced by classifying each surficial geologic unit as a liquefaction potential classification using geologic, hydrologic and geotechnical information, but most researchers define their liquefaction categories differently. The CGS identifies areas that indicate the potential for liquefaction and require site-specific geotechnical investigations prior to development, but have no gradation of liquefaction hazard within the area. We compared our liquefaction potential calculations to the CGS liquefaction zones in four areas: (1) Oakland, (2) Southern San Francisco Bay, (3) San Francisco, and (4) the San Fernando Valley. The CGS liquefaction mapping criteria are described in CGS's Special Publication #118 (California Geological Survey 2004) and are summarized as:

1. Areas known to have experienced historical liquefaction;
2. Areas of uncompacted fills that are saturated, or may become saturated;
3. Areas where geotechnical data indicate the soils are potentially liquefiable; and
4. If subsurface data are not sufficient for quantitative evaluation of liquefaction, then liquefaction potential is based on age of deposit, expected PGA, and depth to groundwater.

The comparison of our results to the CGS categories for this sites are shown in Appendix A, E, F and I.

For San Bernardino, CA, Matti and Carson (1991) determined the percentage of susceptible FS values for each subpopulation and categorized the liquefaction susceptibility between High to Low as follows:

1. High – 80% of FS values are less than or equal to 1.0
2. Moderately High – 60 to 80% of the FS values are less than or equal to 1.0
3. Moderate – 30 to 60% of the FS values are less than or equal to 1.0
4. Low – Less than 30% of the FS values are less than or equal to 1.0

Matti and Carson (1991) found that liquefaction susceptibility is generally greatest in the youngest Holocene alluvial fan deposits. For our LPI distributions, we also show the highest LPI values are within the Latest Holocene geologic units (see Appendix C for figures of San Bernardino distributions).

Knudsen et al. (2000) defined liquefaction susceptibility categories for each geologic unit in the San Francisco Bay area, including Oakland, Southern San Francisco Bay, and San Francisco areas, as a function of groundwater depth and liquefaction calculations using both M6.5 and M8.0 earthquake scenarios. This methodology is based on Tinsley et al. (1985) that defines the liquefaction categories as:

1. Very High or High – Liquefaction is expected to occur in M6.5 event
2. Moderate – Liquefaction expected for a M8.0 event, but not a M6.5
3. Low or Very Low – Liquefaction not expected in a M8.0 event

The comparison of our results to the liquefaction susceptibility categories are shown above in Figure 6 for the Oakland, CA site and can be found in the appendicies for the other sites. In Oakland, the V_s LPI distributions best match the reported liquefaction susceptibility categories.

The SPT and CPT LPI distributions are difficult to distinguish and at times contradicted the Knudsen et al. (2000) liquefaction susceptibility categories.

In the St. Louis area, Pearce and Baldwin (2005) produced a decision flow chart for liquefaction susceptibility evaluation based on historic liquefaction, age of deposit, groundwater level, and SPT data. Pearce and Baldwin (2005) determined that the Cahokia Alluvium deposits had a High to Moderate liquefaction susceptibility, while the Peoria Loess and Vandalia Till had a Very Low susceptibility to liquefaction. By grouping our calculated LPI values by these geologic units, we also find that the Cahokia Alluvium has the highest liquefaction susceptibility and the loess and till deposits had a lower median and mean LPI, although the distribution of LPI values is quite large. The Boston project (Baise and Brankman 2004) used a form of this chart in the liquefaction hazard map development.

For the Oakland, CA area, Holzer et al. (2006) based their liquefaction susceptibility ratings on the findings by Toprak and Holzer (2003), which determined that liquefaction surface effects generally occur where LPI $\geq$ 5 for each geologic unit. Therefore, they determined that the percentage of surface area of a geologic unit expected to exhibit liquefaction surface effects can be evaluated from the percentage of CPT profiles with LPI $\geq$ 5. In Shelby county, TN, Rix and Romero-Hudock (2006) used a similar methodology to Holzer et al. (2006) except that they evaluated the probability of exceeding LPI values of 5 and 15 for each geologic unit over a range of PGA and M_w. Using this method, liquefaction hazard maps can easily be produced for a variety of seismic demands for the region. We reviewed the SPT data for Shelby county and found a similar trend in the liquefaction potential by geologic unit (see Appendix G for figures), although our LPI values, overall, seem to have lower LPI distributions. Similar to the results of Rix and Romero-Hudock (2006), we did find that Qal (Holocene alluvium) and Qtl (Pleistocene loess-covered terrace) geologic units had slightly higher mean LPI values, but it should be noted that the LPI distributions for each geologic unit range between non-liquefiable and very high liquefiability. Rix and Romero-Hudock (2006) recommended site-specific studies for artificial fill (af) deposits because of the uncertainty in the density of fill units.

Liquefaction hazard mapping requires a good amount of both engineering and geologic judgment. The current state-of-the-practice for liquefaction mapping correlates surficial geologic unit with liquefaction susceptibility, which must assume that soil properties are statistically homogenous for a given geologic unit. Figure 2 presents the liquefaction potential determined from geotechnical data for two geologic units in the St. Louis area, the Cahokia alluvium and the Peoria Loess. The results are presented as box-plots, histograms, and cumulative distributions. Each figure presents the same information but using a different graphical technique. Box-plots are used in this report and by Lenz and Baise (2006), histograms are used by Baise et al. (2006), and cumulative distributions are used by Holzer et al. (2006) and Rix and Romero-Hudock (2006). Each presentation illustrates how broadly variable the geotechnical data are within the geologic unit and how the distributions between geologic units vary. The box-plots have the advantage that they also indicate variation in mean and median and are more easily interpreted than either the histograms or the cumulative distributions; however the cumulative distributions are useful for associating a probability value with a geologic unit.

As observed in Figure 2, a single geologic unit may not have a uniform liquefaction hazard. For example, Holzer et al. (2006) delineated some liquefaction boundaries different from geologic unit boundaries in the Oakland, CA area. This requires an intimate knowledge of the geologic setting, which was not accessible to us in our review of these projects, and may not be accessible to researchers producing regional liquefaction hazard maps. All of the liquefaction hazard maps we reviewed integrated data from geologic, hydrologic and geotechnical sources, which is necessary to produce a comprehensive liquefaction hazard map.

Figure 12 presents the liquefaction potential determined from geotechnical data (SPT) in the Southern San Francisco Bay region sorted by 1) age of geologic unit, 2) geologic unit, 3) groundwater level, and 4) geologist interpreted liquefaction susceptibility (Knudsen et al. 2000). This figure illustrates how each of these pieces of data are correlated with liquefaction potential. The fourth category (geologist interpretation) would be a compilation of the previous three categories with additional interpretation of geotechnical data and should be the most accurate estimate. From the figure, it is evident that liquefaction potential is highly variable within each of these categories. Although the Holocene and Modern units tend to have most of the high LPI values, the Late Holocene has a median value near LPI=5. Within the geologic units, the mean values hover around LPI=5, whereas the median values are more variable. Each geologic unit distribution has a significant portion of LPI>5 values. Since the geologic unit is generally the mapped unit, it is important to note how broad the LPI distributions are within each unit. Parsing the data by groundwater exhibits a consistent trend (the deeper the groundwater, the lower the LPI values). Finally, the liquefaction hazard categories exhibit a trend in the mean values consistent with the hazard ratings, but the median values are not consistent (High hazard has a lower median value then Medium hazard) and the Very High, High, and Medium categories have significant overlap. As shown in Figure 6, the V_s LPI values showed a more consistent classification for the Oakland area hazard categories than either CPT or SPT LPI values. Figure 12 illustrates the importance of combining geology, age, and groundwater with geotechnical data to determine liquefaction hazard.

4.7 Regional variability of liquefaction potential

Many researchers have documented the uncertainty and inherent variability in soil properties and have characterized the variability of soil properties using mean and coefficient of variation (Baecher and Christian 2003; Holzer et al. 2005; Phoon and Kulhawy 1999). However, many times the uncertainty and variability of soils is overlooked during regional liquefaction hazard mapping. The CGS and Knudsen et al. (2000) do not discuss potential variability of soils, nor how they addressed it in their studies. Matti and Carson (1991) recognized that not all soil samples are expected to liquefy in the High Susceptibility category and give a range of percentages of susceptible soils for each liquefaction category. Pearce and Baldwin (2005) show each SPT pair of $(N_1)_{60}$ versus CSR plotted with the Simplified Procedure threshold curves for liquefaction for each geologic unit, but do not address the variability within each plot or how they determined the PGA trigger given the variability of the data. Holzer et al. (2006) and Rix and Romero-Hudock (2006) acknowledge that each geologic unit has a distribution of liquefaction potential, but they assume that the distributions are statistically homogenous to map regional liquefaction hazards by geologic unit. Holzer et al. (2006) plotted the cumulative frequency distribution of LPI values for each geologic unit, but then applied a single probability to the entire geologic unit or subunit. Rix and Romero-Hudock (2006) provide an example

histogram for a geologic unit, which shows the variability of LPI values, and then created liquefaction hazard maps using a probability range bounded by the LPI ≥5 and LPI≥15 for each geologic unit.

The movement towards characterizing, or at least recognizing, the variability of liquefaction potential across geologic units is necessary since it has been shown that soil properties are variable and uncertainties exist in sampling procedures. Figure 13 shows the variability of LPI (calculated from SPTs) within regional geologic units in the Salt Lake City, UT and San Fernando, CA regions. In Salt Lake City, several geologic units are sampled and the distributions of LPI vary in mean, median, and distribution width. The median values are generally low; however the distributions are highly skewed with large LPI outliers. All of the units except one (Qbc) show some portion of the distribution above the LPI≥5 cutoff, indicating that the units have liquefaction potential and should be classified appropriately. Using the cumulative frequency and assuming that the units are statistically homogenous, the resulting probabilities of exceeding the LPI≥5 cutoff for Salt Lake City are shown in Table 6. The Holocene clay, silt and sand deposit (Qcs) and artificial fill (a) have the highest probabilities of 45% and 33%. As a comparison, in San Fernando, CA, the liquefaction potential is low (primarily LPI=0) as a result of a relatively deep groundwater level (average groundwater level is approximately 10 m) and as a result the geologic units having less variability; therefore, the assigned liquefaction probabilities are more straight forward.

If sufficient geotechnical data are collected, geostatistics can be used as a tool to evaluate spatial correlation and then directly interpolate between liquefaction potential values to show variability within a unit. For a number of sites we reviewed, we were able to characterize the spatial correlation using geostatistics and then use ordinary kriging to produce interpolated maps of LPI values. In order to evaluate spatial correlation and, if appropriate, interpolate between LPI values, we use a semivariogram model which characterizes the spatial correlation of the dataset. An exponential model is typical for soil parameters which are expected to have a low variance at close distances and then increase to a plateau at greater distances. Although, we expect that LPI semivariograms would all follow an exponential model if the density and distribution of the dataset was sufficient, linear models sometimes provide the best fit to a given dataset. If a dataset does not have any spatial correlation, the semivariogram will be a nugget model (flat). Our assumption is that a sloped linear model indicates that the dataset does not have sufficient density or spatial extent to characterize the true correlation structure of the data. Of the 12 datasets that we have reevaluated, we evaluated the spatial correlation of 11 datasets at eight sites. Six of these datasets were SPT data; four were CPT, and one was V_s. Of the 11 datasets, five resulted in nugget models and six resulted in exponential models. All of the CPT and V_s databases showed an exponential semivariogram model, as did the SPT dataset for Salt Lake City. Five of six SPT datasets resulted in nugget models (i.e. no spatial correlation).

Figure 14 shows the empirical and model semivariograms estimated at four sites: Oakland, CA; San Francisco, CA; San Bernardino, CA; and Salt Lake City, UT. The empirical semivariograms and associated models for the CPT, SPT, and V_s LPI data sets from the Oakland site provide an interesting comparison for different types of geotechnical data. The CPT and V_s LPI datasets are both drawn from the same sCPT tests and use the CPT lithology whereas the SPT data are distributed differently across the site. The CPT and V_s semivariograms are fit with exponential

models. The CPT semivariogram model shows spatial correlation up to at least 6 km with little scatter in the empirical data. The V_s semivariogram, also fit by an exponential model, has a lower nugget (lower initial semivariance) but reaches the same sill (plateau) as the CPT near 10 km. The lower nugget value in the V_s data indicate that there is more similarity (correlation) in LPI values at short distances as compared with the CPT LPI values. The nugget semivariogram model we fit to the SPT data indicates that the data set has no spatial correlation. The lack of spatial correlation may be partially due to the SPT data not being as consistently dense as the CPT data across the region or as a result of the higher degree of error in the test. The SPT semivariance is higher overall than the CPT and the V_s with quite a bit of scatter.

The nugget semivariogram model shown for the San Francisco SPT dataset was typical of SPT data and indicates no spatial correlation in the data. The exception to this is the Salt Lake City SPT data discussed below. The exponential semivariogram for the San Bernardino CPT data was also typical for CPT data (but with a lower nugget than in Oakland) and indicates spatial correlation over 6 km.

For the Salt Lake City data, both CPT and SPT LPI datasets exhibited spatial correlation over several kilometers; however, the SPT LPI values were significantly higher resulting in higher semivariance (see Appendix B for a close-up of the CPT LPI semivariogram). The CPT profiles were all clustered in a single area and had very low LPI values (<5), while the SPT are more distributed over a larger area and as typical for SPT had more scatter. To be able to better compare the two datasets, we chose a subset of data from a region that had similar density and spatial distributions of SPT and CPT locations. The resulting semivariograms for this subarea still show a large disparity in semivariance as a result of the generally low CPT values (LPI<4). Figure 15 shows the distributions of SPT and CPT LPI values by geologic unit in the focused region as well as semivariograms for both. The SPT semivariogram over the smaller region is linear rather than exponential whereas the CPT semivariogram is still exponential in shape. The CPT and SPT datasets are similarly distributed, use the same interpolated groundwater levels, reach sufficient depths, and have the same design earthquake and ground motions. An examination of the high SPT LPI values identified large sampling intervals (~10 ft) as a potential cause of the discrepancy. For the two geologic units, the median SPT LPI values are both 0 and the mean values are only slightly higher then the CPT values. If we consider the previous observation that SPT LPI distributions tend to include high outliers combined with the large sampling intervals, then the difference in distributions is no longer unexpected.

As an alternative to using geologic units to classify liquefaction potential, we test a direct interpolation of LPI between locations using geostatistical methods when spatial correlation exists (as determined by the semivariogram). At the Oakland site, we can estimate LPI values across the study region using ordinary kriging for both the CPT and V_s datasets, and the results are shown in Figure 16. Interpolated values are only shown when the estimate variance is lower than the population variance (i.e. when the interpolated value has a lower variance than an estimate made with the population mean). As a result of the high sample density and low variance, both maps cover the entire area of study. It is important to note that the interpolated values here disregard geologic boundaries; therefore, these maps are an intermediate step and a true liquefaction hazard map should combine the results of interpolated LPI values and geologic boundaries. The CPT based map shows relatively high hazard (orange and red) across the entire

region; while the V_s based map results in high hazard primarily near the coast and coincident with the artificial fill units. The V_s maps match more closely the published liquefaction hazard maps for the area than the one produced from CPT data (Holzer et al. 2006; Knudsen et al. 2000). Since both datasets are collocated and use the same lithology to determine liquefiability, the difference is in the layering of the datasets, the liquefaction potential relationships (CPT vs. V_s correlations), and the differences in spatial correlation. The V_s semivariogram has a very low nugget value indicating that the interpolated value is going to be most strongly influenced by nearby points. The CPT semivariogram has a higher nugget and therefore, the resulting interpolated values represent an average over a larger area. The V_s profiles are generally comprised of 2-5 layers of constant V_s whereas the CPT profiles are highly variable throughout the profile. To investigate the affect of I_c on the CPT map, we produced a kriged map of the CPT assuming that the cutoff for the I_c was 2.4 instead of 2.6 as shown in Figure 17. Using an I_c cutoff of 2.4, the V_s and CPT kriged maps more closely correspond with the published maps of the area but the CPT map still has higher hazard in the inland units.

To test how well geostatistical methods work for a single discrete geologic unit, we use the CPT-based LPI values within the Qds (Latest Pleistocene to Holocene dune sand or Merritt Sand) geologic unit. We chose this unit because Holzer et al. (2006) described this unit as being more liquefiable in the western and northern portions. As is seen in Figure 18, the model semivariogram for these 15 CPT profiles shows good spatial correlation up to about 1 km with a low nugget value. There is one low outlier near 1 km in the empirical semivariogram which is due to there being a low number of CPT pairs at this distance. Using this model semivariogram, we use ordinary kriging to interpolate the LPI values across this deposit as shown in Figure 18. The outline of this Qds unit is indicated on the full site map in Figure 16. The kriged map shows lower LPI values along the eastern portion and higher values in the northern and middle portions of the deposit, which is similar to the liquefaction hazard given by Holzer et al. (2006) but provides more detail.

As a second example of geostatistical interpolation, we found spatial correlation with the CPT and SPT data in Salt Lake City (Figure 14). We used ordinary kriging to interpolate the SPT LPI values, both over the entire site and within a subunit of the Holocene to Pleistocene terrace gravel (Qtg) geologic unit as shown in Figure 19. The larger map shows high LPI zones along the western portion of the site and low zones to the south and western portion of the site. The western portion of the map is dominated by the geologic unit Qcs (Holocene clay, silt, and sand), which is a very young unit deposited in the Great Salt Lake when lake levels were higher, while many of the borings taken in the southern portion of the site are within artificial fill units. Both the Qcs and artificial fill units show higher LPI distributions (as seen in Figure 13) than the other units in the area. The subarea map shows that the Qtg unit could be subdivided into two zones.

Of the eleven datasets, six of them presented spatial correlation including: (1) Oakland CPT, (2) Oakland V_s, (3) Salt Lake City SPT, (4) Salt Lake City CPT, (5) San Bernardino CPT, and (6) Evansville CPT. Interpolated maps of LPI values for each of these sites can be found in the appendicies. If a sufficient dataset is collected, LPI can be interpolated between observation points; thus providing a more detailed map of liquefaction potential than achieved using geologic unit boundaries alone. In general, the SPT datasets do not show sufficient spatial correlation for interpolation. However, the V_s and CPT–based LPI values showed significant spatial correlation

across the evaluated regions allowing for direct interpolation. The resulting maps of LPI values show pockets of high and low hazard within geologic units, which can be useful information if these delineations cannot be made in the field. In addition, spatial correlation can be estimated within geologic units and then used for interpolation of LPI values providing a more detailed map of spatial variability of liquefaction potential.

5.0 CONCLUSIONS

We outline a common methodology for evaluating geotechnical data for liquefaction potential and including the information in regional liquefaction hazard maps. The methodology is based on the Seed-Idriss Simplified Procedure as updated in Youd et al. (2001) and relies on the liquefaction potential index. We also outline recently published probability methods that can be used for liquefaction evaluation. Box-plots and cumulative distributions are used to evaluate the population variability for geologic units and to report liquefaction potential in terms of probability of liquefaction within geologic units. In addition, the semivariogram is used to assess the spatial correlation of LPI values and to determine if the liquefaction potential can be interpolated between data points for an assessment of spatial distribution of liquefiable soil.

Using the outlined methods, nine sites (12 datasets) are reevaluated to identify issues and challenges in regional liquefaction hazard mapping projects. The primary issues are: 1) the importance of an accurate and appropriate ground water table, 2) the effect of soil type restrictions (I_c), 3) the effect of geotechnical data type, and 4) the population and spatial variability of LPI over geologic units. Depending on the regional conditions, either groundwater or soil type can play a major role in determining the liquefiability of soils. The choice of SPT, CPT, and V_s and the inherent spatial variability of liquefaction potential were issues at all sites.

A comparison of CPT, SPT, and V_s resulted in some very interesting conclusions. In general LPI results vary as a result of geotechnical data type. This bias has been reported elsewhere (Andrus et al. 2004; Juang et al. 2002) and can be accounted for by using different Factor of Safety limits for the various data (as well as using the appropriate I_c cutoff). The high CPT LPI values reported here for Oakland, CA are in part a result of the conservative assumption that I_c <2.6 defines liquefiable soils. In Oakland, CA, the I_c <2.4 cutoff more closely matches the published liquefaction maps. In general, the SPT based LPI values are the most variable and positively skewed whereas the CPT and V_s LPI distributions are narrower with less scatter and fewer outliers. At the Oakland site, where all three measurements are available and mapped liquefaction hazard maps can be compared with LPI distributions, the V_s LPI distributions match the mapped liquefaction hazard categories more accurately than either CPT or SPT LPI distributions. This indicates that V_s may be more consistent with geologic interpretations (i.e. V_s profiles in a specific unit are more similar than SPT or CPT profiles in the same unit). The semivariogram analysis at Oakland, CA indicate that the V_s and CPT datasets are spatially correlated to a distance of at least 6 km, but the SPT data set does not show spatial correlation. The V_s dataset is also highly correlated at shorter distances (more so than the CPT dataset) resulting in a more detailed interpolated map that closely matches the published liquefaction maps for the region. The spatial correlation results at the Oakland site are similar to those found at other sites. In general, CPT-based and V_s-based LPI values show spatial correlation and SPT-based LPI values do not.

We have identified differences in LPI values between the three types of geotechnical data. These differences most likely result from In addition, we evaluate the consistency of LPI values derived from SPT, CPT, and V_s over geologic units and susceptibility categories. Further research should be performed to determine which estimate is the most accurate at identifying liquefiable soils (rather than the most consistent to geologically mapped units).

Our analysis provided significant evidence of both the spatial and population variability of liquefaction potential within mapped geologic units. Overlap between low to high hazard generally exists between geologic units. Liquefaction potential should be assigned to mapped units in a way that reflects the distribution of liquefiable soils (using probability or spatial analysis). Because of the wide distribution of LPI values in a given geologic unit, it is imperative that sufficient geotechnical data are collected across the unit to insure an unbiased and characteristic sample.

In general, dense geotechnical data sets are needed to properly evaluate the liquefaction potential for regional mapping. Integration of varying geotechnical data should be done with care and should take into account the bias that results from each data type (SPT, CPT, and V_s). Poor spatial coverage of geotechnical data can lead to biased results and mischaracterization of LPI distributions. From the analysis of geotechnical datasets presented here, CPT and V_s based LPI values have less variability within geologic units than SPT based LPI values and show significant spatial correlation. The high variability of SPT based LPI values leads to a lack of spatial correlation of values. Therefore, we recommend using CPT and V_s measurements for liquefaction hazard mapping projects whenever possible. Although we only had a single V_s dataset, the V_s LPI results closely matched the published liquefaction hazard maps. We recommend further investigation into which type of data most accurately characterizes liquefaction potential with a focus on CPT and V_s. Finally, issues of soil type need to be addressed when using CPT and V_s and the growing literature on the liquefiability of silty soils should assist in this matter.

6.0 PUBLICATIONS AND CONFERENCE PRESENTATIONS ORIGINATING FROM THIS RESEARCH

1. Lenz, J. A. and Baise, L. G. (2006). Spatial variability of liquefaction potential in regional mapping using CPT and SPT data, *Soil Dynamics and Earthquake Engineering*, Accepted in October 2006.
2. Lenz, J. A. and Baise, J.G. (2007). Variability of LPI across geologic units for regional liquefaction mapping, GeoDenver 2007.

7.0 REFERENCES

Anderson, L. R., Keaton, J. R., Spitzley, J. E., and Allen, A. G. (1994). "Liquefaction potential map for Salt Lake County, Utah." *Rep. No. Utah Geological Survey Contract Report 94-4*.

Andrews, D. C., and Martin, G. R. (2000). "Criteria for liquefaction of silty sands." *Proc., 12th World Conference on Earthquake Engineering*.

Andrus, R. D., Piratheepan, P., Ellis, B. S., Zhang, J., and Juang, C. H. (2004). "Comparing liquefaction evaluation methods using penetration-V_S relationships." *Soil Dyn.Earthquake Eng.,* 24(9-10), 713-721.

Andrus, R. D., and Stokoe II, K. H. (2000). "Liquefaction resistance of soils from shear-wave velocity." *J.Geotech.Geoenviron.Eng.,* 126(11), 1015-1025.

Baecher, G. B., and Christian, J. T. (2003). *Reliability and Statistics in Geotechnical Engineering.* John Wiley & Sons, England.

Baise, L. G., and Brankman, C. M. (2004). "Liquefaction Hazard Mapping in Boston, Massachusetts: Collaborative Research with William Lettis & Associates, Inc., and Tufts University." *Rep. No. USGS Award No. 02HQGR0036 and 02HQGR004* .

Baise, L. G., Higgins, R. B., and Brankman, C. M. (2006). "Liquefaction hazard mapping - Statistical and spatial characterization of susceptible units." *J.Geotech.Geoenviron.Eng.,* 132(6), 705-715.

Boore, D. M. (2003). "A compendium of P- and S-wave velocities from surface- to-borehole logging: Summary and reanalysis of previously published data and analysis of unpublished data." *Rep. No. U.S. Geological Survey Open-File Report 03-191*.

Boore, D. M., Joyner, W. B., and Fumal, T. E. (1997). "Empirical near-source attenuation relations for horizontal and vertical components of peak ground acceleration, peak ground velocity, and pseudo-absolute acceleration response spectra." *Seismol. Res. Lett.,* 68(1), 154-179.

Brankman, C. M. and Baise L. B. (2006). "Liquefaction susceptibility mapping in Boston, Massachusetts." *Engineering and Environmental Geology,* submitted 2006.

Bray, J. D., and Sancio, R. B. (2006). "Assessment of the liquefaction susceptibility of fine-grained soils." *J.Geotech.Geoenviron.Eng.,* 132(9), 1165-1177.

Broughton, J., and Van Arsdale, R. (2004). "Surficial geologic map of the Northwest Memphis Quadrangle, Shelby County, Tennessee, and Crittenden County, Arkansas." *Rep. No. Scientific Investigations Map 2838,* U.S. Geological Survey.

Bryant, B. H. (1990). "Geologic map of the Salt Lake City 30' x 60' quadrangle, north-central Utah, and Uinta County, Wyoming, with a section on palynologic data from Cretaceous and lower Tertiary rocks in the Salt Lake City 30' x 60' quadrangle by D.J. Nichols and B.H. Bryant." *Rep. No. U.S. Geological Survey Miscellaneous Investigations Series Map, I-1944, 1 sheet, scale 1:100,00* .

California Department of Conservation, Division of Mines and Geology. (2000). "Recommended criteria for delineating seismic hazard zones in California." *Rep. No. Special Publication 118,* California Division of Mines and Geology.

California Geological Survey. (2004). "Recommended criteria for delineating seismic hazard zones in California." *Rep. No. Special Publication 118*.

California State Water Rights Board. (1962). "Report of Referee, in the Superior Court of the State of California in and for the County of Los Angeles, The City of Los Angeles, a Municipal Corporation, Plaintiff vs. City of San Fernando, a Municipal Corporation, et al., Defendants." No. 650079(v. 1), 258 p.

Carson, S. E., and Matti, J. C. (1986). "Contour map showing minimum depth to ground water, San Bernardino Valley and vicinity, California 1973-1983." *Rep. No. U.S. Geological Survey Open-File Report 86-225*.

Cetin, K. O., Seed, R. B., Der Kiureghian, A., Tokimatsu, K., Harder Jr., L. F., Kayen, R. E., and Moss, R. E. S. (2004). "Standard penetration test-based probabilistic and deterministic assessment of seismic soil liquefaction potential." *J.Geotech.Geoenviron.Eng.,* 130(12), 1314-1340.

Cox, R. (2004). "Surficial geologic map of the Northest Memphis Quadrangle, Shelby County, Tennessee." *Rep. No. Scientific Investigations Map 2839,* U.S. Geological Survey.

Cressie, N. (1985). "Fitting variogram models by weighted least-squares." *Journal of the International Association for Mathematical Geology,* 17(5), 563-586.

Frankel, A. D., Petersen, M. D., Mueller, C. S., Haller, K. M., Wheeler, R. L., Leyendecker, E. V., Wesson, R. L., Harmsen, S. C., Cramer, C. H., Perkins, D. M., and Rukstales, K. S. (2002). "Documentation for the 2002 update of the National Seismic Hazard Maps." *Rep. No. USGS OFR 02-420,* U.S. Geological Survey.

Goovaerts, P. (1997). *Geostatistics for natural resources evaluation.* Oxford University Press, New York.

Gray, H. H. (1989). "Quaternary geologic map of Indiana." 1:500,000(Indiana).

Grimley, D., and Lepley, S. (2001a). "Surficial geologic materials map of the Columbia Bottom (IL) 7.5' quadrangle." *Rep. No. Illinois State Geologic Survey STATEMAP product*.

Grimley, D., and Lepley, S. (2001b). "Surficial geologic materials map of the Wood River (IL) 7.5' quadrangle." *Rep. No. Illinois State Geologic Survey STATEMAP product*.

Grimley, D., Phillips, A., and Lepley, S. (2001). "Surficial geologic materials map of the Monks' Mound (IL) 7.5' quadrangle." *Rep. No. Illinois State Geological Survey STATEMAP product*.

Helley, E. J., and Graymer, R. W. (1997). "Quaternary geology of Alameda County, and parts of Contra Consta, Santa Clara, San Mateo, San Francisco, Stanislaus, and San Joaquin counties, California: A digital database." *Rep. No. Open-File Rep. 97-97,* U.S. Geological Survey.

Hitchcock, C. S., and Wills, C. J. (2000). "Quaternary geology of the San Fernando Valley, Los Angeles County, California." 1:48000 Map Sheet 50.

Hitchcock, C. S., and Wills, C. J. (1998). "Quaternary geologic mapping and seismic hazards of San Fernando Valley, California." *GSA Abstracts with Programs, Cordilleran Section Meeting,* 30(5), p. 20.

Holzer, T. L., Bennett, M. J., Noce, T. E., Padovani, A. C., and Tinsley III, John C. (2002). "Liquefaction Hazard and Shaking Amplification Maps of Alameda, Berkeley, Emeryville, Oakland, and Piedmont, California: A Digital Database." *Rep. No. USGS Open-File Report 02-296,* U.S. Geological Survey.

Holzer, T. L., Bennett, M. J., Noce, T. E., Padovani, A. C., and Tinsley III, J. C. (2006). "Liquefaction Hazard Mapping with LPI in the Greater Oakland, California, Area." *Earthquake Spectra,* 22(3), 693-708.

Holzer, T. L., Bennett, M. J., Noce, T. E., and Tinsley III, J. C. (2005). "Shear-wave velocity of surficial geologic sediments in Northern California: Statistical distributions and depth dependence." *Earthquake Spectra,* 21(1), 161-177.

Hwang, H., Chien, M. C., and Lin, Y. W. (1999). "Investigation of soil conditions in Memphis, Tennessee." *Rep. No. USGS Award No. 1434-HQ-98-GR-00002*.

Hynes Jr., L. F., and Olsen, R. S. (1999). "Influence of confining stress on liquefaction resistance." *Proc., Int. Workshop on Phys. and Mech. of Soil Liquefaction,* 145-152.

Iwasaki, T., Tokida, K., Tatsuoka, F., Watanabe, S., Yasuda, S., and Sato, H. (1982). "Microzonation for soil liquefaction potential using simplified methods." *Proc., 3rd International Earthquake Microzonation Conference,* 1319-1330.

Jefferies, M. G., and Davies, M. P. (1993). "Use of CPTu to estimate equivalent SPT N_{60}." *Geotech Test J,* 16(4), 458-468.

Juang, C. H., Jiang, T., and Andrus, R. D. (2002). "Assessing probability-based methods for liquefaction potential evaluation." *J.Geotech.Geoenviron.Eng.,* 128(7), 580-589.

Kayen, R. E., Mitchell, J. K., Seed, R. B., Lodge, A., Nishio, S., and Coutinho, R. (1992). "Evaluation of SPT-, CPT-, and shear wave-based methods for liquefaction potential assessment using Loma Prieta data." *Proc., 4th Japan-U.S. Workshop on Earthquake-Resistant Des. of Lifeline Fac. and Countermeasures for Soil Liquefaction,* 177-204.

Kayen, R.E. et al. (in preparation). "Shear Wave Velocity-Based Probabilistic and Deterministic Assessment of Seismic Soil Liquefaction Potential." *J. Geotech. Geoenviron. Eng.*.

Knudsen, K. L., Sowers, J. M., Witter, R. C., Wentworth, C. M., Helley, E. J., Nicholson, R. S., Wright, H. M., and Brown, K. H. (2000). "Preliminary maps of Quaternary deposits and liquefaction susceptibility, nine-county San Francisco Bay region, California: A digital database." *Rep. No. USGS Open-File Report 00-444,* U.S. Geological Survey.

Kohlhase, R. C. (1987). "Ground-water levels and pumpage in hte East St. Louis area, Illinois 1981-1985." *Rep. No. Illinois State Water Survey Circular 168 (ISWS/CIR-168/87)*.

Lenz, J. A., and Baise, L. G. (submitted 2006). "Spatial variability of liquefaction potential in regional mapping using CPT and SPT data." *Soil Dyn.Earthquake Eng.*.

Liao, T., Zavala, G., McGillivray, A., Camp, W. M., III, and Mayne, P. W. (2001). "Cone penetration testing for seismic hazards evaluation in Memphis & Shelby County, Tennessee." *Rep. No. USGS Grant 00HQGR0025 Final Report*.

Liao, S. S. C., Veneziano, D., and Whitman, R. V. (1988). "Regression-Models for evaluating liquefaction probability." *J. Geotech. Eng.,* 114(4), 389-411.

Liao, T., Mayne, P. W., Tuttle, M. P., Schweig, E. S., and Van Arsdale, R. B. (2002). "CPT site characterization for seismic hazards in the New Madrid seismic zone." *Soil Dyn.Earthquake Eng.,* 22(9-12), 943-950.

Lineback, J. A. (1979). "Quaternary Deposits of Illinois." 1:500,000.

Luna, R., and Frost, J. D. (1998). "Spatial liquefaction analysis system." *J.Comput.Civ.Eng.,* 12(1), 48-56.

Matti, J. C., and Carson, S. E. (1991). "Liquefaction susceptibility in the San Bernardino Valley and Vicinity, Southern California - A regional evaluation." *Rep. No. U.S. Geological Survey Bulletin 1898,* Denver, CO.

Moore, D. W., and Diehl, S. F. (2004a). "Surficial geologic map of the Southeast Memphis Quadrangle, Shelby County, Tennessee." *Rep. No. Scientific Investigations Map 2822,* U.S. Geological Survey.

Moore, D. W., and Diehl, S. F. (2004b). "Surficial geologic map of the Southwest Memphis Quadrangle, Shelby County, Tennessee, and Crittenden County, Arkansas." *Rep. No. Scientific Investigations Map 2823,* U.S. Geological Survey.

Morton, D. M., and Miller, F. K. (2003). "Preliminary geologic map of the San Bernardino 30' x 60' quadrangle, California." *Rep. No. USGS OFR 03-293,* U.S. Geological Survey, Menlo Park, California.

Moss, R. E. S., Seed, R. B., Kayen, R. E., Stewart, J. P., Der Kiureghian, A., and Cetin, K. O. (2006). "CPT-based probabilistic and deterministic assessment of in situ seismic soil liquefaction potential." *J.Geotech.Geoenviron.Eng.,* 132(8), 1032-1051.

Ng, K. W., Chang, T. S., and Hwang, H. H. M. (1989). "Surface Conditions of Memphis and Shelby County." *Rep. No. Technical Report NCEER-89-0021*.

Nicholson, S. W., Dicken, C. L., Horton, J. D., Labay, K. A., Foose, M. P., and Mueller, J. A. L. (2005). "Preliminary integrated Geologic Map Databases for the United States: Kentucky, Ohio, Tennessee, and West Virginia." 1:100,000(Kentucky).

Pearce, J. T., and Baldwin, J. N. (2005). "Liquefaction susceptibility mapping, St. Lous, Missouri and Illinois." *Rep. No. Award 03HQGR0029,* U.S. Geological Survey - National Earthquake Hazards Reduction Program.

Petersen, M. D., Bryant, W. A., Cramer, C. H., Cao, T., Reichle, M. S., Frankel, A. D., Lienkaemper, J. J., McCrory, P. A., and Schwartz, D. P. (1996). "Probabilistic seismic hazard assessment for the State of California." *Rep. No. California Department of Conservation, Division of Mines and Geology Open-File Rep. 96-08 (also U.S. Geological Survey Open-File Rep. 96-706)*.

Phillips, A. (1999). "Surficial geologic materials map of the Cahokia (IL) 7.5' quadrangle." *Rep. No. Illinois State Geologic Survey STATEMAP product*.

Phillips, A., Grimley, D., and Lepley, S. (2001). "Surficial geologic materials map of the Granite City (IL) 7.5' quadrangle." *Rep. No. Illinois State Geological Survey STATEMAP product*.

Phoon, K., and Kulhawy, F. H. (1999). "Evaluation of geotechnical property variability." *Canadian Geotechnical Journal,* 36(4), 625-639.

R Development Core Team. (2006). "R: A Language and Environment for Statistical Computing." v.2.3.0.

Ribeiro Jr., P. J., and Diggle, P. J. (2001). "geoR: A package for geostatistical analysis." *R-NEWS,* 1(2).

Rix, G. J., and Romero-Hudock, S. (submitted May, 2006). "Liquefaction potential mapping in Memphis and Shelby County, Tennessee." *Earthquake Spectra*.

Robertson, P. K. (2004). "Evaluating soil liquefaction and post-earthquake deformations using CPT." *Proceedings of the Second International Conference on Site Characterization,* Millpress, Rotterdam, Netherlands, 233-249.

Robertson, P. K., and Wride, C. E. (1998). "Evaluating cyclic liquefaction potential using the cone penetration test." *Canadian Geotechnical Journal,* 35(3), 442-459.

Seed, H. B., and Idriss, I. M. (1971). "Simplified procedure for evaluating soil liquefaction potential." *J Soil Mech found Div ASCE,* 97(SM9), 1249-73.

Sonmez, H. (2003). "Modification of the liquefaction potential index and liquefaction susceptibility mapping for a liquefaction-prone area (Inegol, Turkey)." *Environ.Geol.,* 44(7), 862-871.

Thompson, E. M., Baise, L. G., and Kayen, R. E. (2007). "Spatial correlation of shear-wave velocity in the San Francisco Bay Area sediments." *Soil Dynamics and Earthquake Engineering,* 27(2), 144-152.

Tinsley, J. C., Youd, T. L., Perkins, D. M., and Chen, A. T. F. (1985). "Evaluating liquefaction potential." GPO, Washington, DC, USA, 263-315.

Toprak, S., and Holzer, T. L. (2003). "Liquefaction potential index: Field assessment." *J.Geotech.Geoenviron.Eng.,* 129(4), 315-322.

Van Arsdale, R. (2004a). "Surficial geologic map of the Ellendale Quadrangle, Shelby County, Tennessee." *Rep. No. Scientific Investigations Map 2836,* U.S. Geological Survey.

Van Arsdale, R. (2004b). "Surficial geologic map of the Germantown Quadrangle, Shelby County, Tennessee." *Rep. No. Scientific Investigations Map 2837,* U.S. Geological Survey.

Youd, T. L., and Idriss, I. M. (2001). "Liquefaction resistance of soils: Summary report from the 1996 NCEER and 1998 NCEER/NSF workshops on evaluation of liquefaction resistance of soils." *J.Geotech.Geoenviron.Eng.,* 127(4), 297-313.

Youd, T. L., Idriss, I. M., Andrus, R. D., Arango, I., Castro, G., Christian, J. T., Dobry, R., Liam Finn, W. D., Harder L.F., J., Hynes, M. E., Ishihara, K., Koester, J. P., Liao, S. S. C., Marcuson III, W. F., Martin, G. R., Mitchell, J. K., Moriwaki, Y., Power, M. S., Robertson, P. K., Seed, R. B., and Stokoe II, K. H. (2001). "Liquefaction resistance of soils: Summary report from the 1996 NCEER and 1998 NCEER/NSF workshops on evaluation of liquefaction resistance of soils." *J.Geotech.Geoenviron.Eng.,* 127(10), 817-833.

Guidelines for Regional Liquefaction Hazard Mapping

by:

Laurie G. Baise[1]

and

Jennifer A. Lenz[1]

[1]Department of Civil and Environmental Engineering
Tufts University
113 Anderson Hall, Medford, MA 02155
phone: 617-627-2211 fax: 617-627-3994
email: laurie.baise@tufts.edu
webpage: http://ase.tufts.edu/cee/faculty/baise/bio.asp

U.S. Geological Survey
National Earthquake Hazard Reduction Program
Award No. 05HQGR0103

August 31, 2006

Non-technical summary:

This project is a one-year study to reevaluate completed regional liquefaction hazard mapping projects and develop guidelines for incorporating geotechnical data in regional liquefaction hazard mapping projects. Many early liquefaction hazard projects relied solely on surficial geology to assess liquefaction hazard. The current trend is to include geotechnical data along with the surficial geology when characterizing the liquefaction susceptibility. Geotechnical data provide detailed information about the soil at a specific location. When pooled over a geologic unit, geotechnical data can provide information on the distribution of liquefiable soils within the mapped unit.

Site		# of Profiles	Geotechnical Data	Surficial Geology	Groundwater Data	PGA
Oakland, CA	SPT	123	CA Geological Survey Geotechnical Database	San Fran 30x60: Knudsen et al. 2000 (USGS ofr00-444)	CA. Geological Survey Geotechnical Database	Interpolated PSHA 10% PE in 50 years + Fa Class D
	CPT	195	Holzer et al, ofr 02-296	San Fran 30x60: Knudsen et al. 2000 (USGS ofr00-444)	CPT profiles	Interpolated PSHA 10% PE in 50 years + Fa Class D
	VS	192	Holzer et al, ofr 02-296 & Thompson et al. (2006)	San Fran 30x60: Knudsen et al. 2000 (USGS ofr00-444)	CPT profiles	Interpolated PSHA 10% PE in 50 years + Fa Class D
Salt Lake City, UT	SPT	215	Utah Liquefaction Advisory Group Boring Database	Utah Geological Survey 30x60. Digitized from Bryant, 1990.	ULAG Boring Database	Interpolated PSHA 2% PE in 50 years + Fa Class D
	CPT	249	Utah Liquefaction Advisory Group CPT database	Utah Geological Survey 30x60. Digitized from Bryant, 1990.	ULAG Boring Database	Interpolated PSHA 2% PE in 50 years + Fa Class D
San Bernardino, CA	CPT	62	USGS CPT dataset	San Bernardino 30x60: USGS ofr03-293	CPT and interpolated USGS groundwater levels	Interpolated PSHA 2% PE in 50 years + Fa Class D
Evansville, IN	CPT	57	USGS CPT dataset	IN: Indiana Geological Survey Misc Map 49 (1989); KY: USGS ofr05-1324	CPT profiles and IN Dept. of Natural Resources Wells database	Interpolated PSHA 2% PE in 50 years + Fa Class D
So. San Francisco Bay, CA	SPT	165	CA Geological Survey Geotechnical Database	San Fran 30x60: Knudsen et al. 2000 (USGS 00-444)	CA. Geological Survey Geotechnical Database	Interpolated PSHA 10% PE in 50 years + Fa Class D
San Fernando, CA	SPT	52	CA Geological Survey Geotechnical Database	LA 30x60: USGS ofr05-1029	CA. Geological Survey Geotechnical Database	Interpolated PSHA 10% PE in 50 years + Fa Class D
Shelby, TN	SPT	692	Hwang et al. (1999) Boring Database	USGS Scientific Investigations Maps	Hwang et al. (1999)	0.4g
St. Louis, IL	SPT	340	Illinois State Geological Survey Boring Database	Illinois Quaterary deposits (Lineback, 1979)	Illinois State Geological Survey Boring Database	0.2g
San Francisco, CA	SPT	54	CA Geological Survey Geotechnical Database	San Fran 30x60: Knudsen et al. 2000 (USGS 00-444)	CA. Geological Survey Geotechnical Database	Interpolated PSHA 10% PE in 50 years + Fa Class D
Boston, MA	SPT	2963	Baise & Brankman 2004 Boring Database	Brankman & Baise (2006)	Baise & Brankman 2004 Boring Database	0.12g

Table 1. Projects reevaluated for this project and the data we used for liquefaction potential calculations.

Site	Data Type	% LPI > 2	% LPI > 5
Oakland, CA	SPT	28	13
	CPT	21	6
	VS	8	2
Salt Lake City, UT	SPT	24	13
	CPT	20	13
San Bernardino, CA	CPT	22	0
Evansville, IN	CPT	29	6
So. San Fran. Bay, CA	SPT	28	7
San Fernando, CA	SPT	12	6
Shelby, TN	SPT	27	13
St. Louis, IL	SPT	25	5
San Francisco, CA	SPT	6	3

Table 2. Percent of 20 m profiles that show an increase in the LPI of more than 2 and 5 between 10 and 20 m.

Liquefaction Potential Index (LPI)	Liquefaction Potential Classification
0	Non-liquefied
0 < LPI ≤ 2	Low
2 < LPI ≤ 5	Moderate
5 < LPI ≤ 15	High
LPI > 15	Very High

Table 3. Liquefaction potential classifications proposed by Sonmez (2003)

Geologic Unit	CPT	SPT	Vs
afbm	0.73	1.61	1.07
Qds	1.28	2.08	4.58
Qpf	0.86	2.23	3
Qhf	1.01	1.22	6.05
Qhl	0.87	1.86	NaN
Qf	0.43	NA	NaN
Qhff	0.66	0.68	1.84
ALL	0.85	1.64	1.98

Table 4. Coefficient of variation by geologic unit for CPT, SPT and V_s data in Oakland, CA.

Oakland, CA - CPT

	All	Profiles ≥ 10m	Profiles ≥ 15m	Profiles ≥ 20m
# of profiles	210	195	142	66

	Profiles ≥ 20 m			
	LPI_{10}	LPI_{15}	LPI_{20}	LPI_{15} Extrapolated
Mean	6.7	7.7	8.0	7.9
Median	4.3	5.7	6.0	5.8
Max	33.9	35.3	35.3	35.3

Oakland, CA - SPT

	All	Profiles ≥ 10m	Profiles ≥ 15m	Profiles ≥ 20m
# of profiles	218	123	97	45

	Profiles ≥ 20 m			
	LPI_{10}	LPI_{15}	LPI_{20}	LPI_{15} Extrapolated
Mean	3.6	5.5	5.7	5.7
Median	0	0.02	0.03	0
Max	23.2	47.6	50.9	47.6

Table 5. Number of profiles with depths greater than 10, 15 and 20 m, and mean, median and maximum LPI values assuming integration depths of 10, 15 and 20 m. The LPI_{15} extrapolated value is calculated by extrapolating the 15 m value to 20 m.

Salt Lake City Cumulative Frequencies

Geologic Unit	LPI ≥ 5 (%)
All	21%
a	33%
Qal	27%
Qbc	0%
Qcs	45%
Qf	14%
Qpc	21%
Qtg	17%

Table 6. Probability of exceeding LPI≥5 for Salt Lake City, UT SPT database using cumulative frequency distributions.

FIGURES

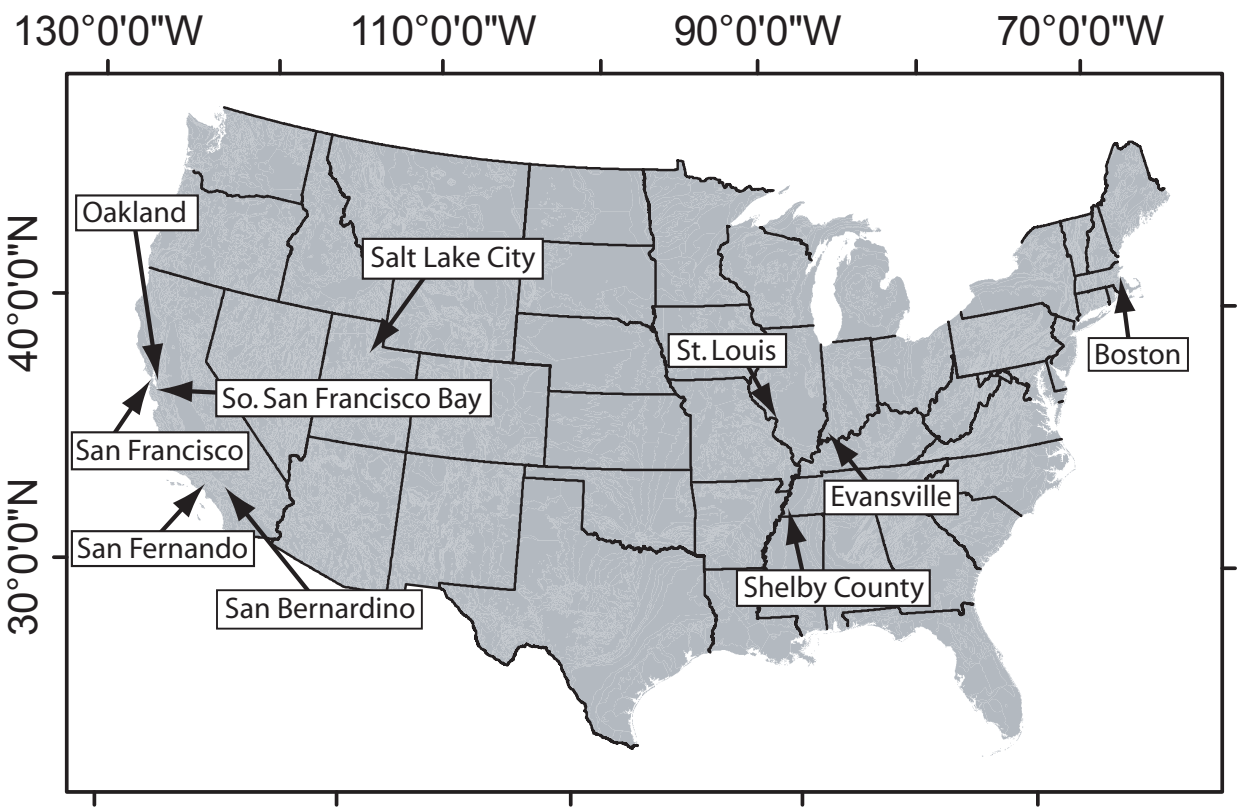


Fig. 1. Vicinity map of 10 sites reviewed for this project.

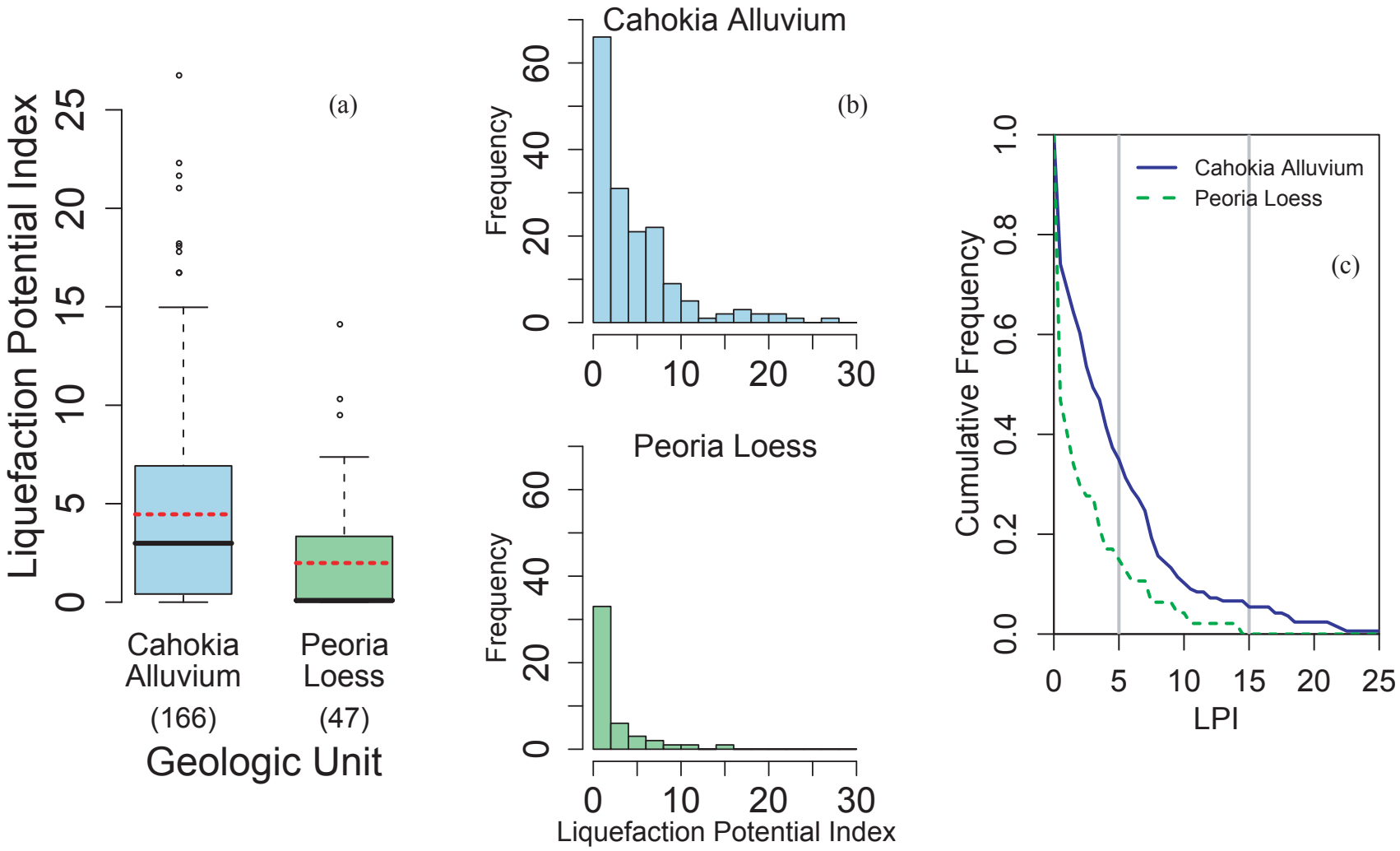


Fig. 2. Two geologic units from the St. Louis SPT database plotted (a) box-plots, (b) histograms, and (c) cumulative frequency plots.

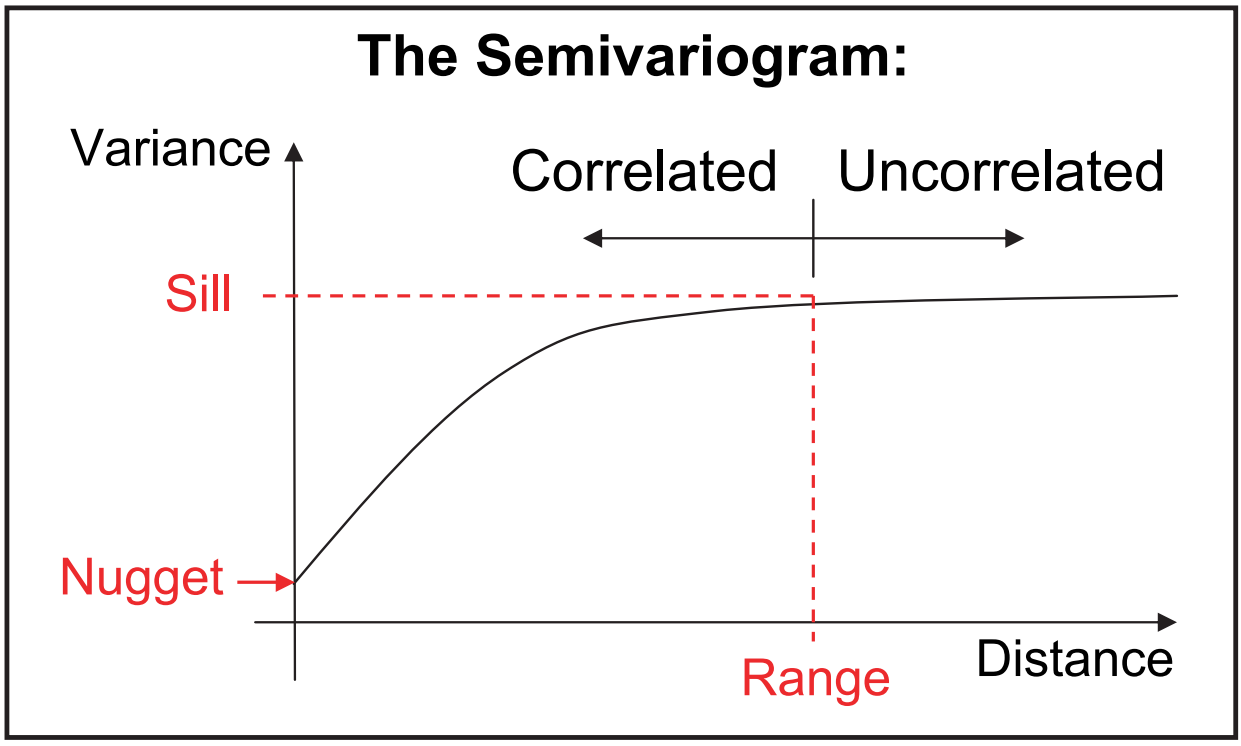


Fig. 3. Typical exponential semivariogram.

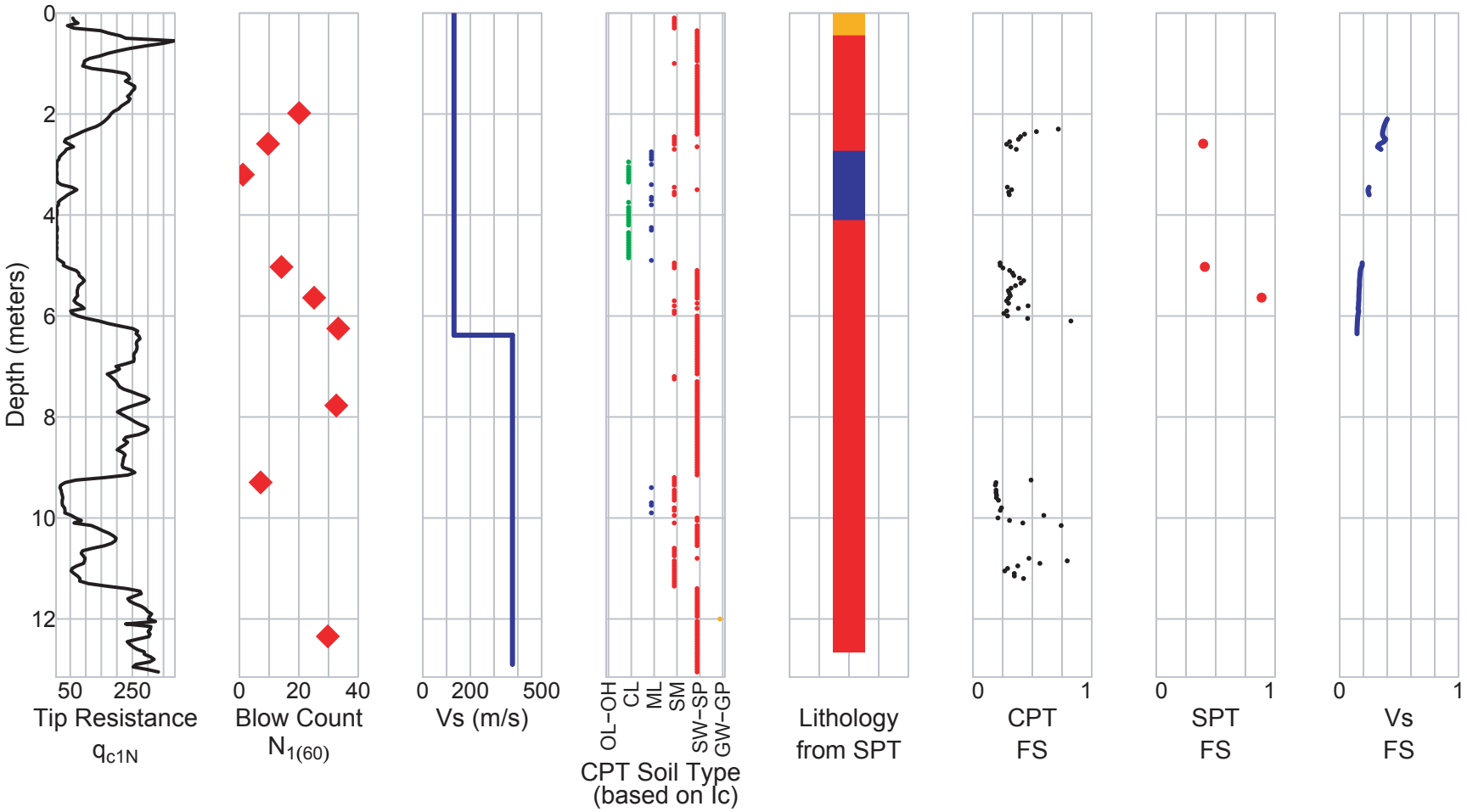


Fig. 4. Comparison between CPT, SPT and Vs profiles within the Oakland, CA area. The distance between these locations is approximately 230 meters and both are located in the surficial geology unit afbm (artificial fill over San Francisco Bay Mud). The characteristics compared are soil density, stratigraphy, and the factor of safety against liquefaction.

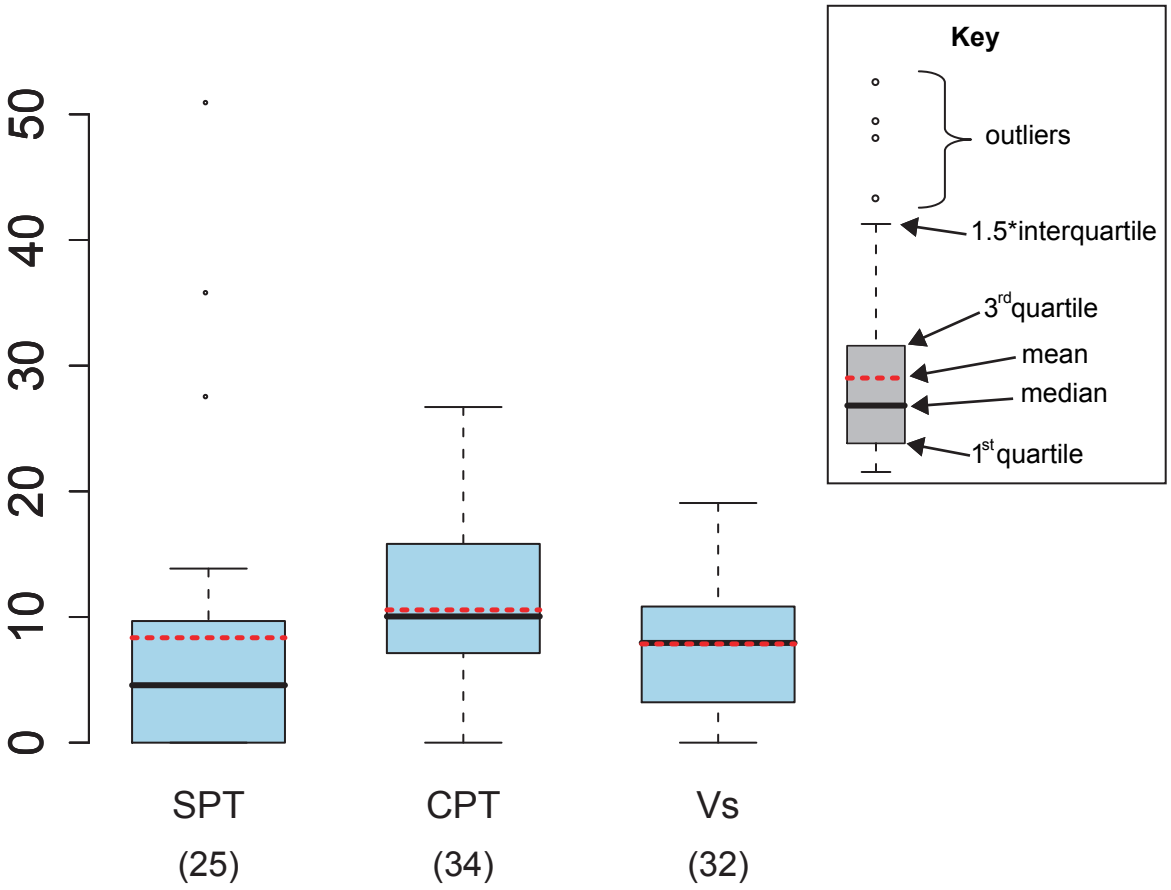


Fig. 5. Distribution of SPT, CPT and Vs based LPI values for a single continuous afbm (artificial fill over San Francisco bay mud) geologic unit.

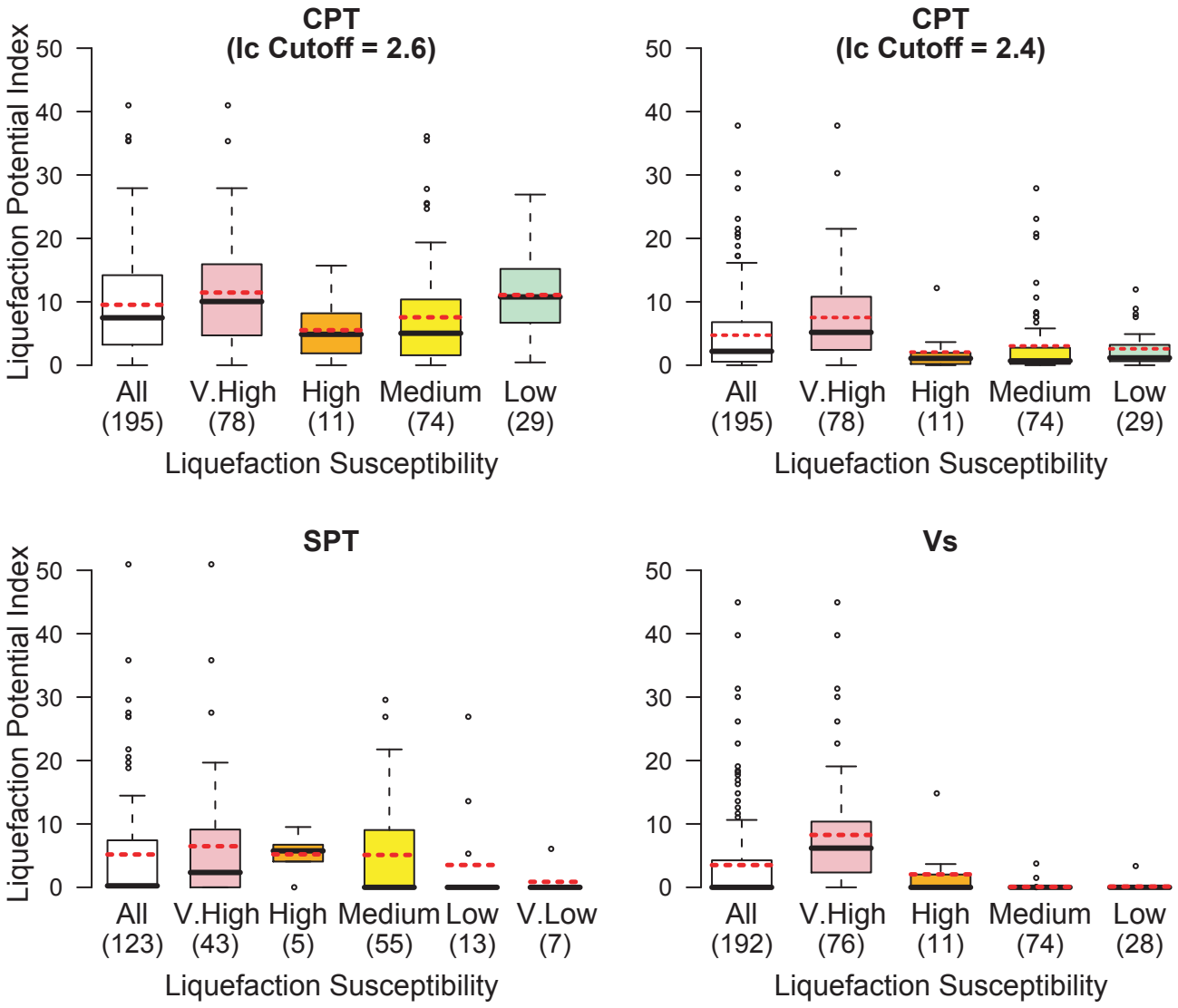


Fig. 6. LPI distributions grouped by liquefaction susceptibility (Knudsen et al., 2000) for the Oakland, CA area for CPT (with two different Ic cutoff values), SPT and Vs.

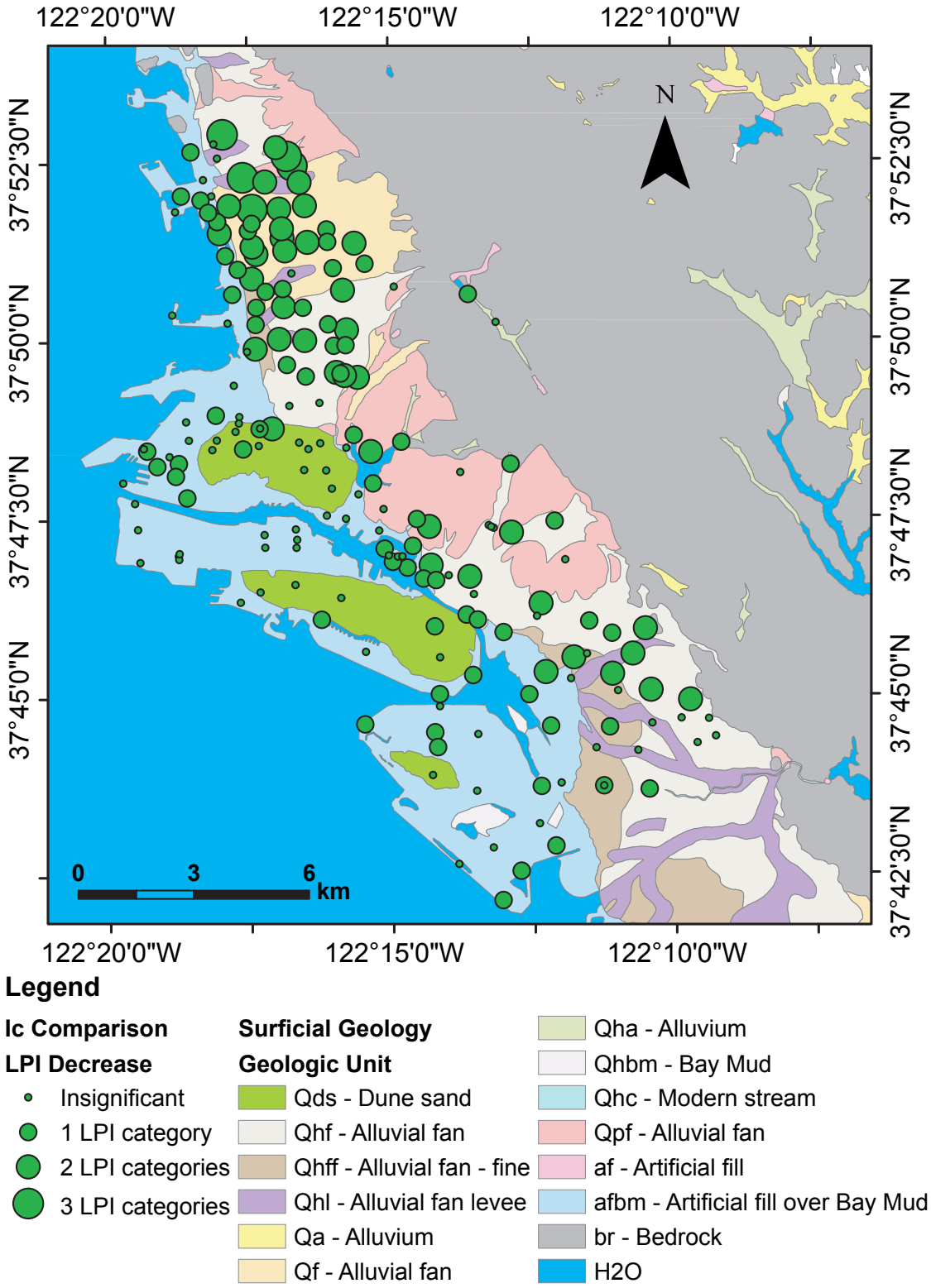


Fig. 7. CPT-based LPI values that would decrease if the Ic cutoff was decreased to 2.4 from 2.6. The size of the points indicates how many LPI categories the profile changed (e.g. a value of 3 LPI categories indicates the LPI decreased from a Very High or High liquefaction potential category to a Low or Non-liquefiable category).

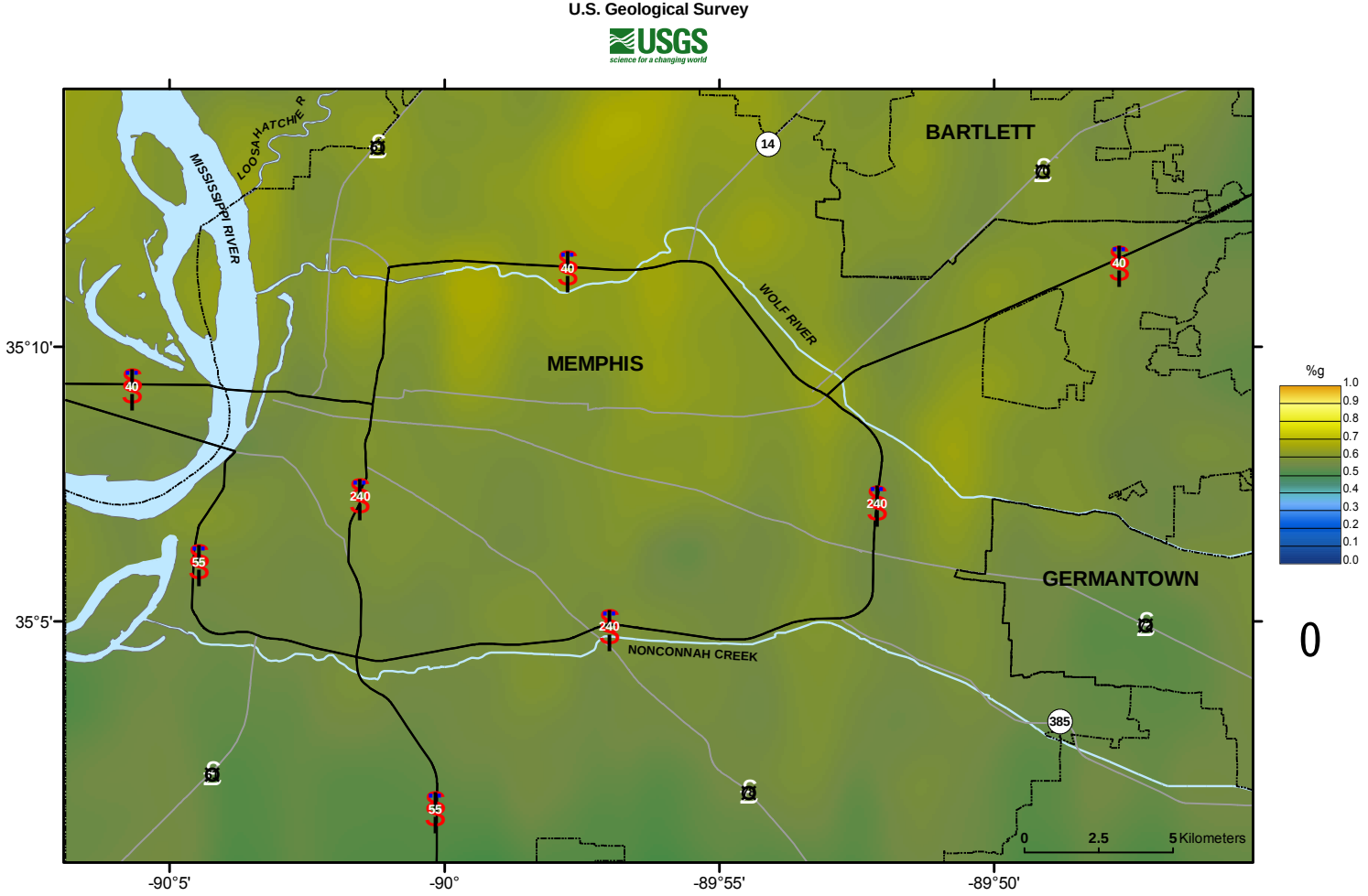


Fig. 8. Results of the PSHA for the Shelby County, TN region. Modified from the USGS urban seismic hazard maps.

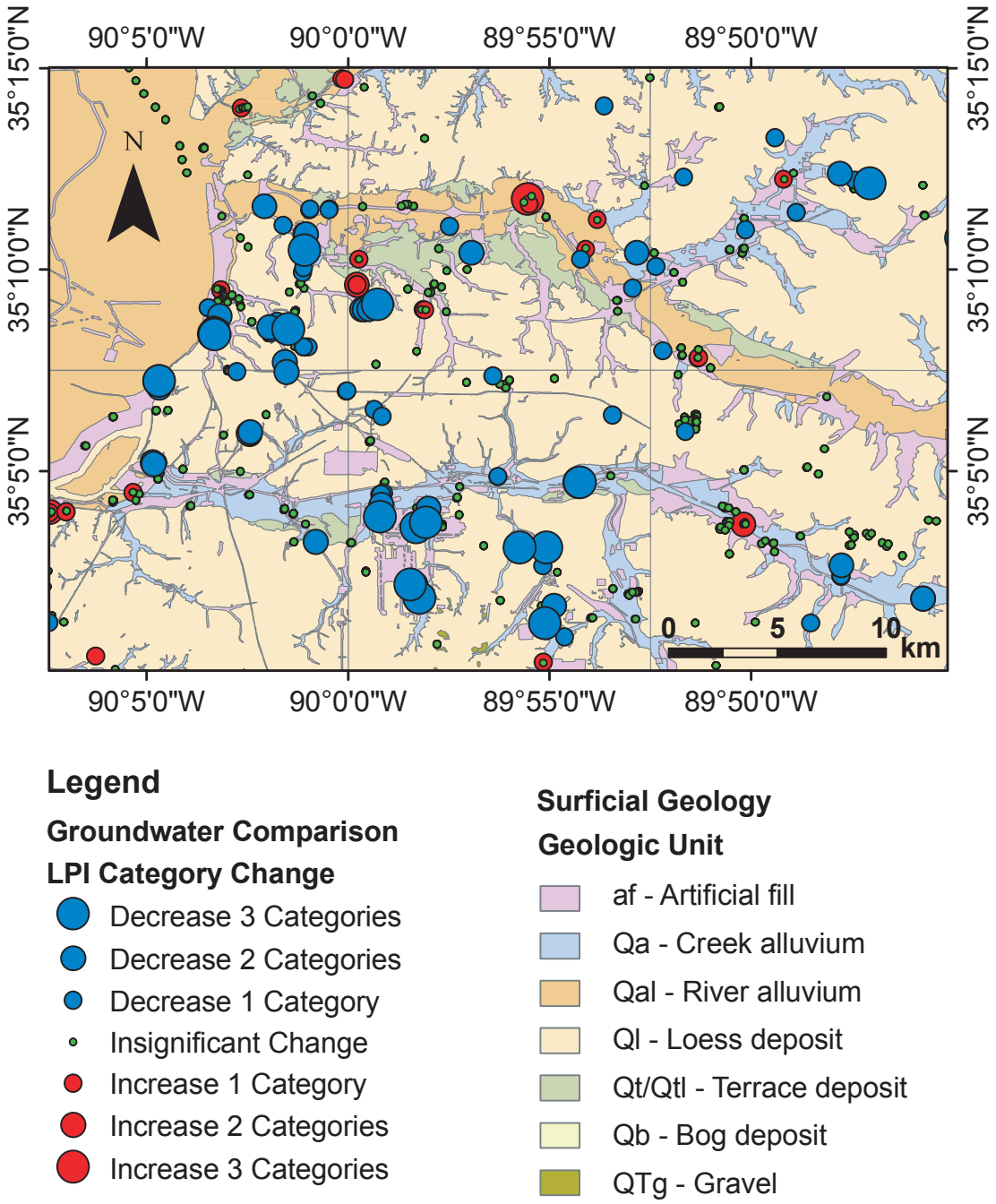


Fig. 9. Change in SPT-based LPI categories in Shelby County, TN between current groundwater levels and an average groundwater level of 6 m. The size of the points indicates how many LPI categories the profile changed.

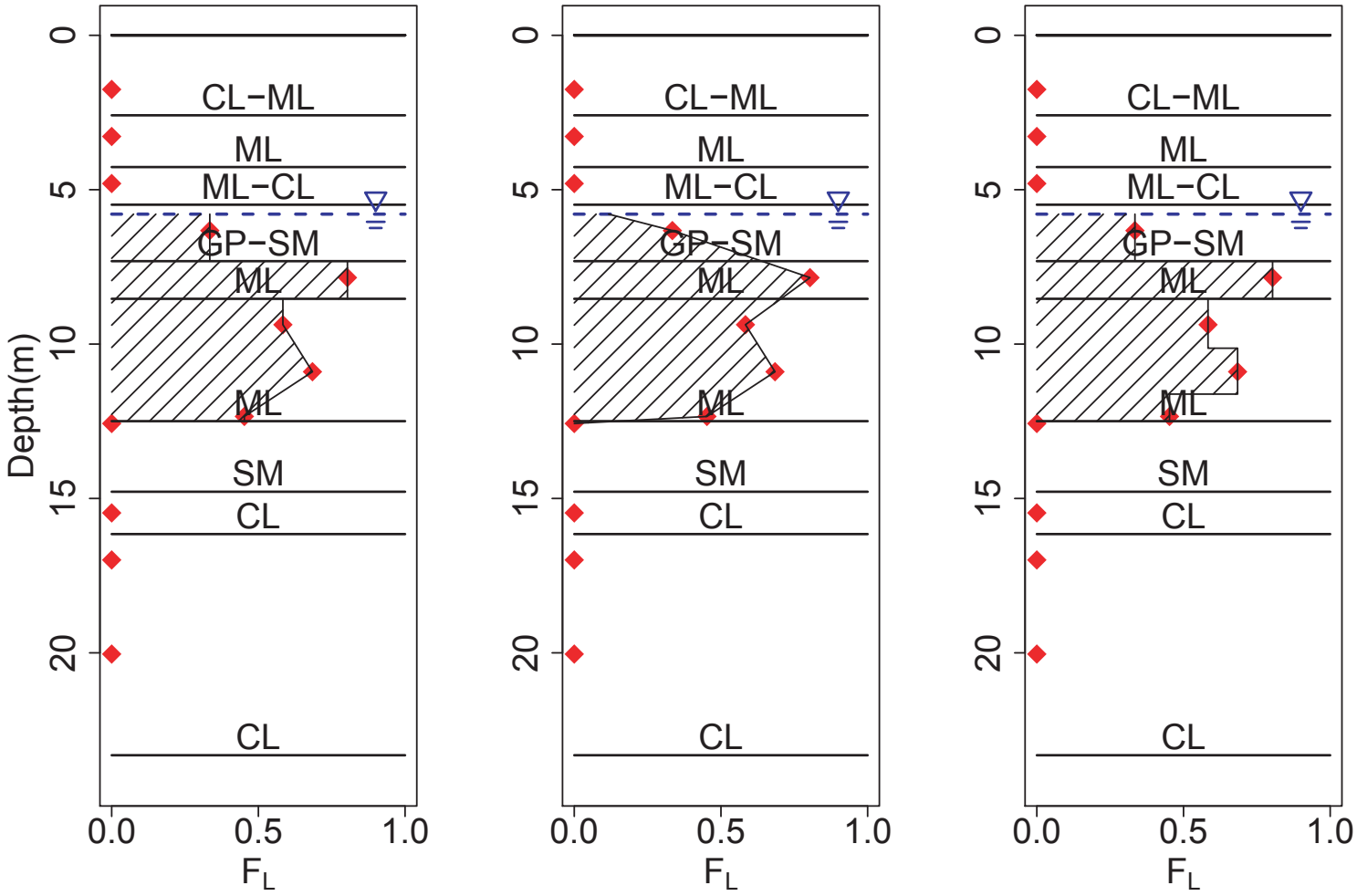


Fig. 10. Examples of integration techniques for a SPT-based LPI value. The case on the left is what we use and assumes each lithologic layer is distict and FL values cannot be interpolated between layers.

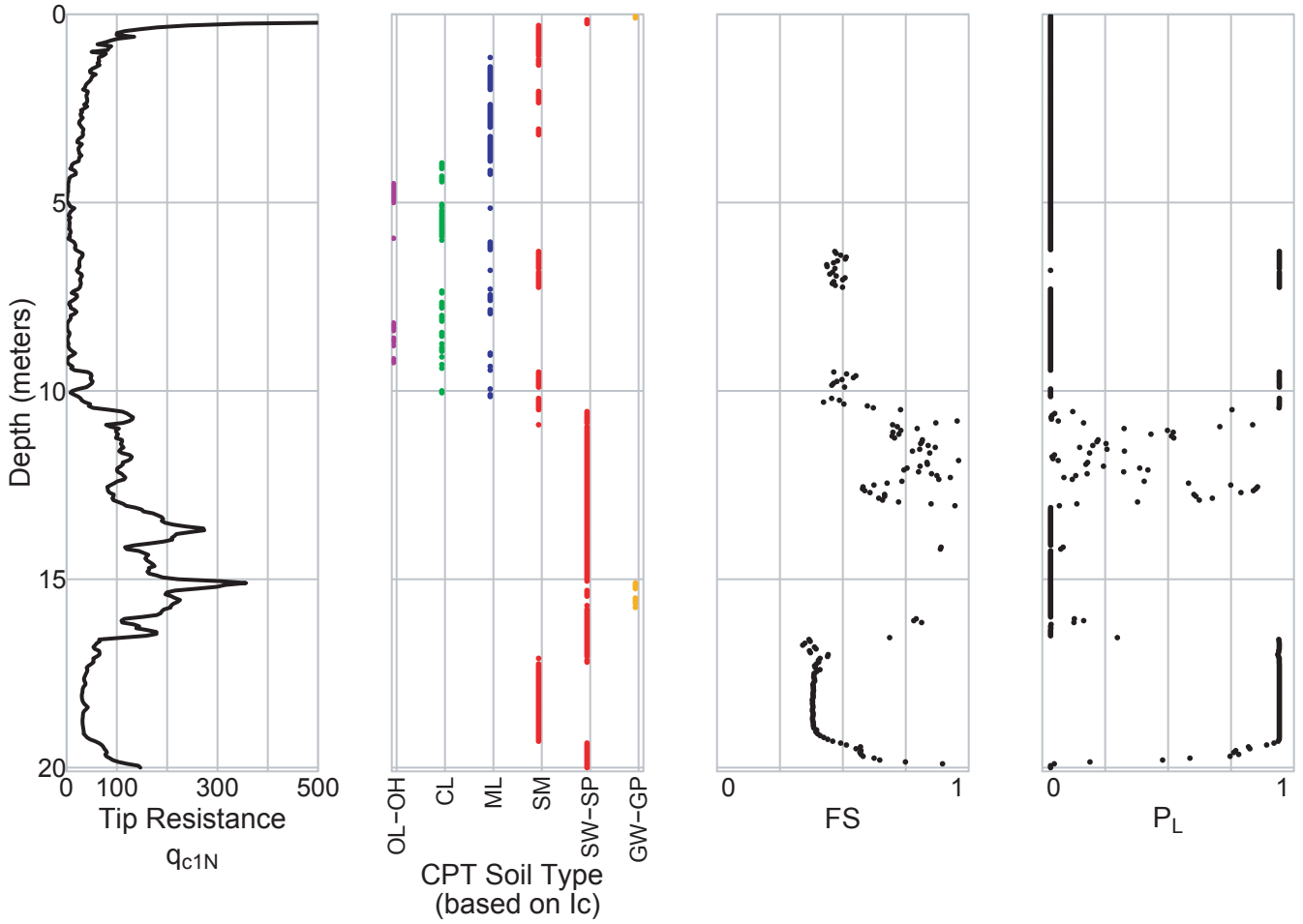


Fig. 11. Example of a CPT profile from the Oakland, CA area showing from left to right, normalized tip resistance, soil behavior based on Ic, factor of safety, and probability of liquefaction. The CPT profiles is located within a Holocene alluvium geologic unit, with a groundwater level at 5.6 m, and a calculated LPI of 8.6.

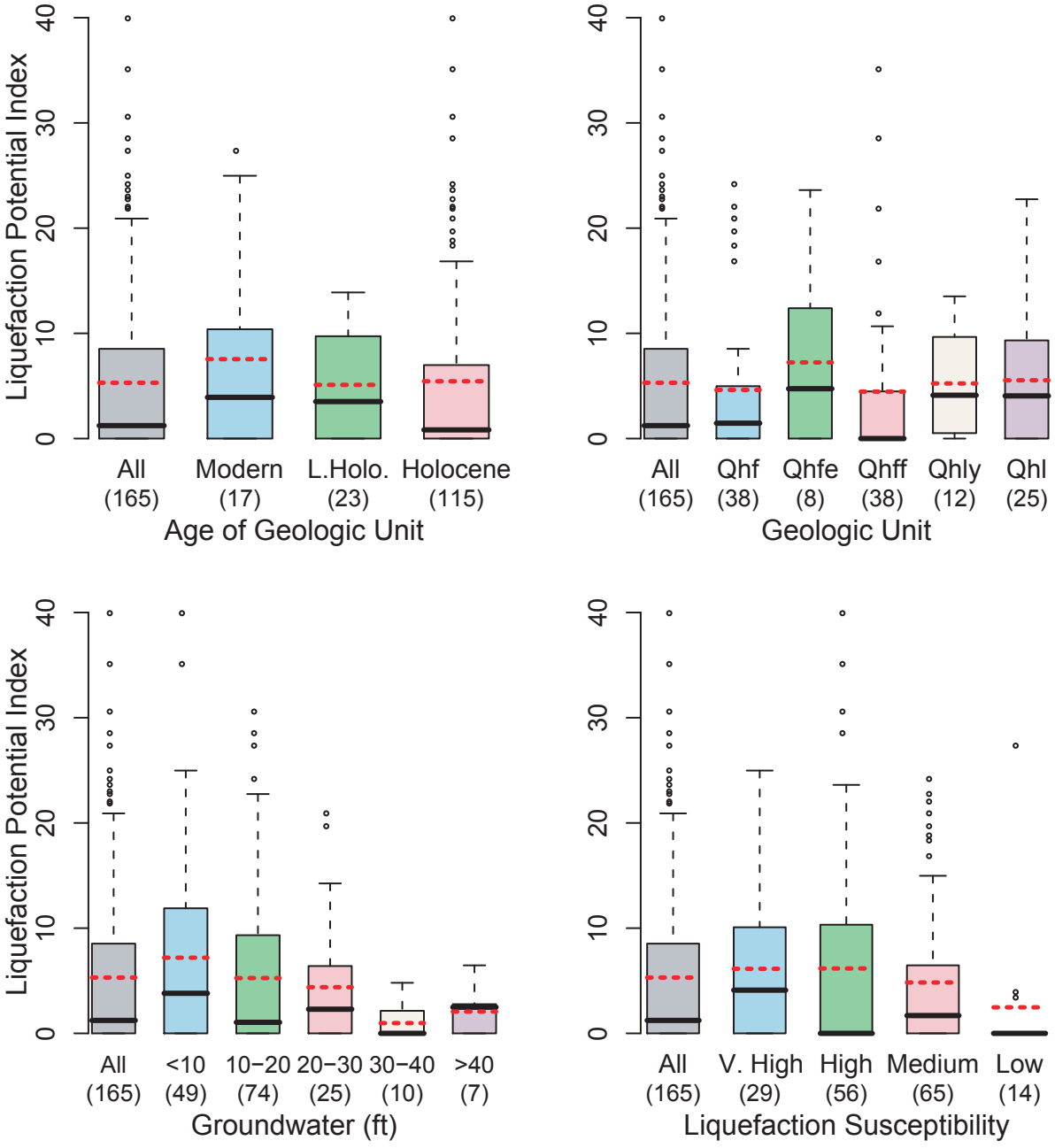


Fig. 12. Liquefaction potential determined from geotechnical data (SPT) in the Southern San Francisco Bay region sorted by 1) age of geologic unit, 2) geologic unit, 3) groundwater level, and 4) geologist interpreted liquefaction susceptibility (Knudsen et al., 2000).

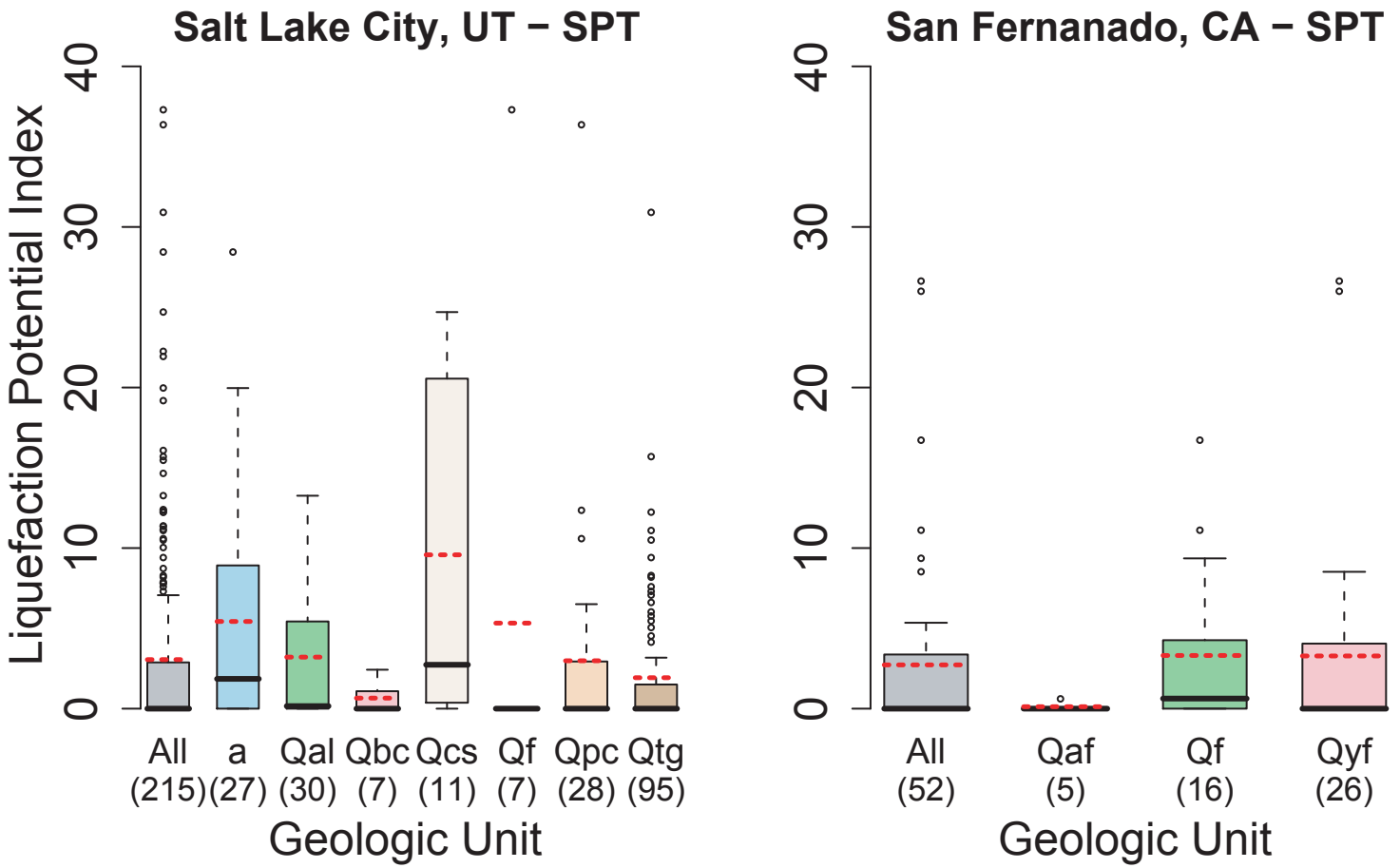


Fig. 13. Variability of SPT-based LPI values within regional geologic units in Salt Lake City, UT and San Fernando, CA.

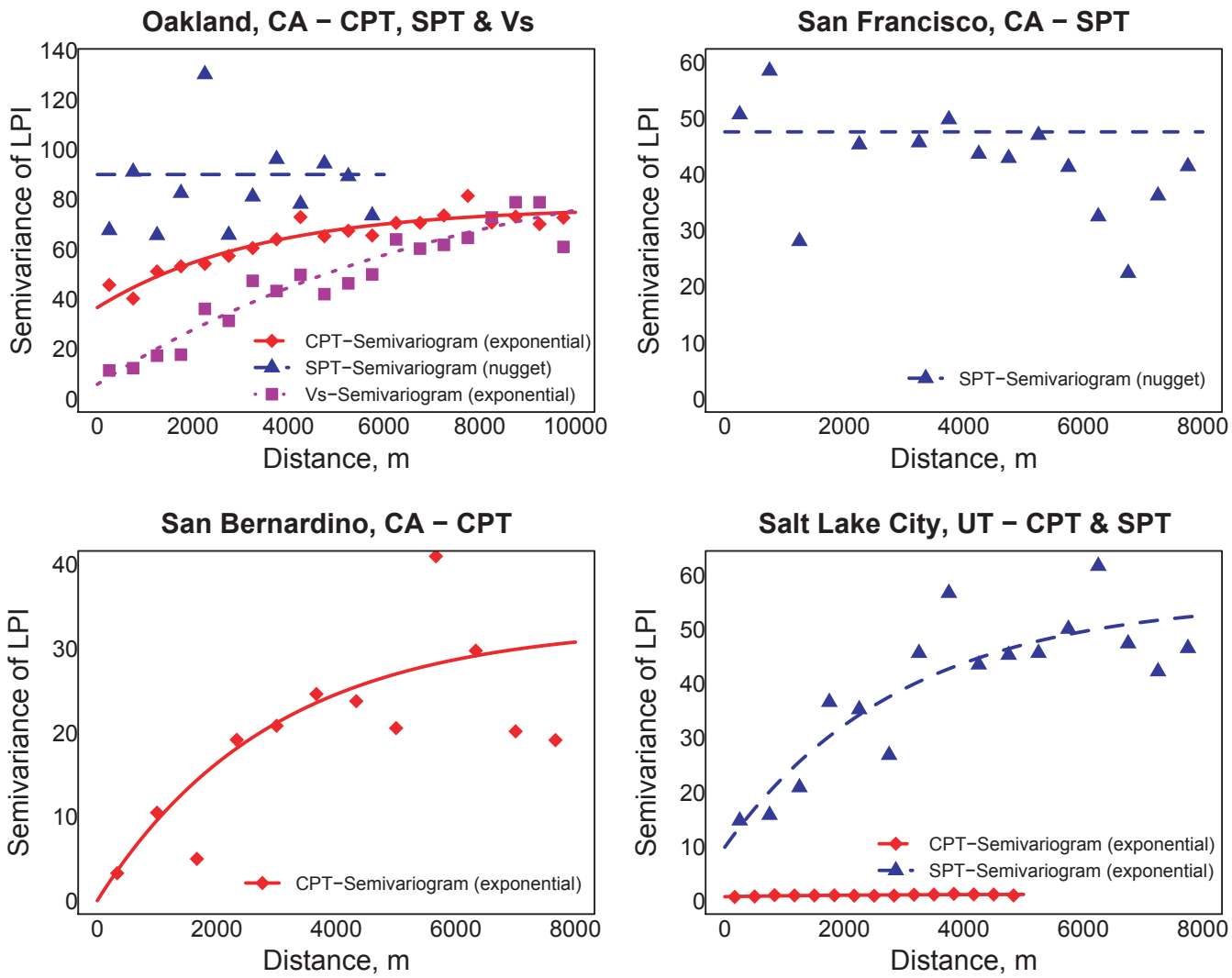


Fig. 14. Estimated semivariograms at four sites showing the empirical data (point values) and model semivariograms. The chosen model semivariogram is noted for each database.

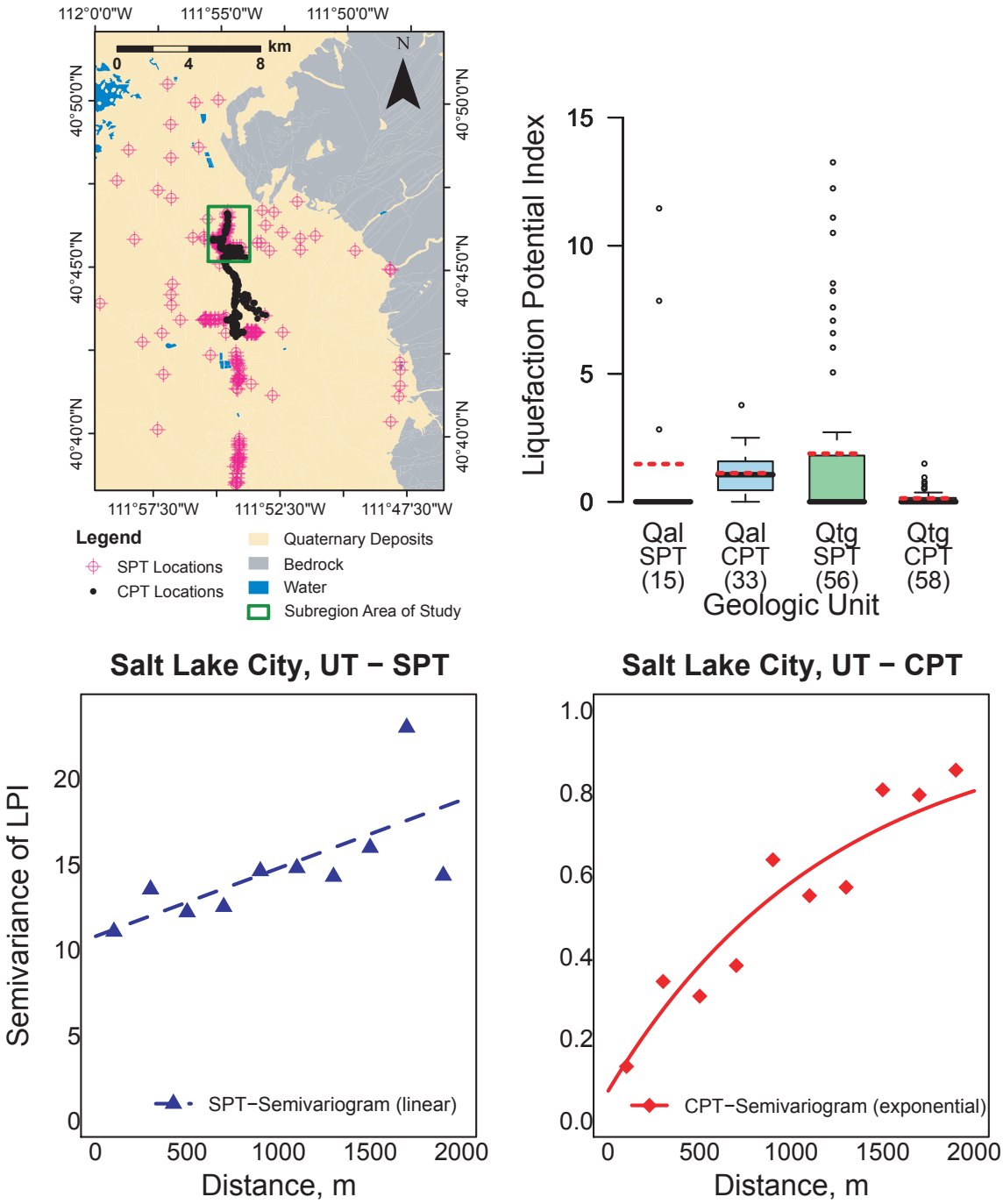


Fig. 15. LPI distributions by geologic unit and semivariograms of both SPT and CPT data within a subregion of the Salt Lake City, UT site.

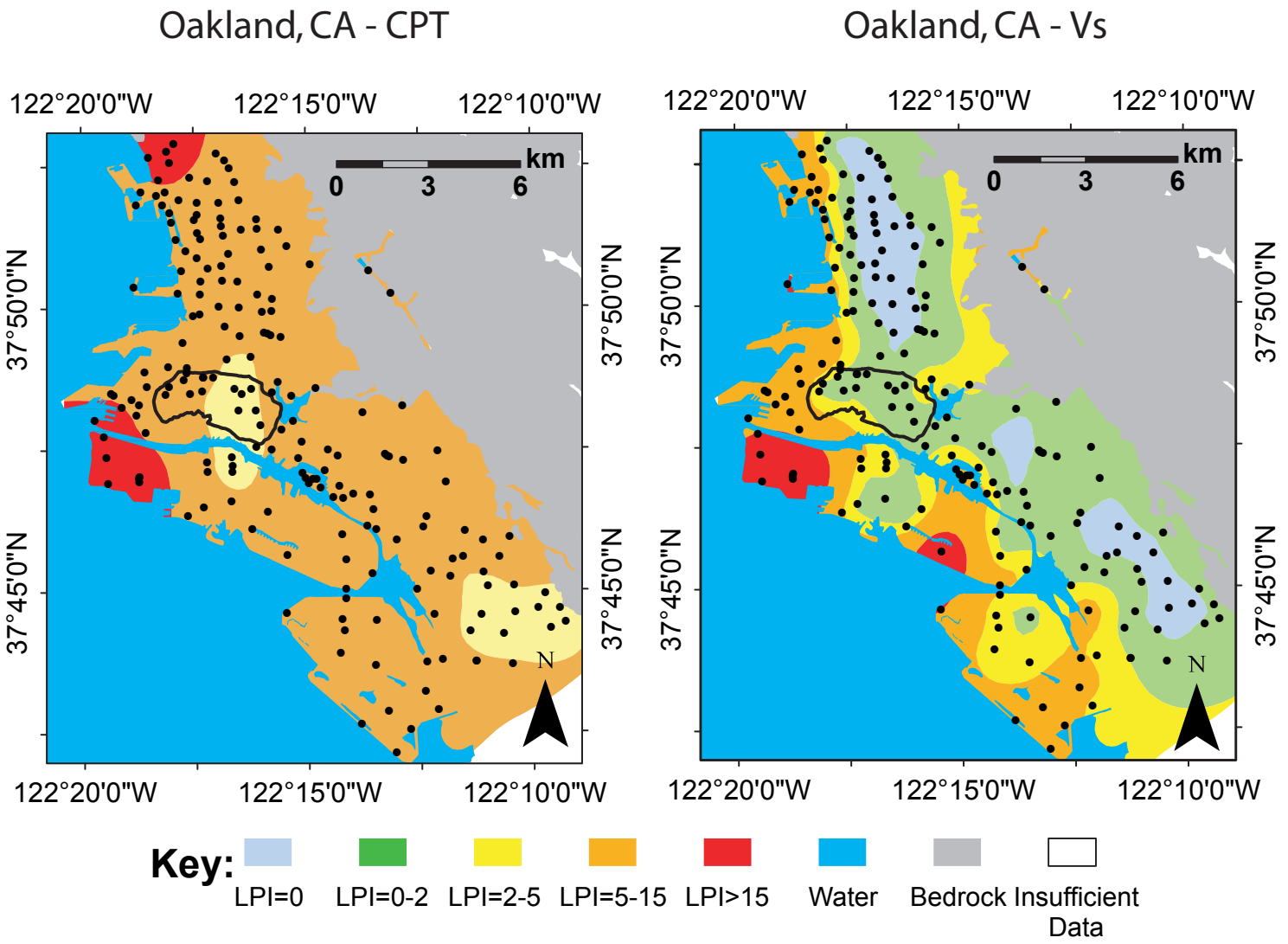


Fig. 16. Ordinary kriging results for CPT- and Vs-based LPI in the Oakland, CA area. Interpolated values are only shown when the estimate variance is lower than the population variance. The latest Pleistocene to Holocene dune sand geologic unit (Qds) outlined on this map is shown in more detail in Fig. 19.

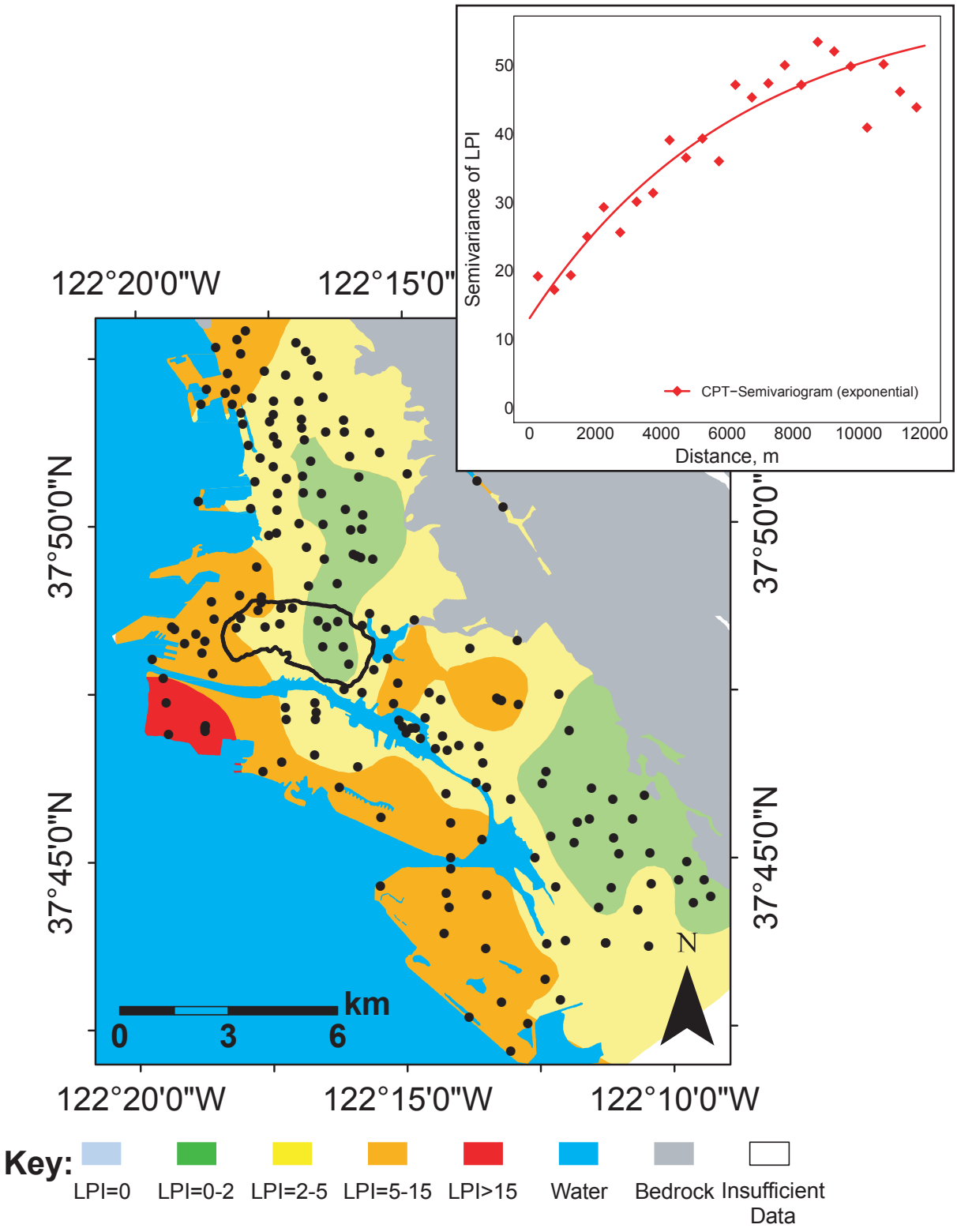


Fig. 17. Ordinary kriging results for CPT-based LPI in the Oakland, CA area using an Ic cutoff value of 2.4 instead of 2.6 as seen in Fig. 17. The inset figure shows the empirical and model semivariogram for this data.

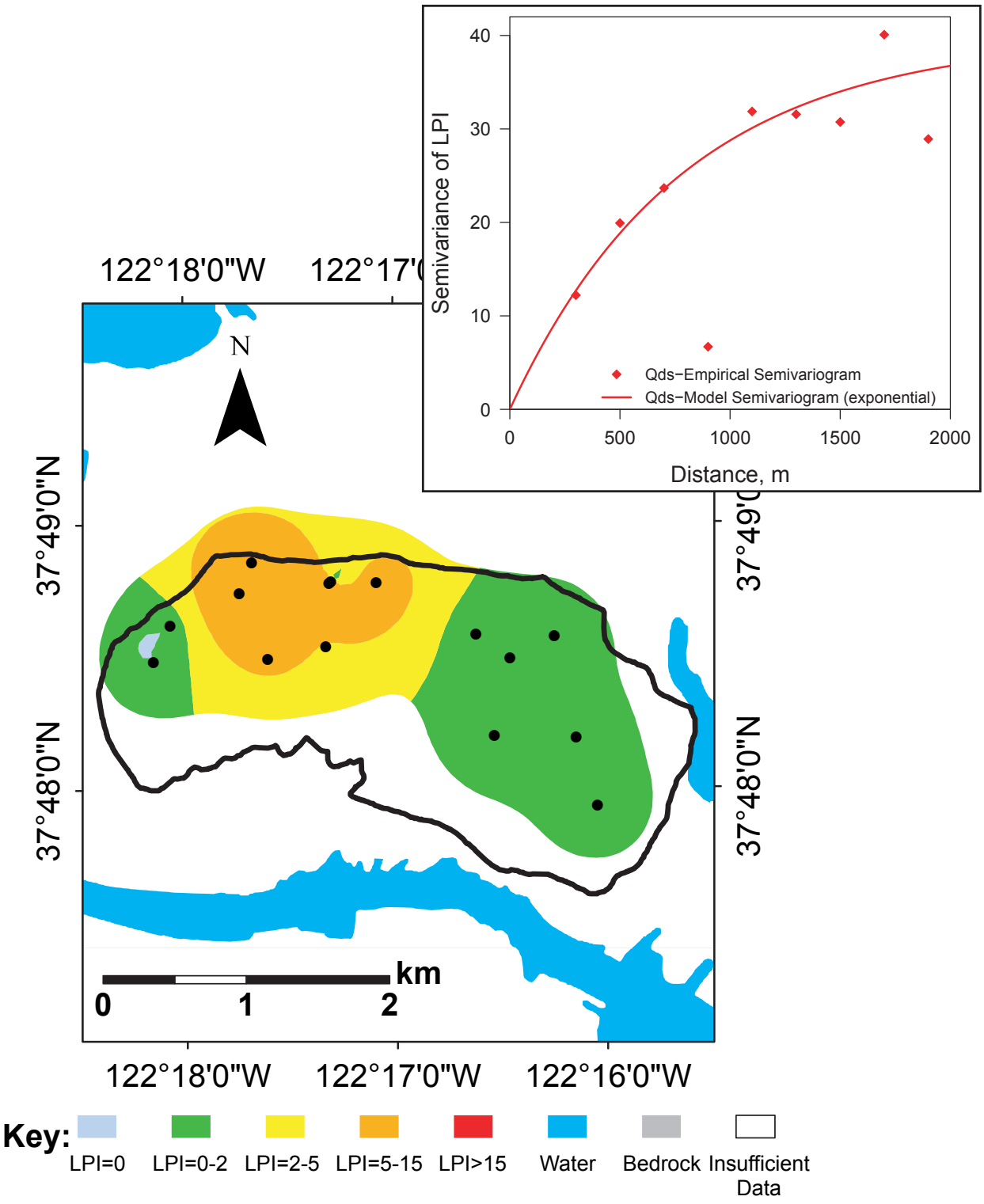


Fig. 18. Ordinary kriging results for CPT-based LPI using and Ic cutoff value of 2.6 within the distinct geologic unit Qds (shown as the black outline) for the Oakland, CA area.

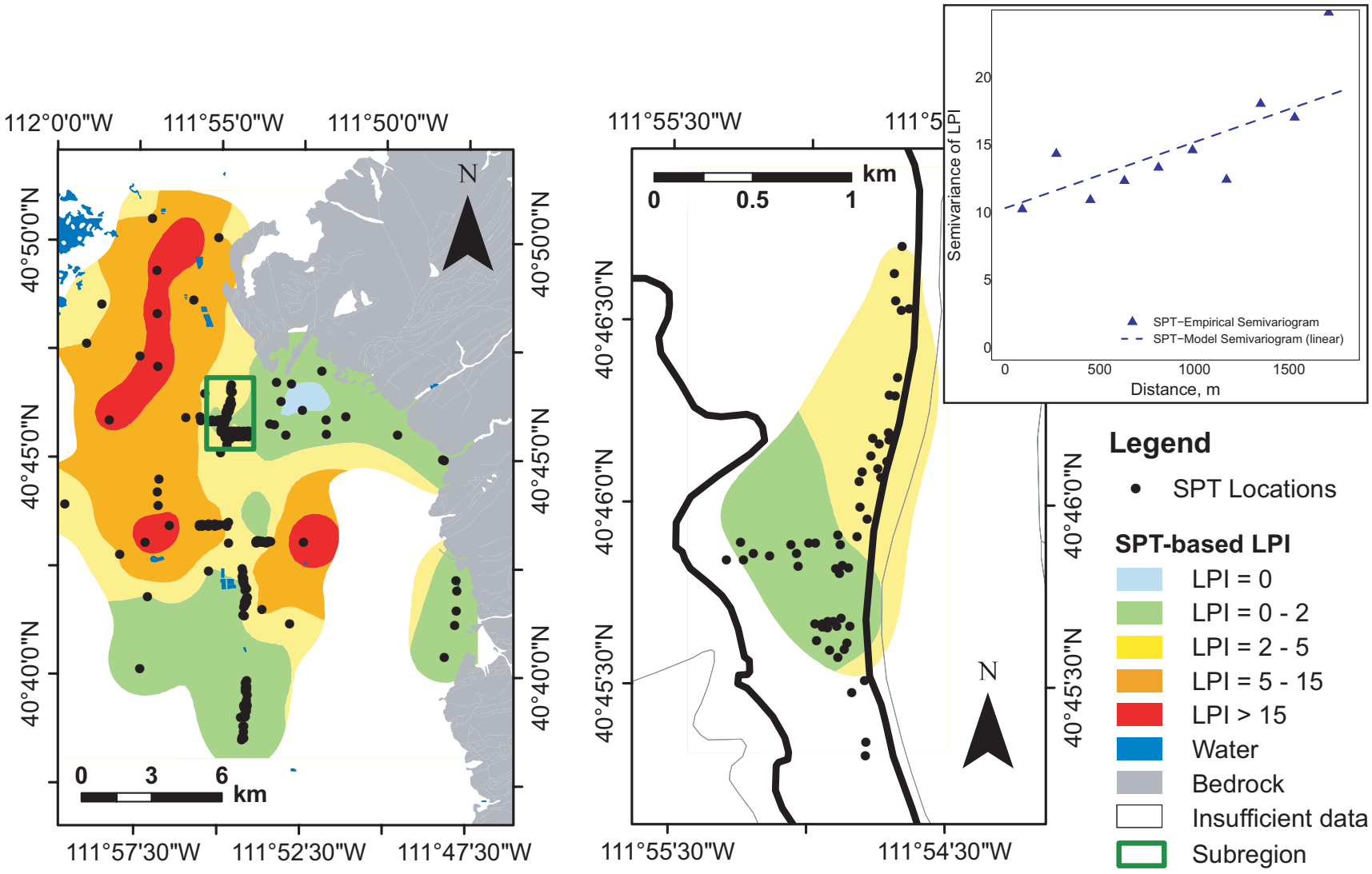


Fig. 19. Ordinary kriging results for SPT-based LPI for the entire Salt Lake City, UT site and a single geologic unit Qtg (Holocene and Pleistocene terrace gravels) from the area outlined in the full map. The inset figures shows the semivariogram for the Qtg geologic unit.

APPENDIX A

Oakland, CA

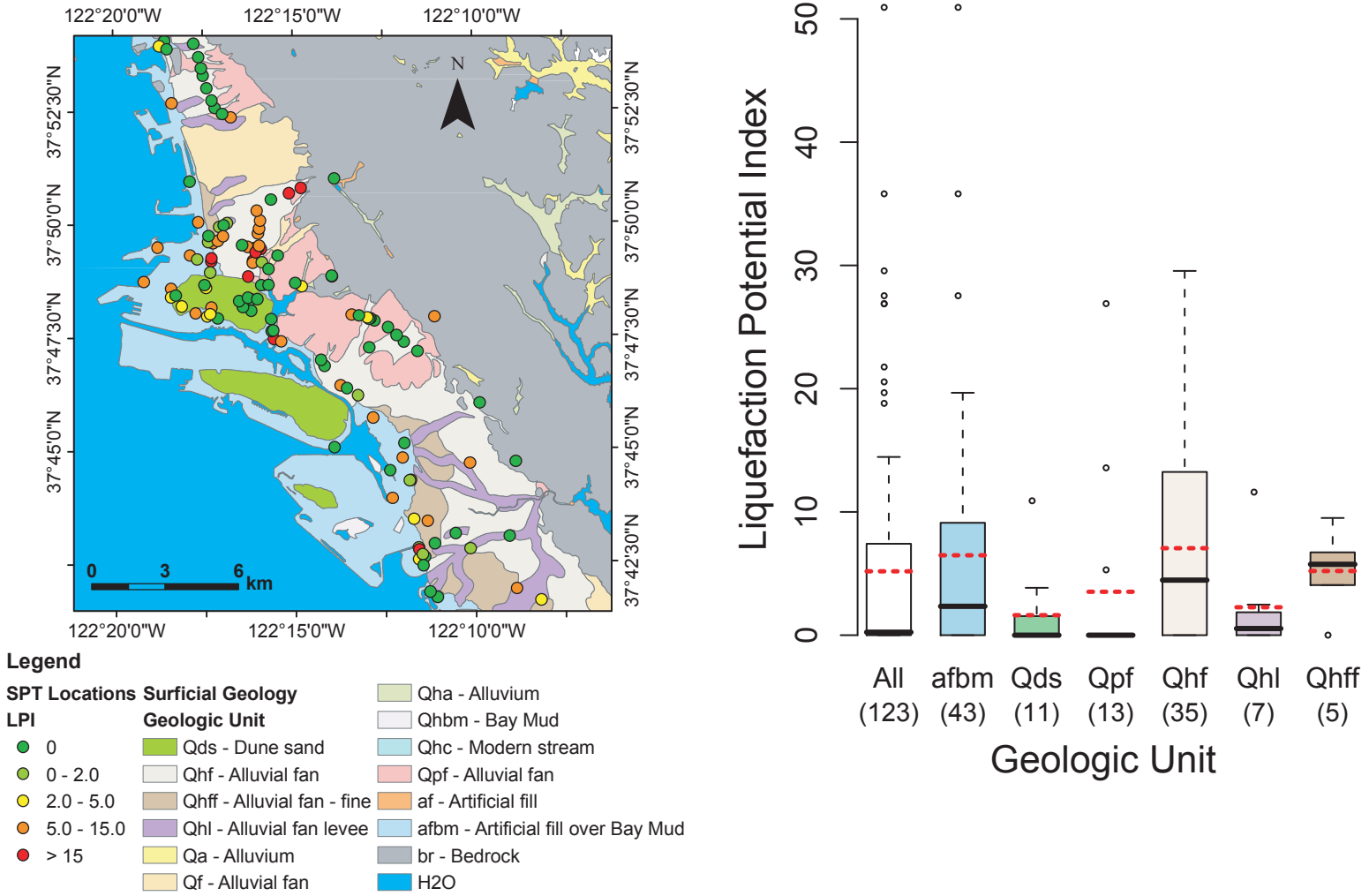


Fig. A.1. SPT-based LPI distributions by geologic unit

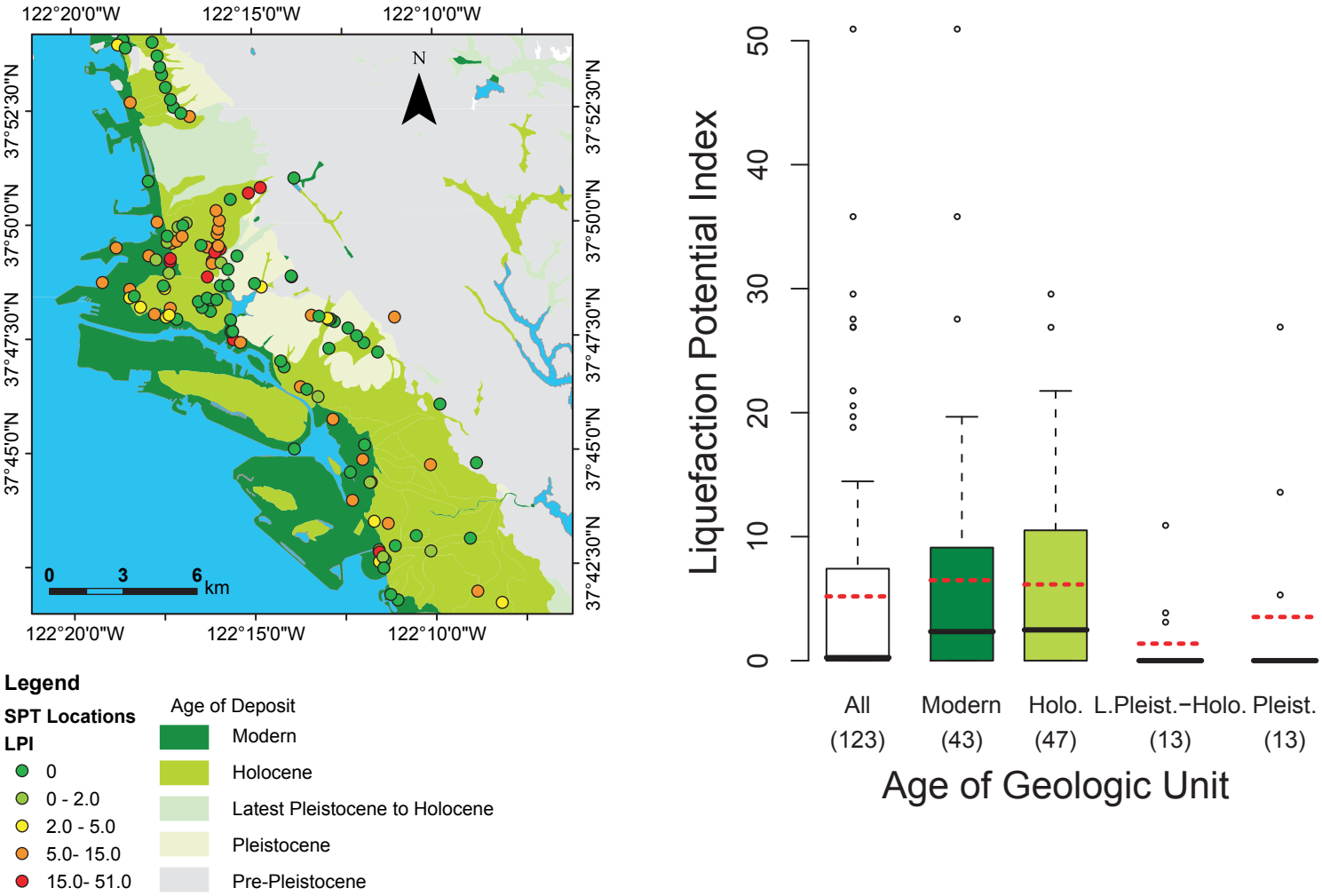


Fig. A.2. SPT-based LPI distributions by age of geologic unit

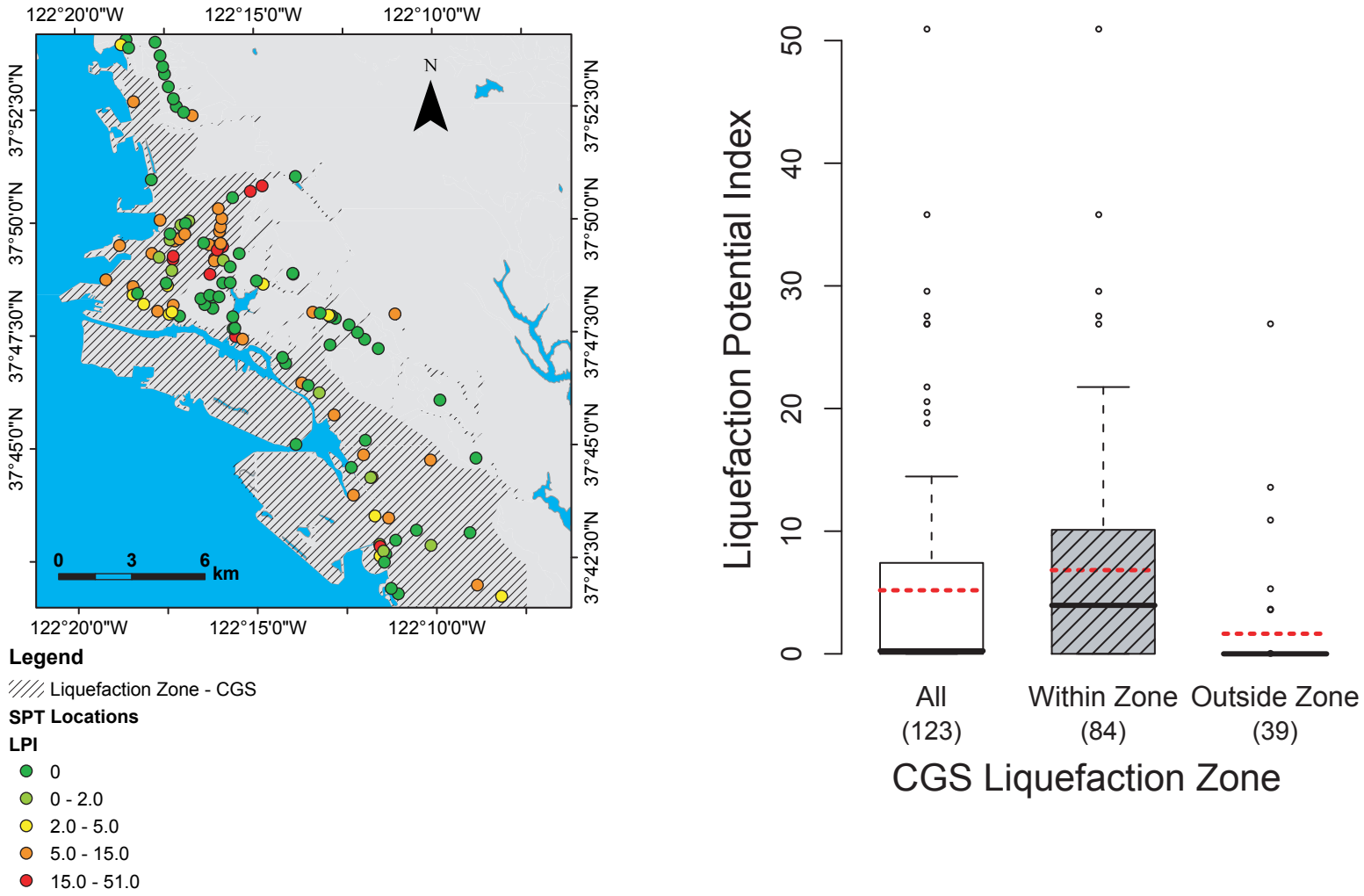


Fig. A.3. SPT-based LPI distributions by California Geological Survey Liquefaction Zone

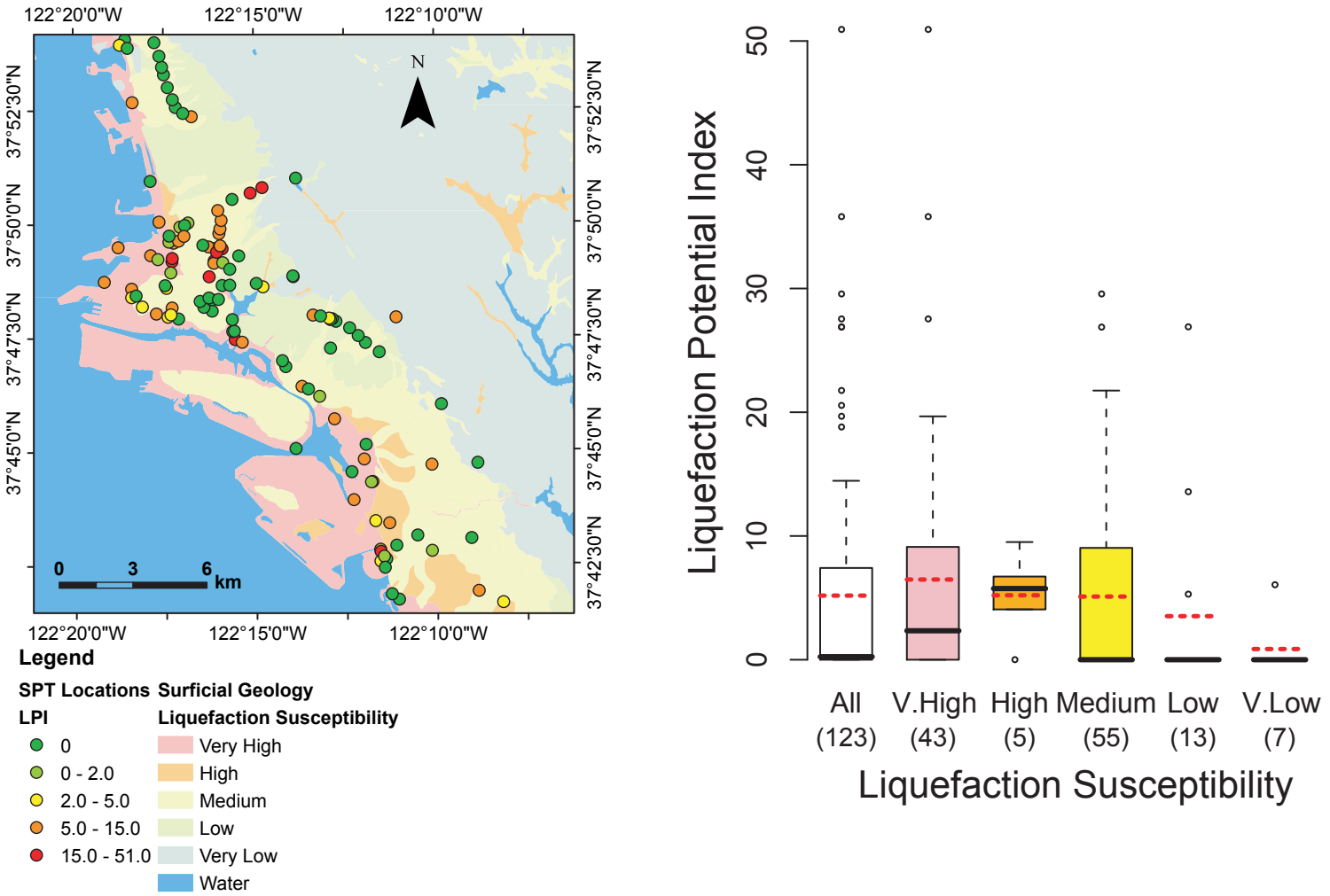


Fig. A.4. SPT-based LPI distributions by liquefaction susceptibility in the Knudsen et al. (2000) geologic maps

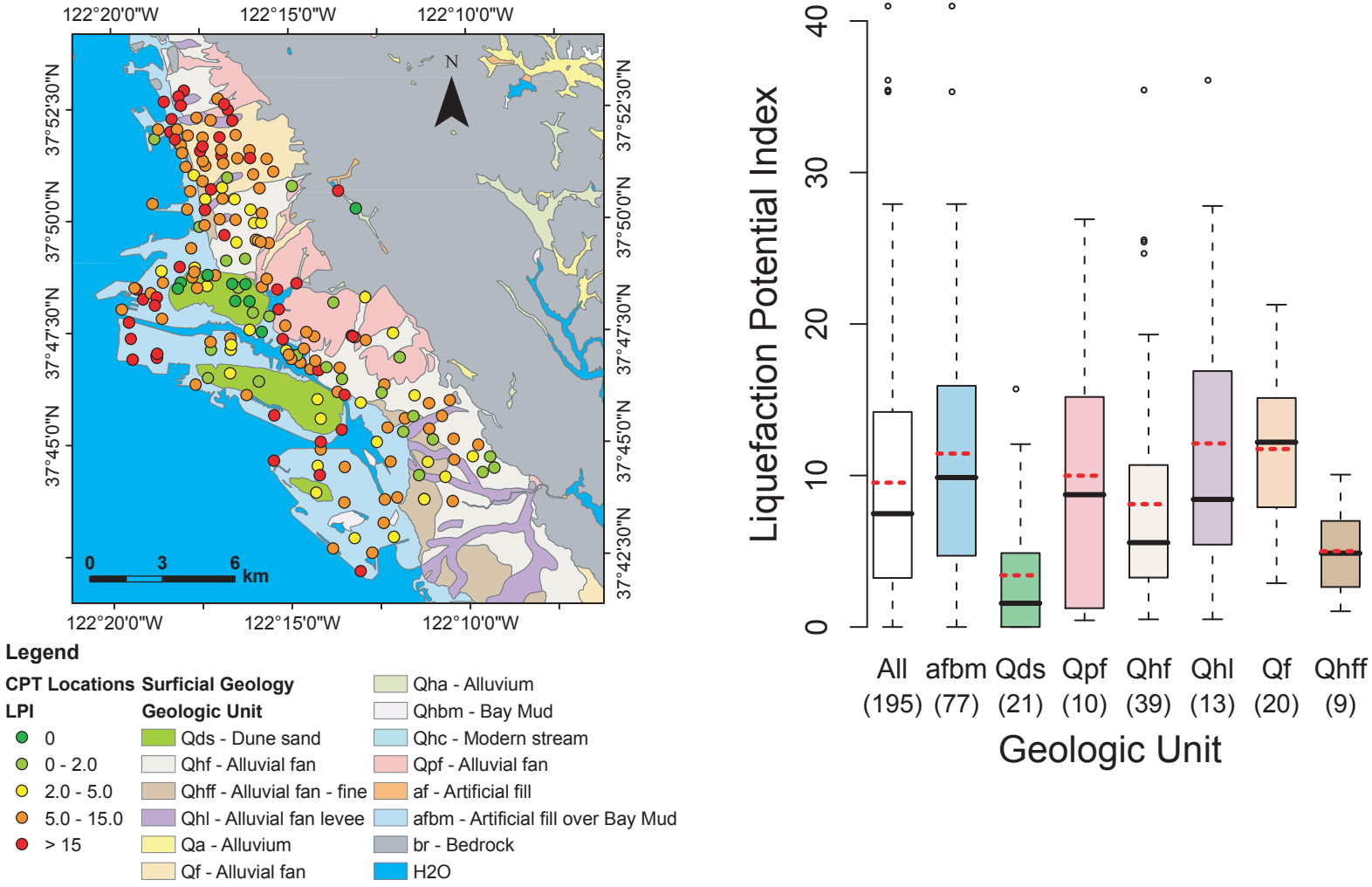


Fig. A.5. CPT-based LPI distributions by geologic unit

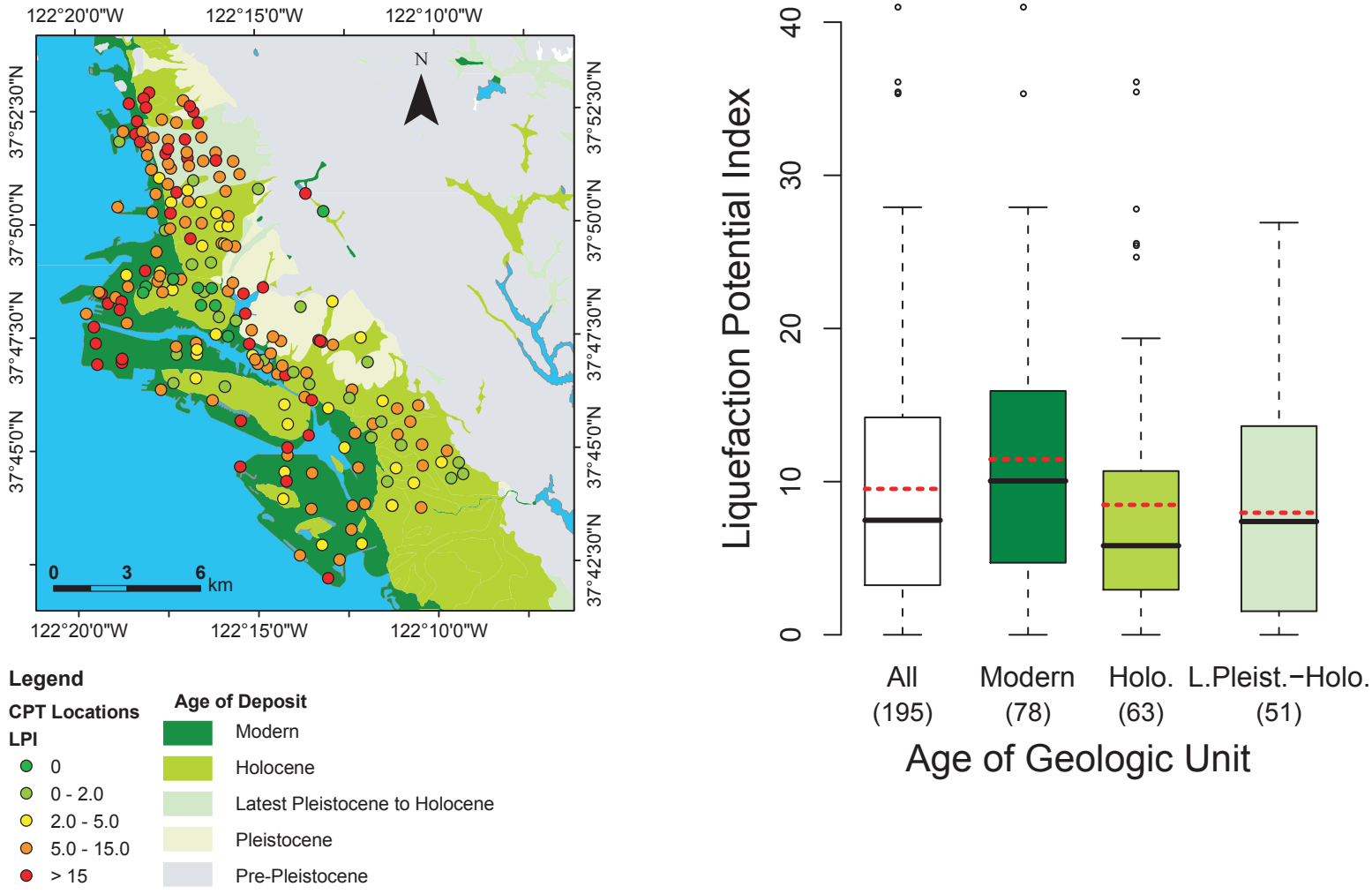


Fig. A.6. CPT-based LPI distributions by age of geologic unit

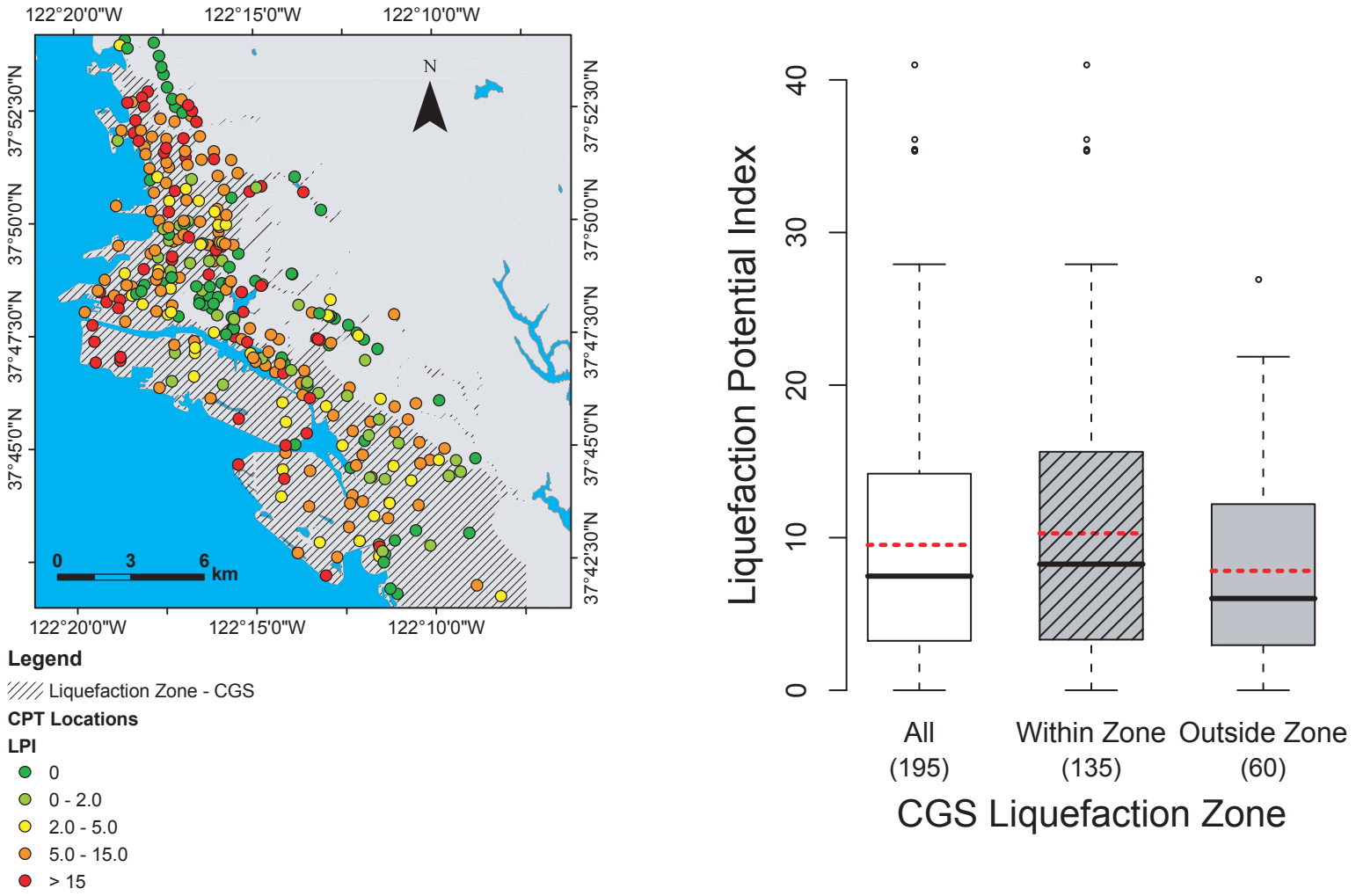


Fig. A.7. CPT-based LPI distributions by California Geological Survey Liquefaction Zone

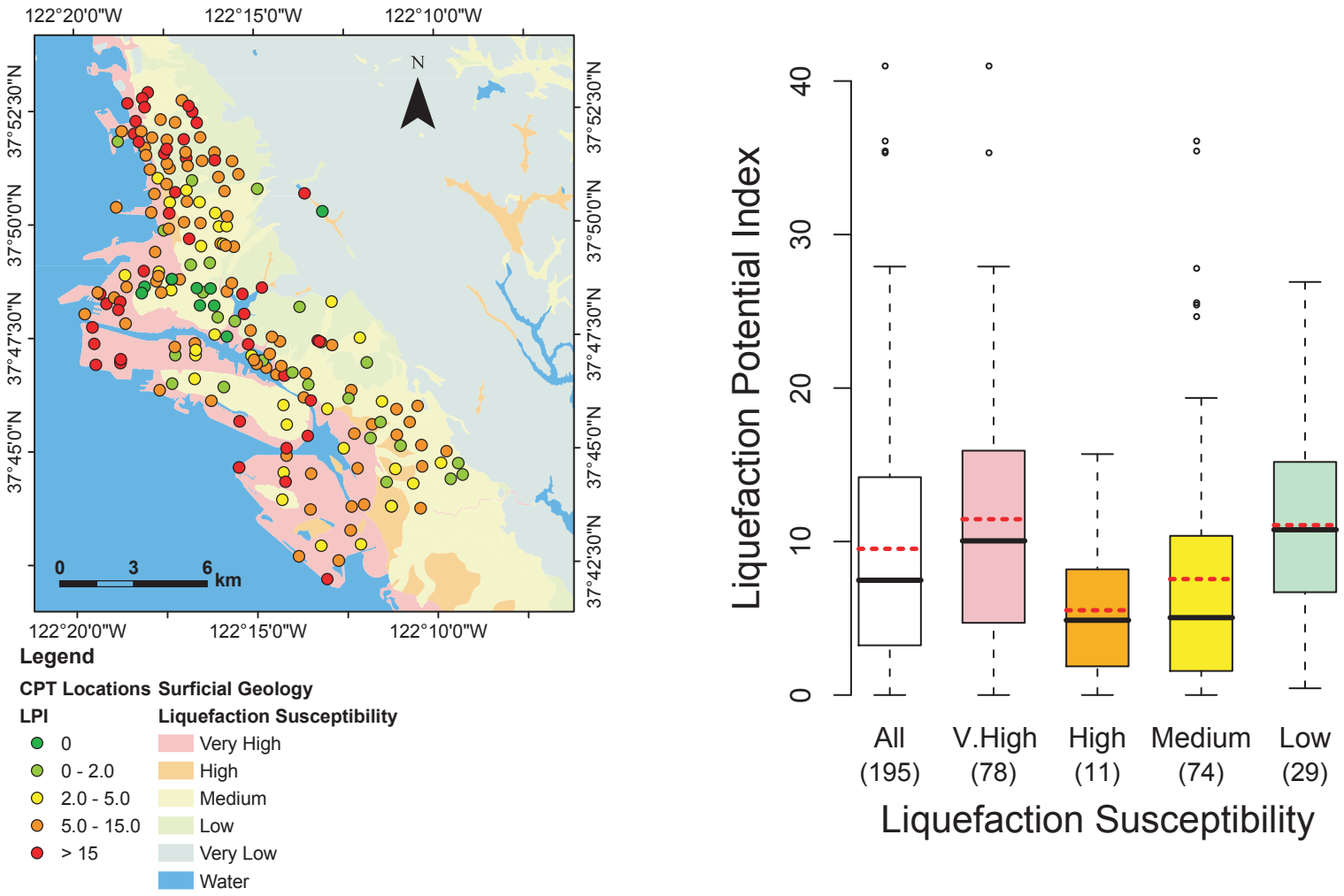


Fig. A.8. CPT-based LPI distributions by liquefaction susceptibility in the Knudsen et al. (2000) geologic maps

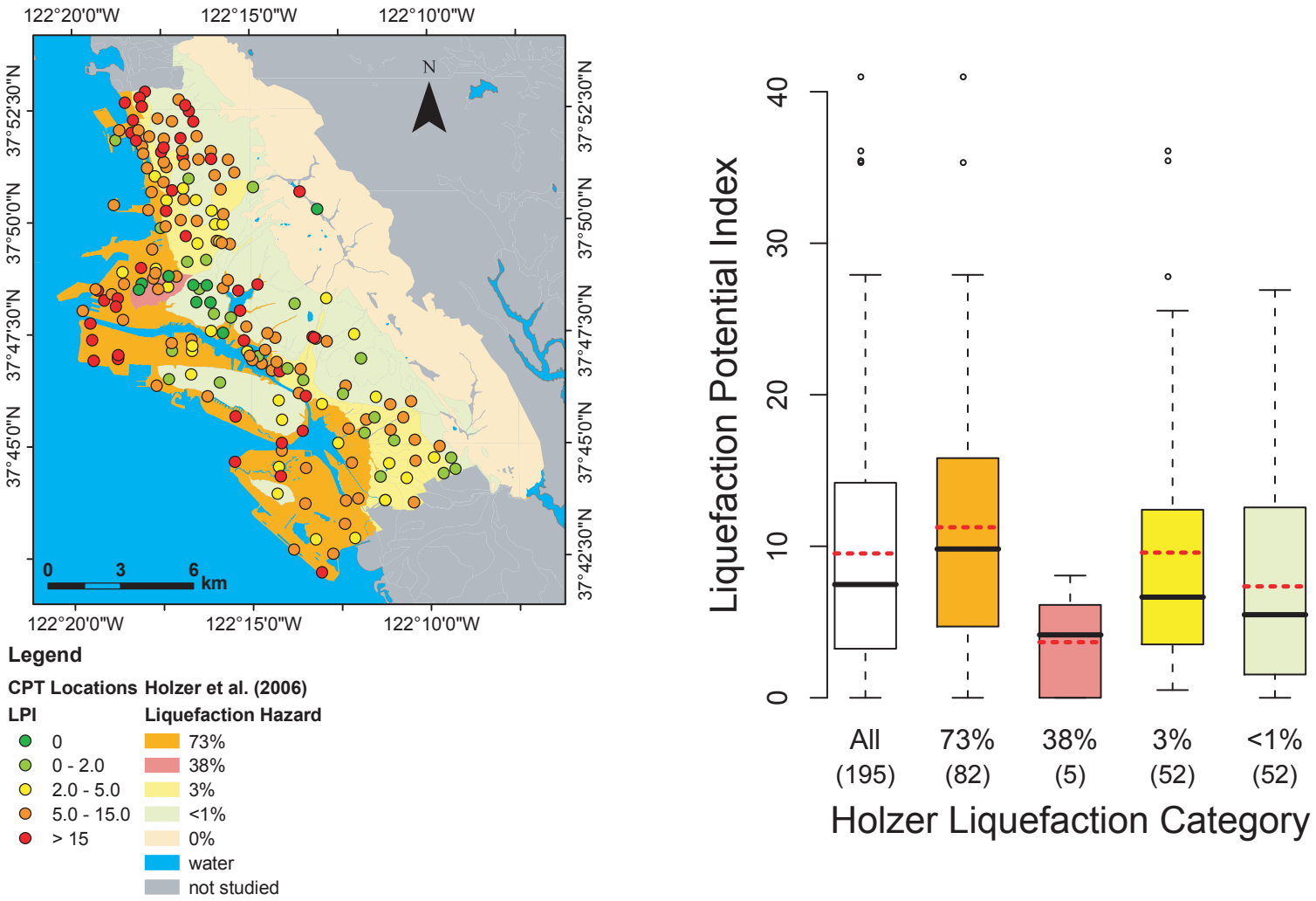


Fig. A.9. CPT-based LPI distributions by liquefaction hazard from the Holzer et al. (2006) maps

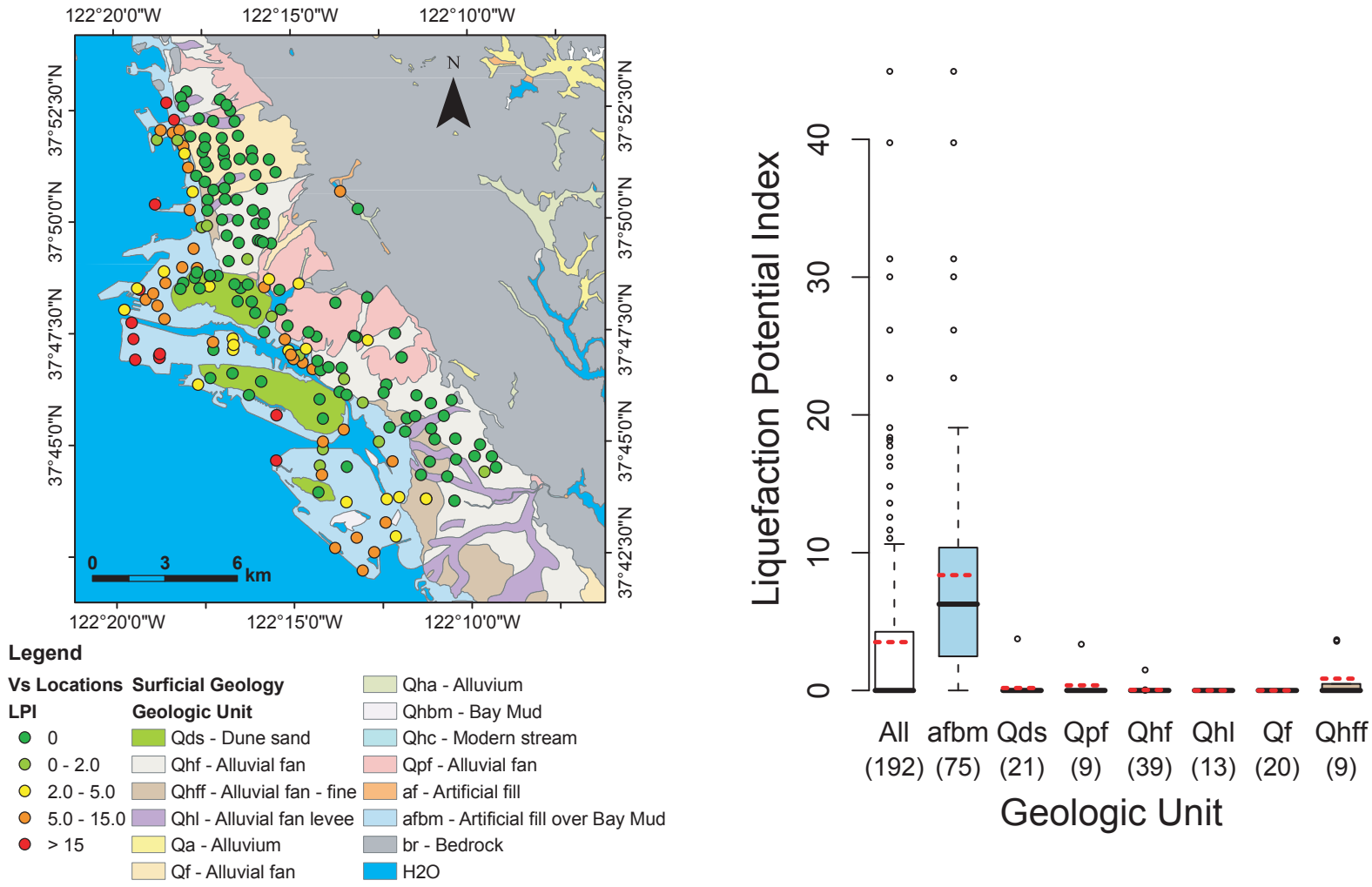


Fig. A.10. Vs-based LPI distributions by geologic unit

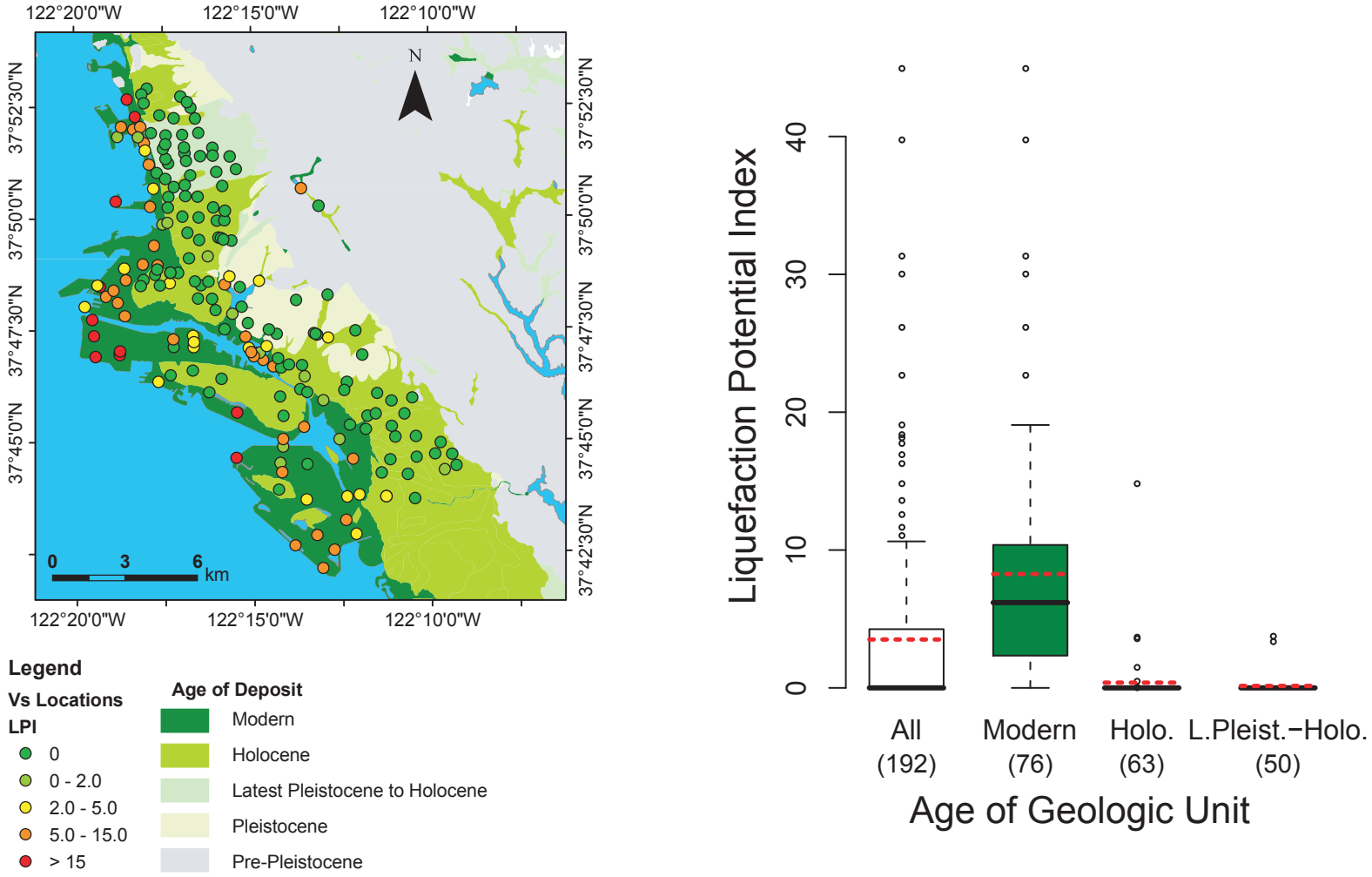


Fig. A.11. Vs-based LPI distributions by age of geologic unit

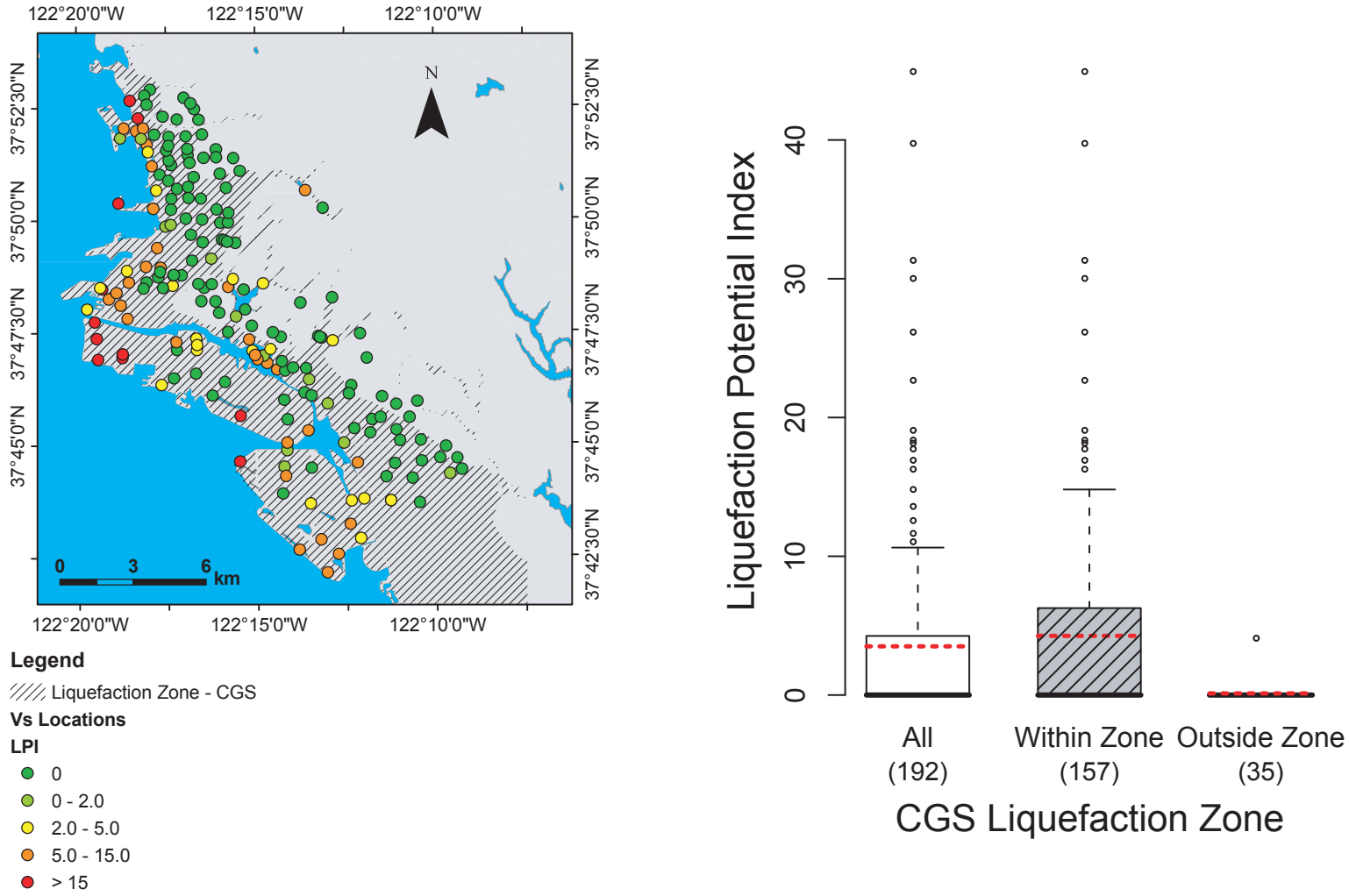


Fig. A.12. Vs-based LPI distributions by California Geological Survey Liquefaction Zone

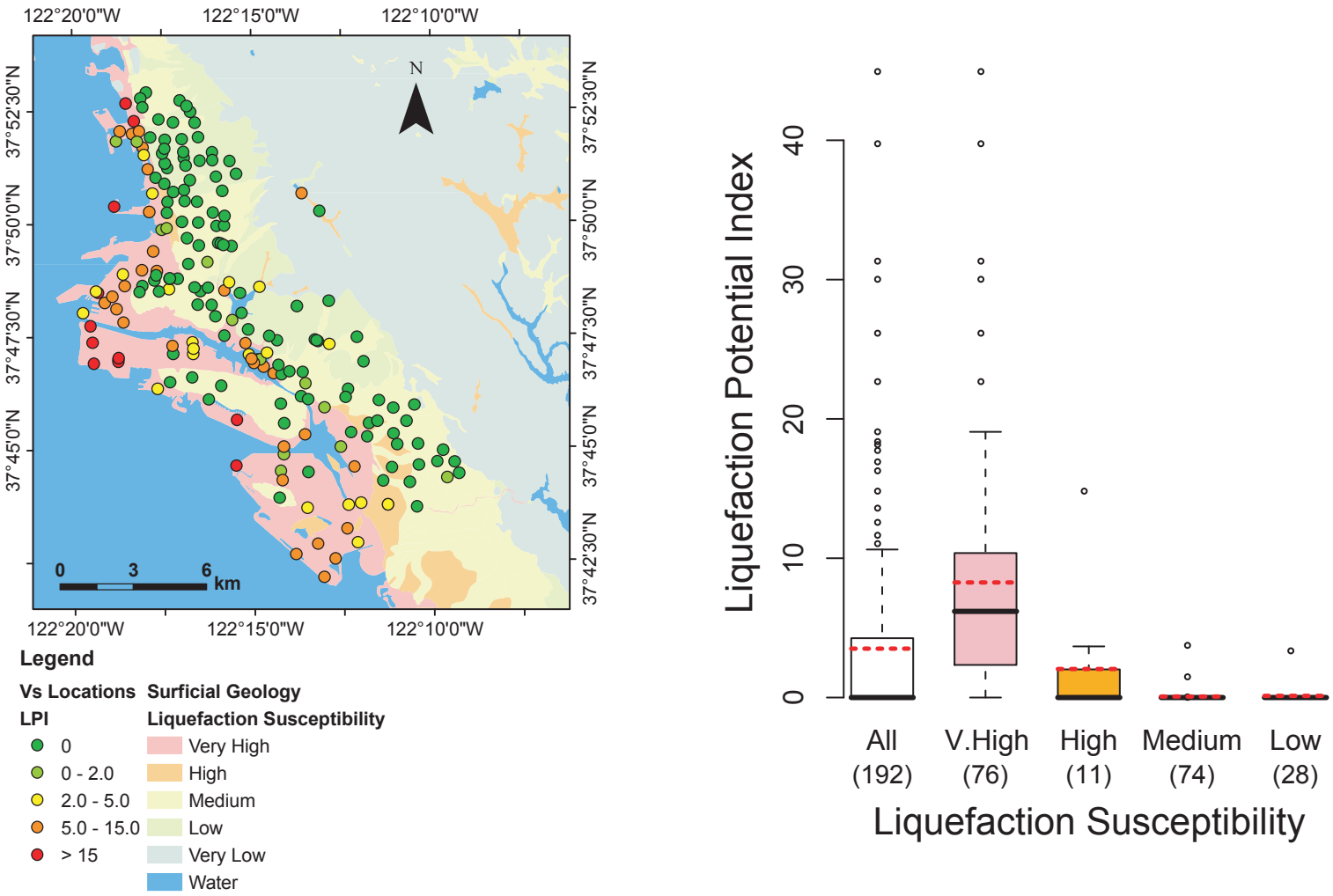


Fig. A.13. Vs-based LPI distributions by liquefaction susceptibility in the Knudsen et al. (2000) geologic maps

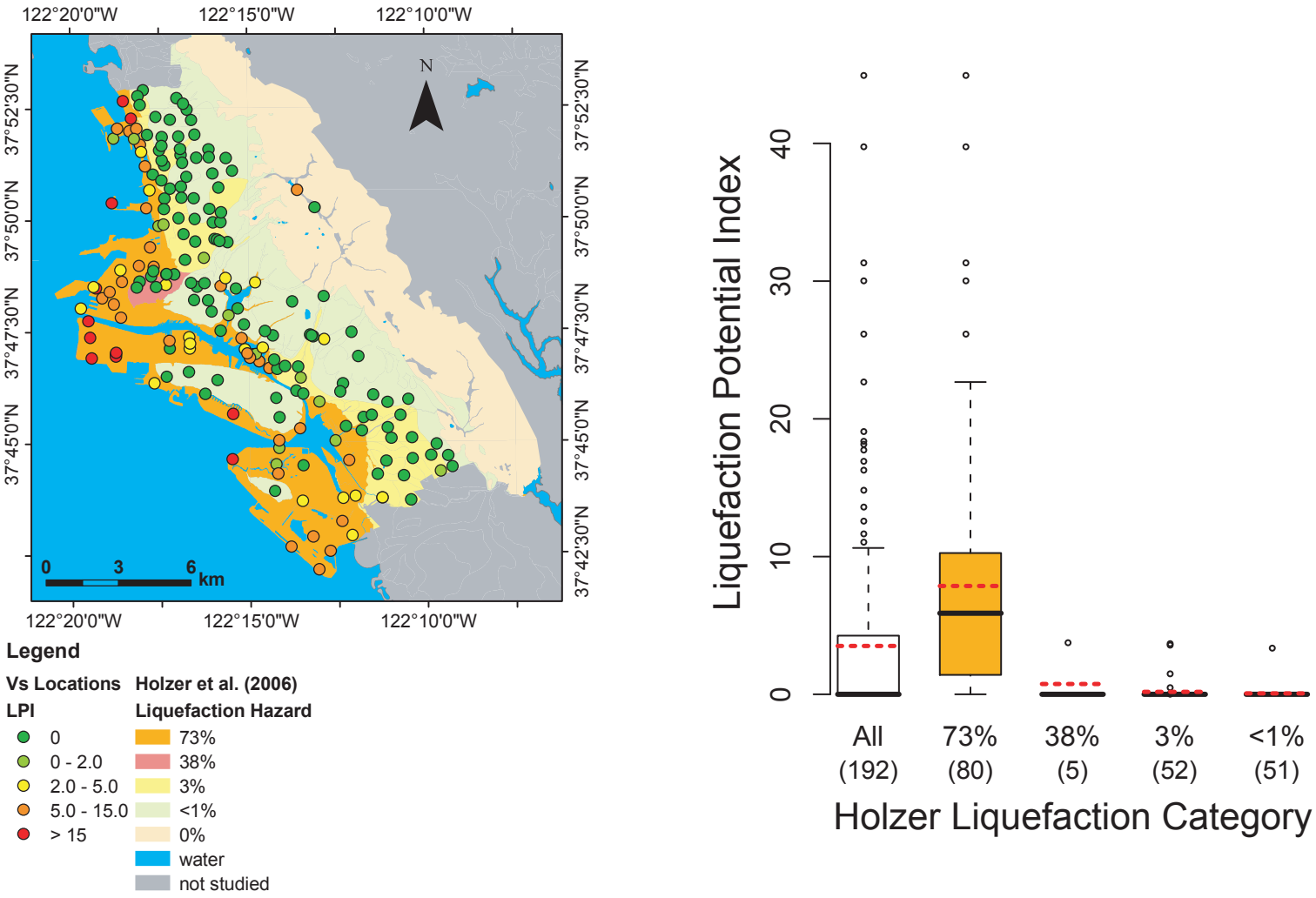


Fig. A.14. Vs-based LPI distributions by liquefaction hazard from the Holzer et al. (2006) maps

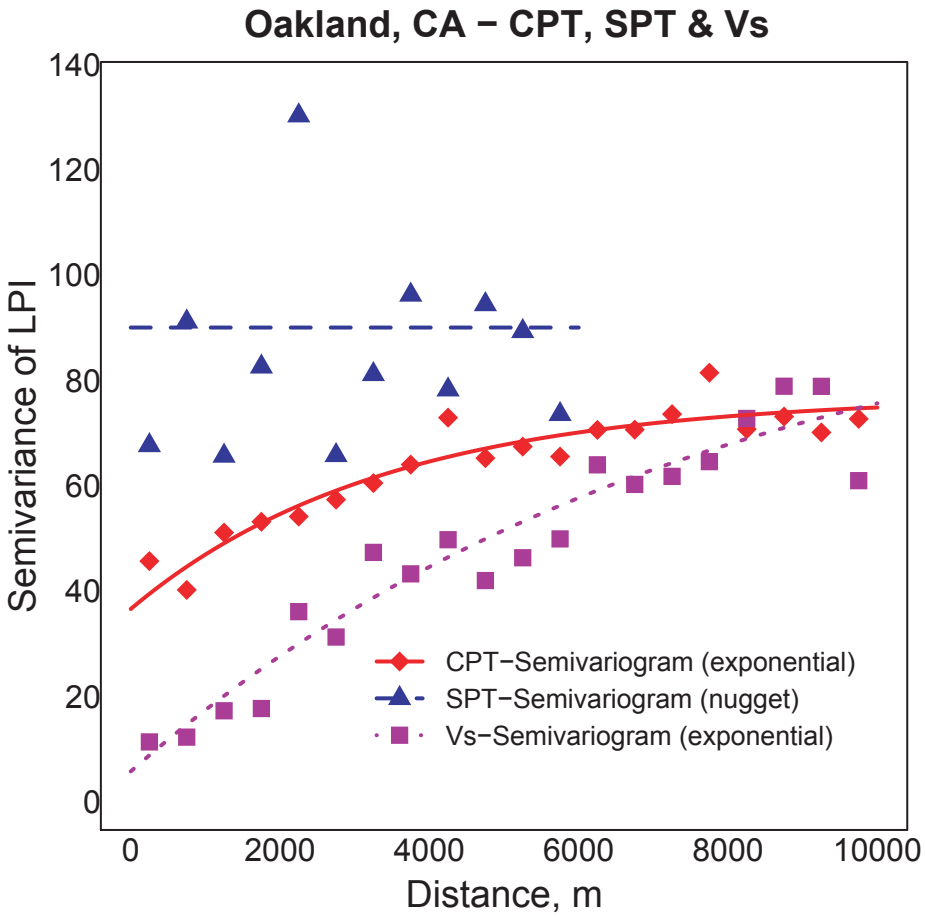


Fig. A.15. Semivariograms for SPT-, CPT-, and Vs-based LPI values.

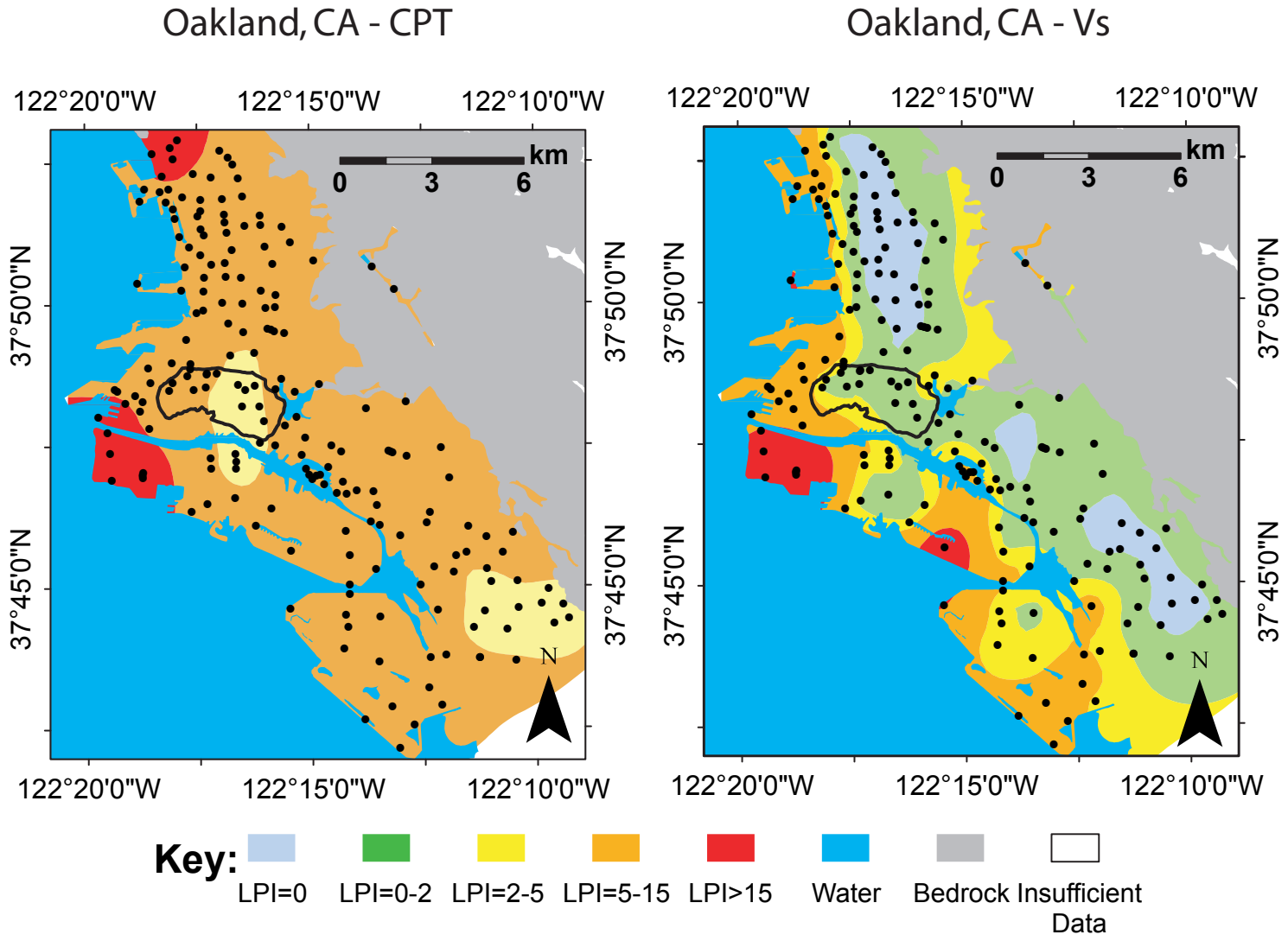


Fig. A.16. Ordinary kriging results for CPT- and Vs-based LPI

APPENDIX B

Salt Lake City, UT

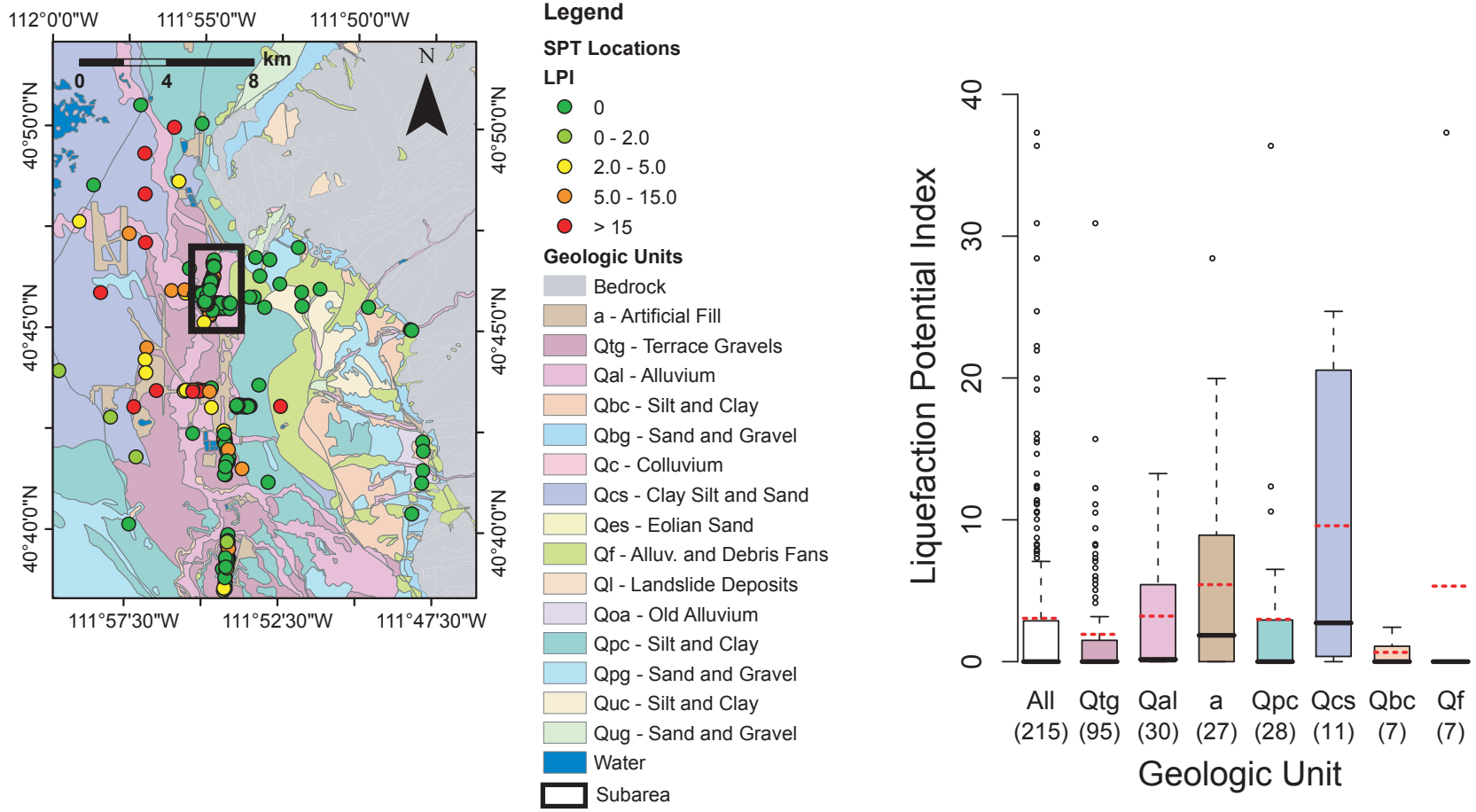


Fig. B.1. SPT-based LPI distributions by geologic unit

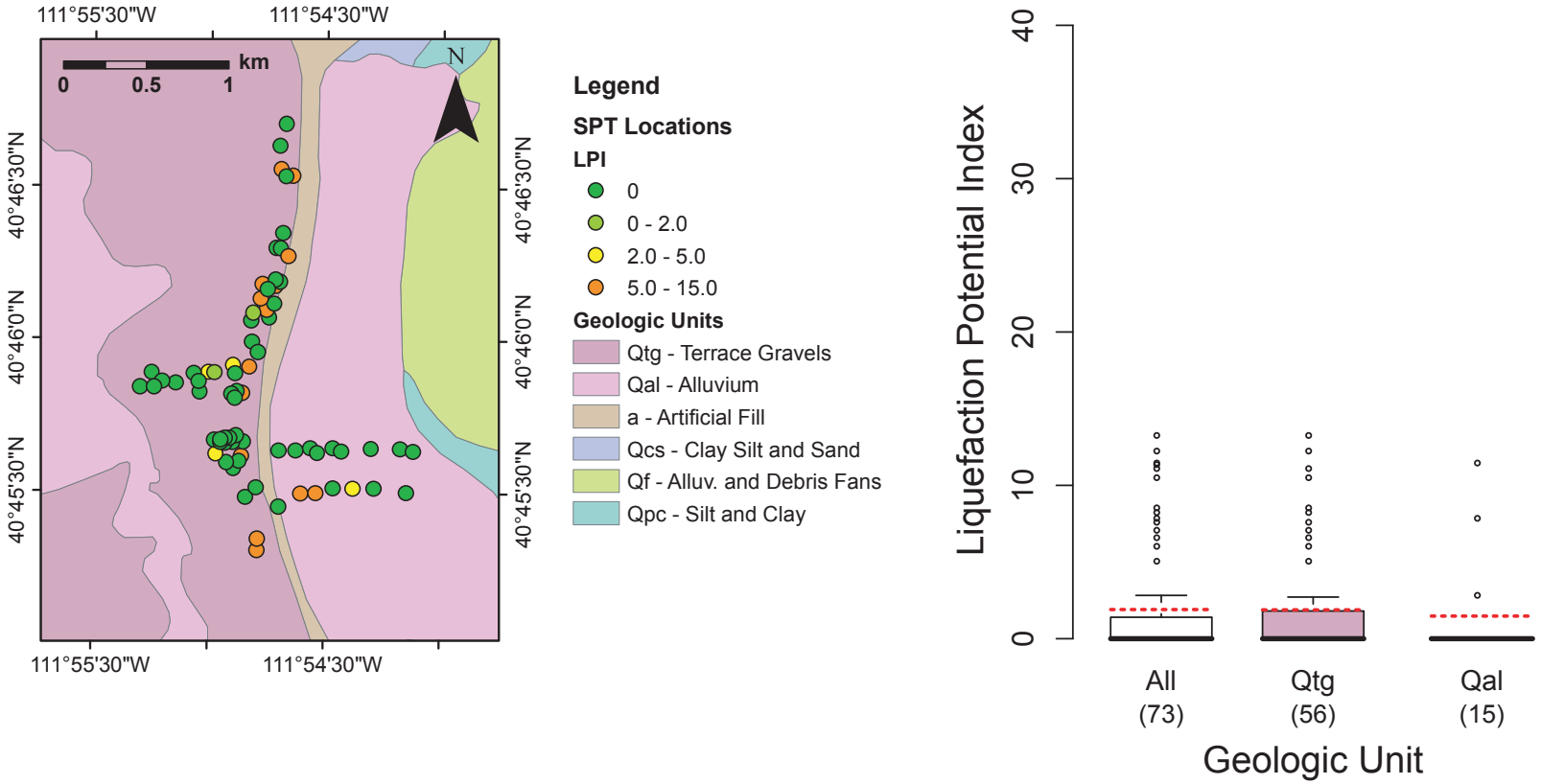


Fig. B.2. LPI distributions by age of geologic unit within subregion

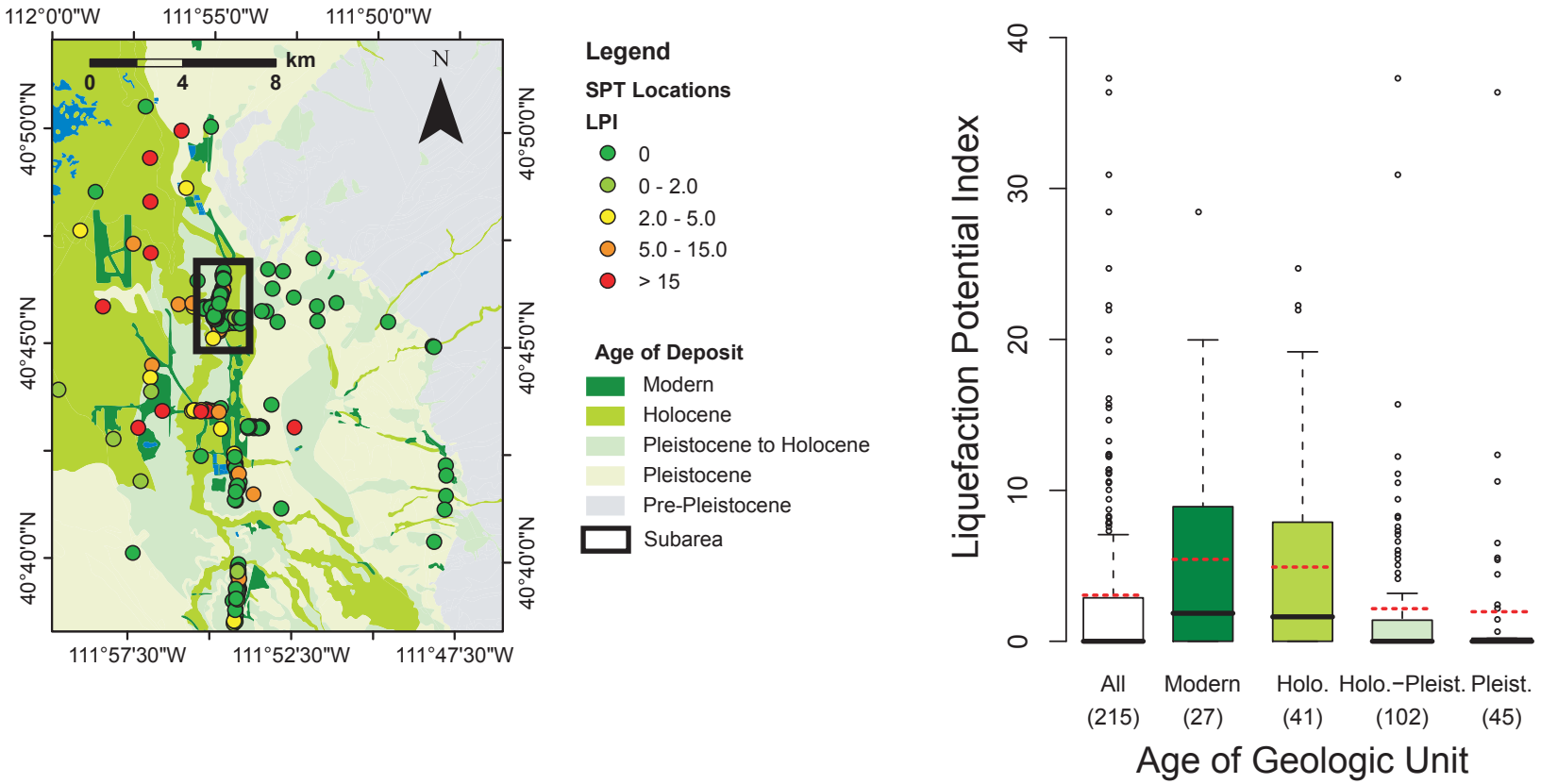


Fig. B.3. SPT-based LPI distributions by age of geologic unit

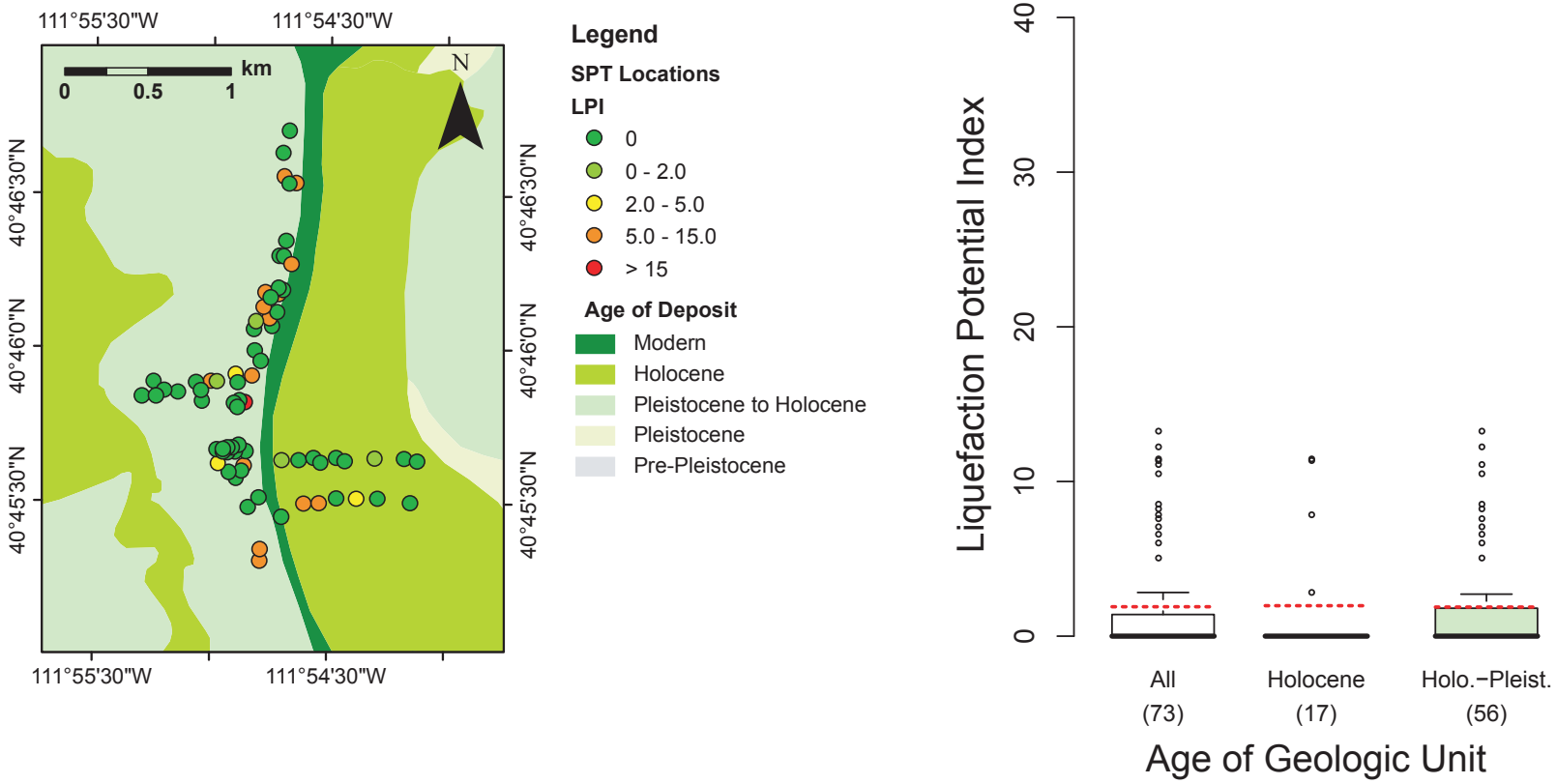


Fig. B.4. SPT-based LPI distributions by age of geologic unit for subarea

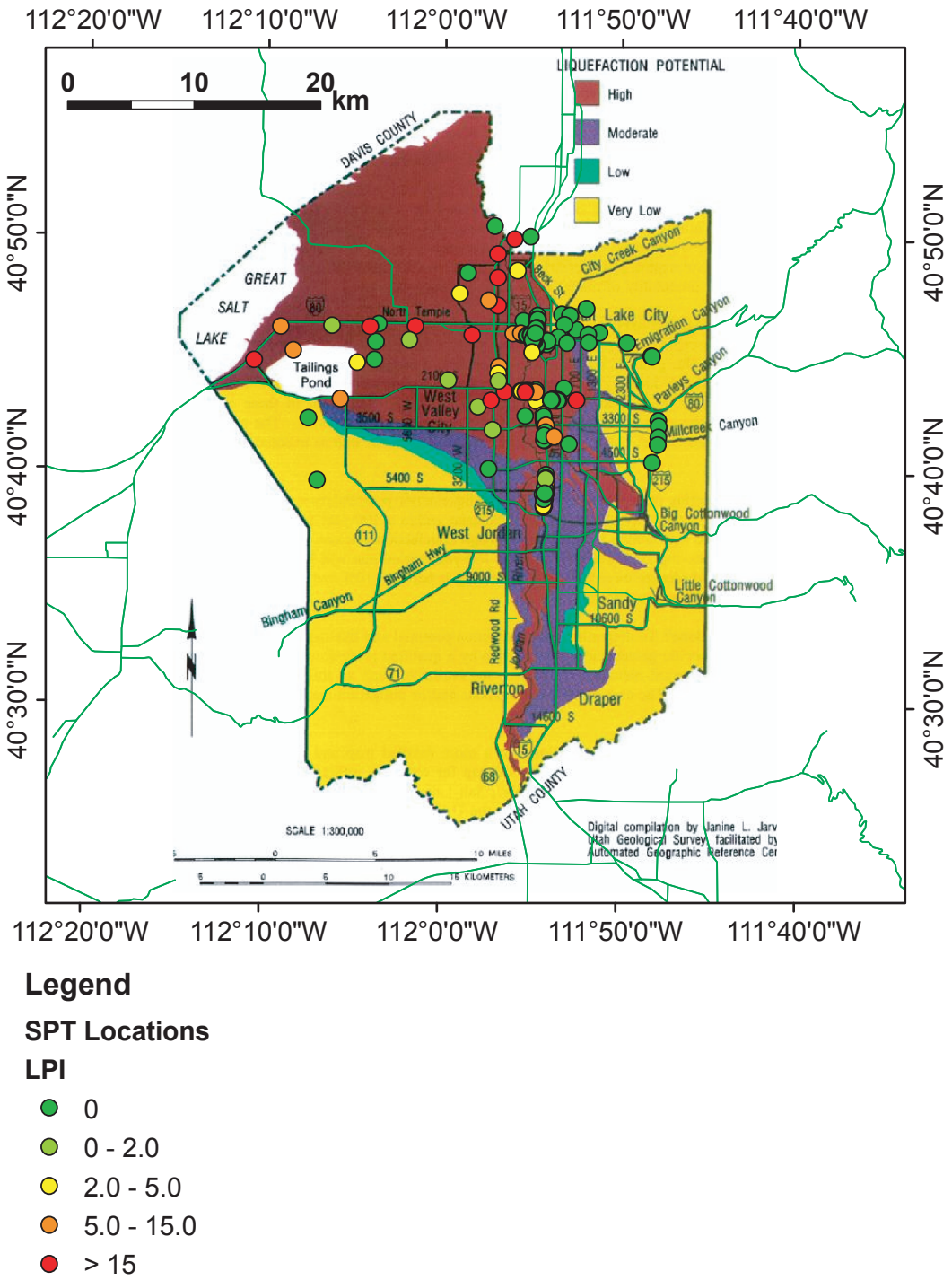
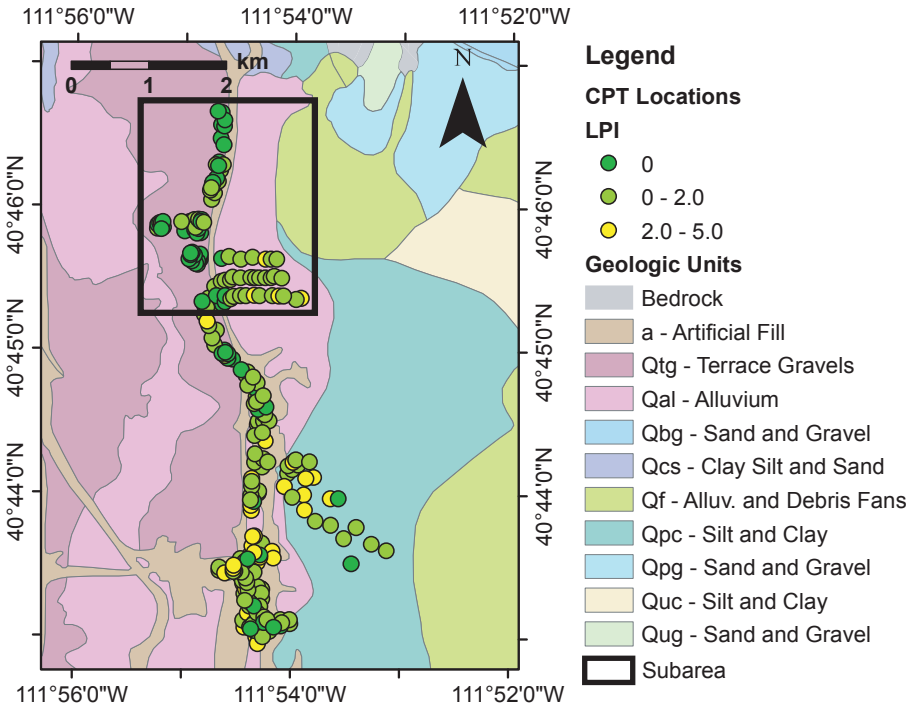


Fig. B.5. SPT-based LPI plotted on liquefaction potential map by Anderson et al. (1994)



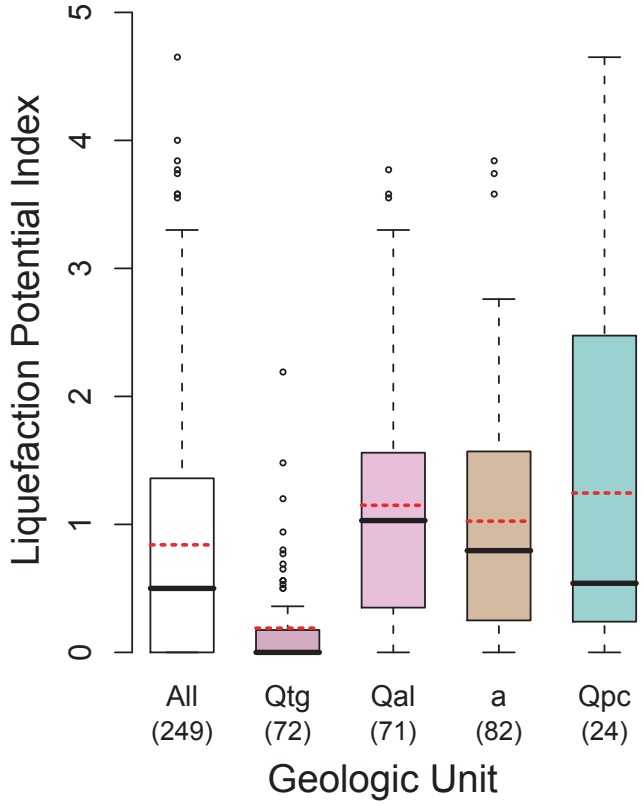


Fig. B.6. CPT-based LPI distributions by geologic unit

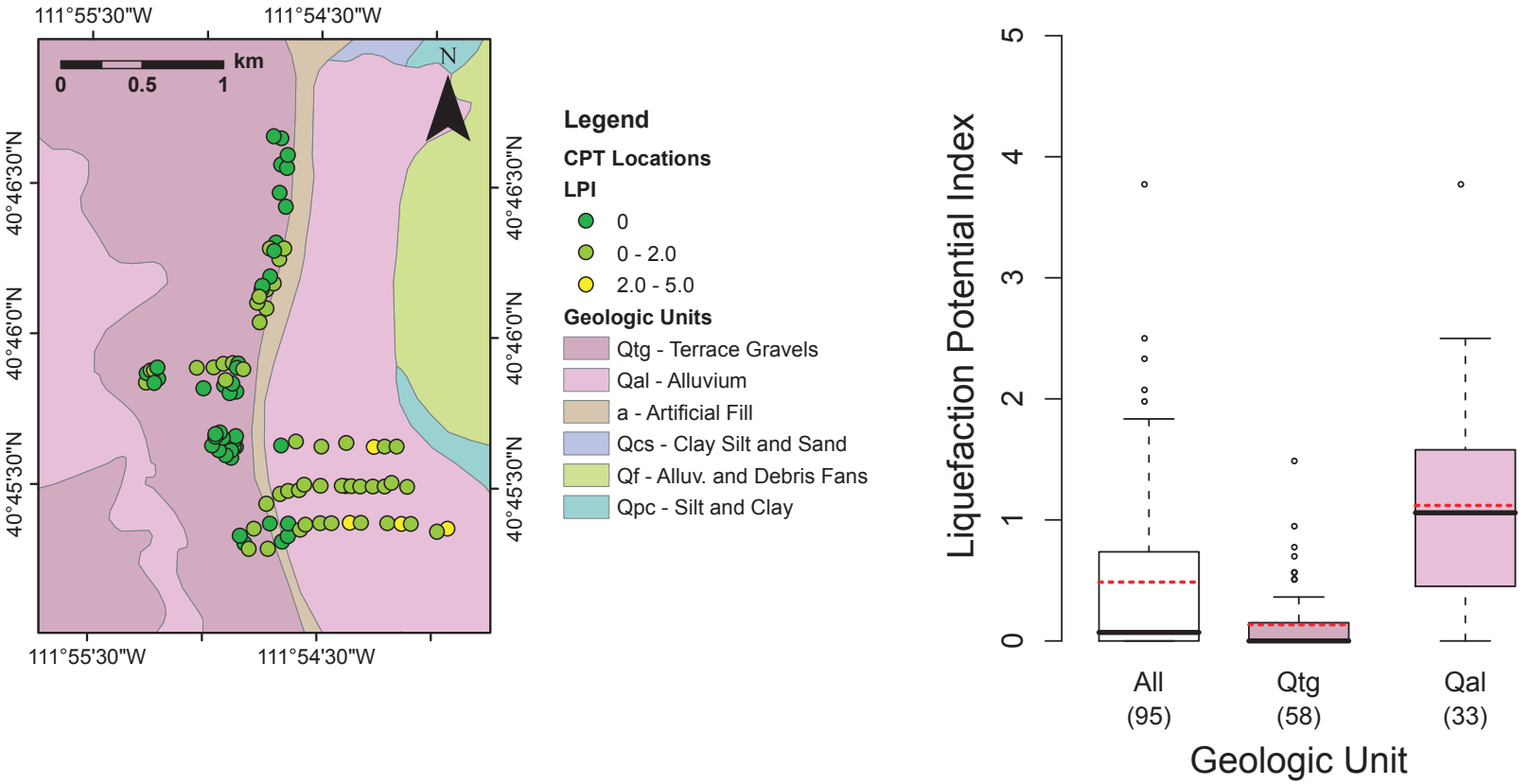


Fig. B.7. CPT-based LPI distributions by geologic unit for subarea

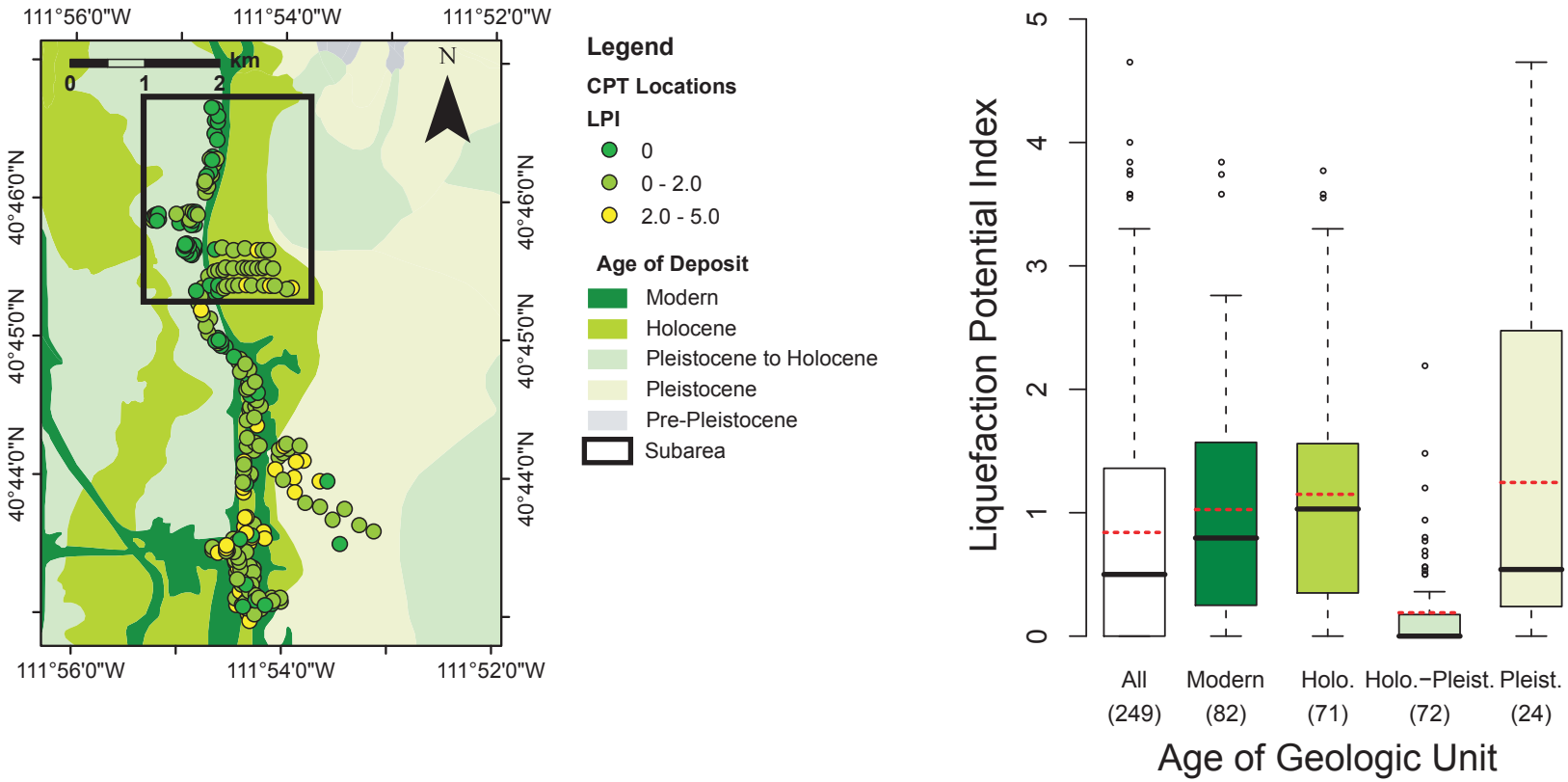


Fig. B.8. CPT-based LPI distributions by age of geologic unit

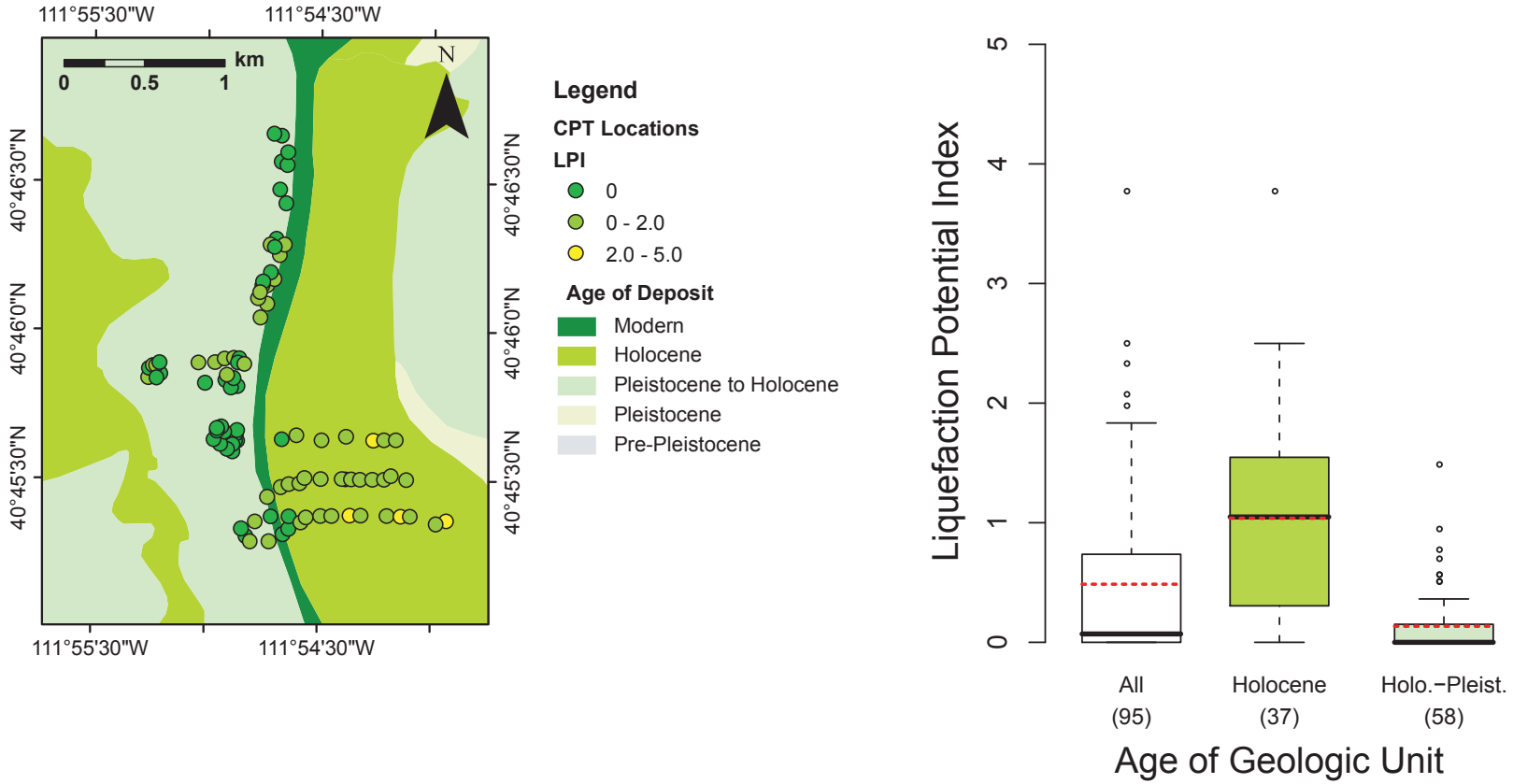


Fig. B.9. CPT-based LPI distributions by age of geologic unit for subarea

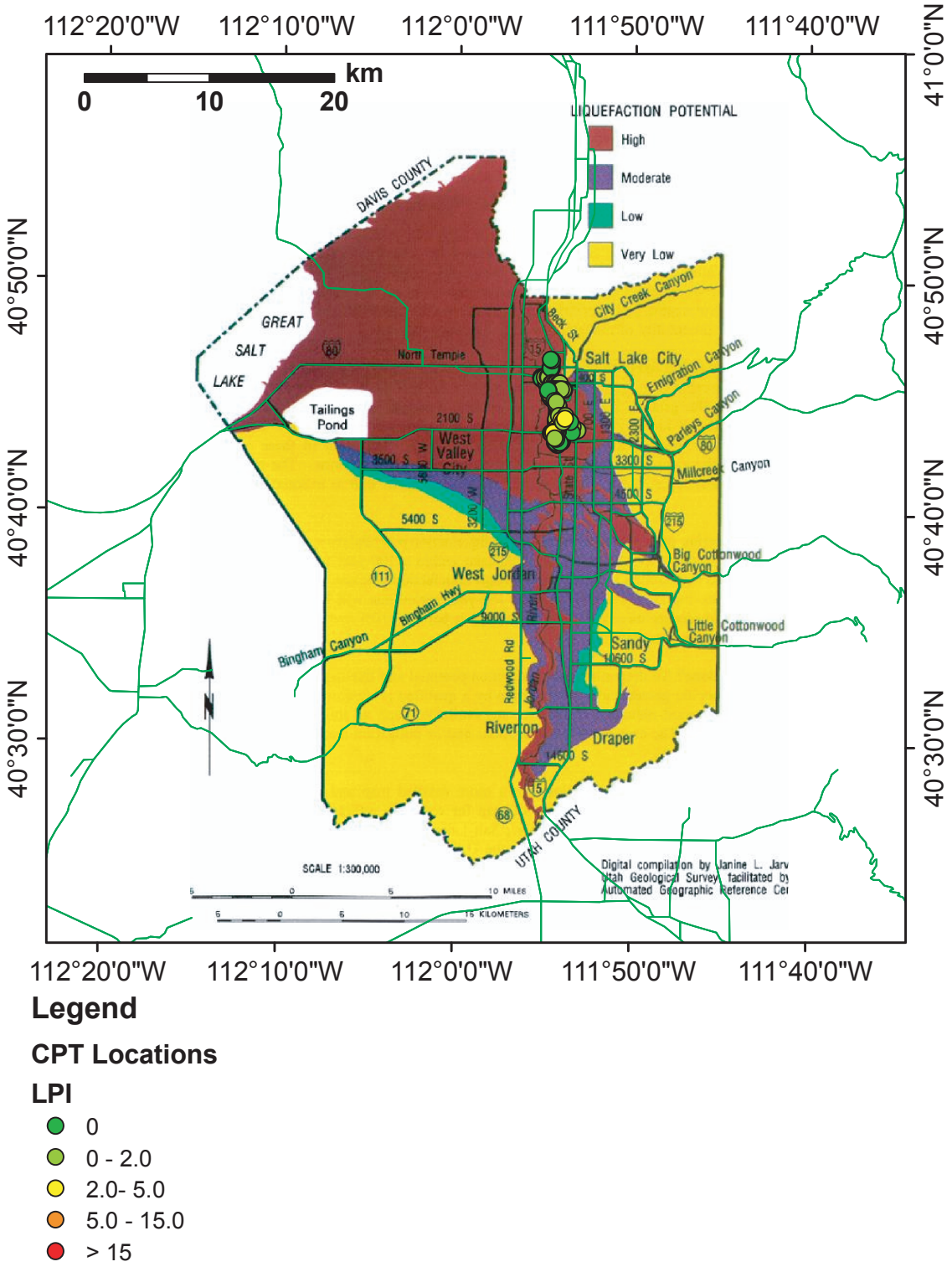


Fig. B.10. CPT-based LPI plotted on liquefaction potential map by Anderson et al. (1994)

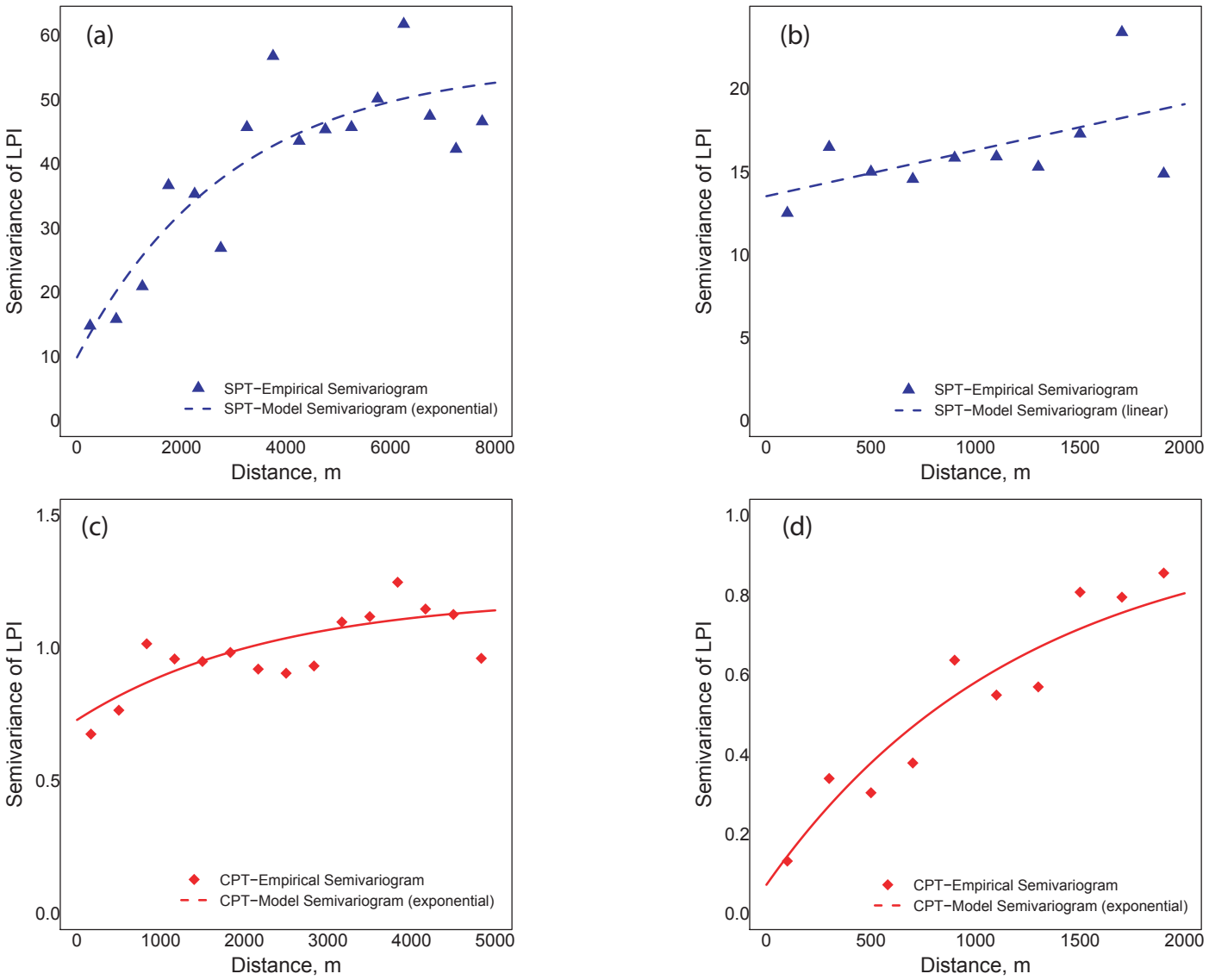


Fig. B.11. Semivariograms for (a) SPT full dataset, (b) SPT subarea, (c) CPT full dataset, and (d) CPT subarea

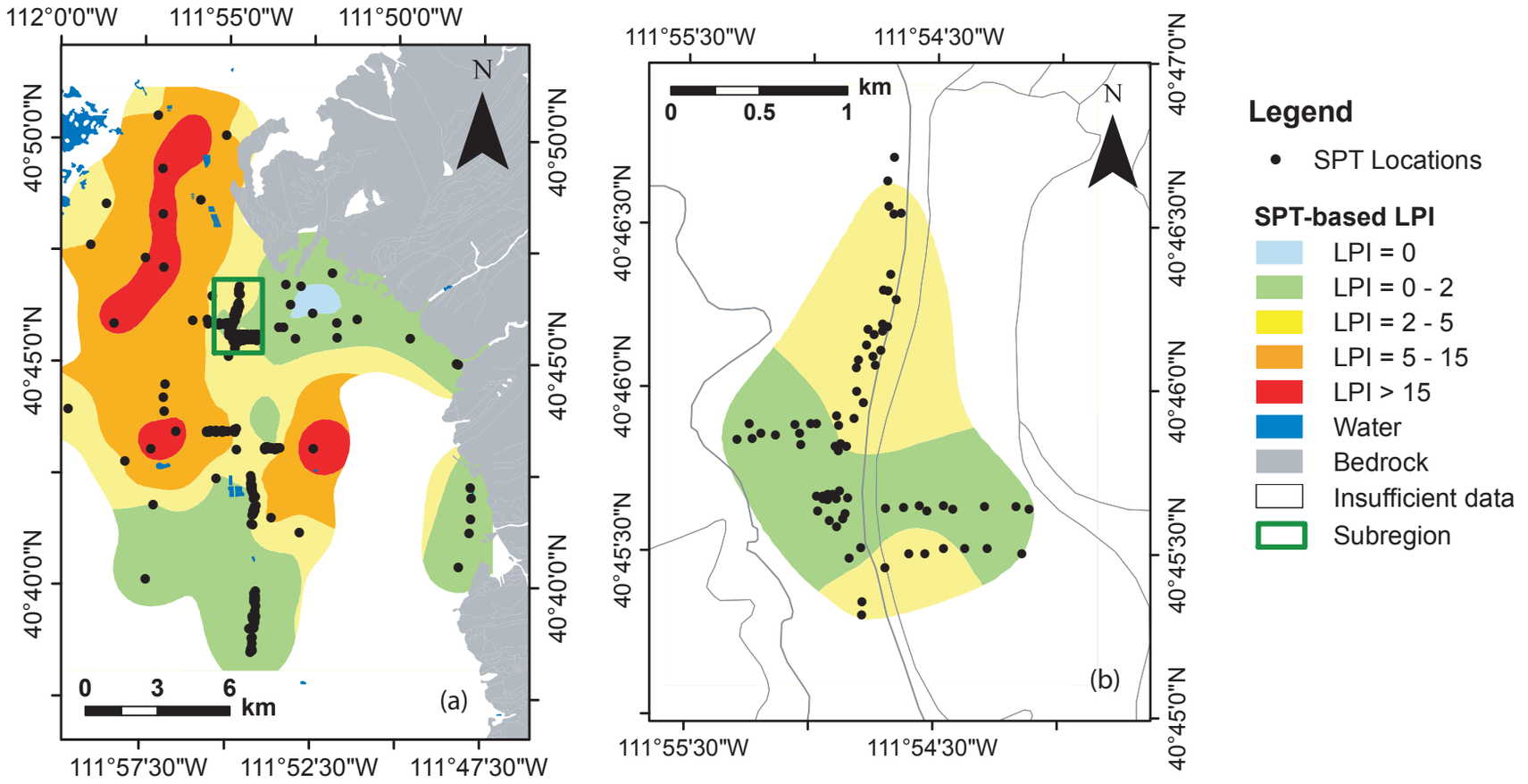


Fig. B.12. Ordinary kriging results for SPT-based LPI for (a) full dataset and (b) subarea

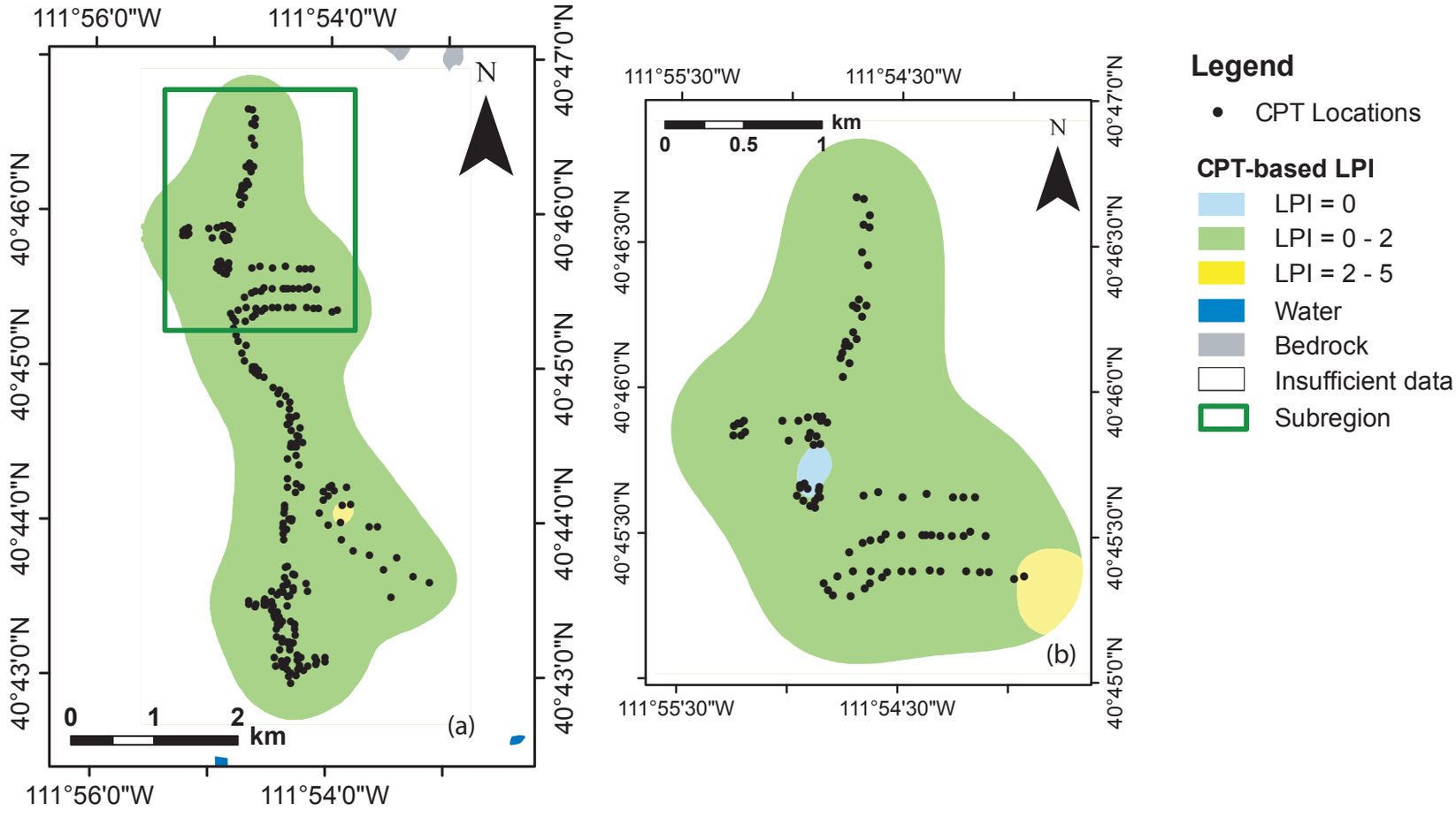


Fig. B.13. Ordinary kriging results for CPT-based LPI for (a) full dataset and (b) subarea

APPENDIX C

San Bernardino, CA

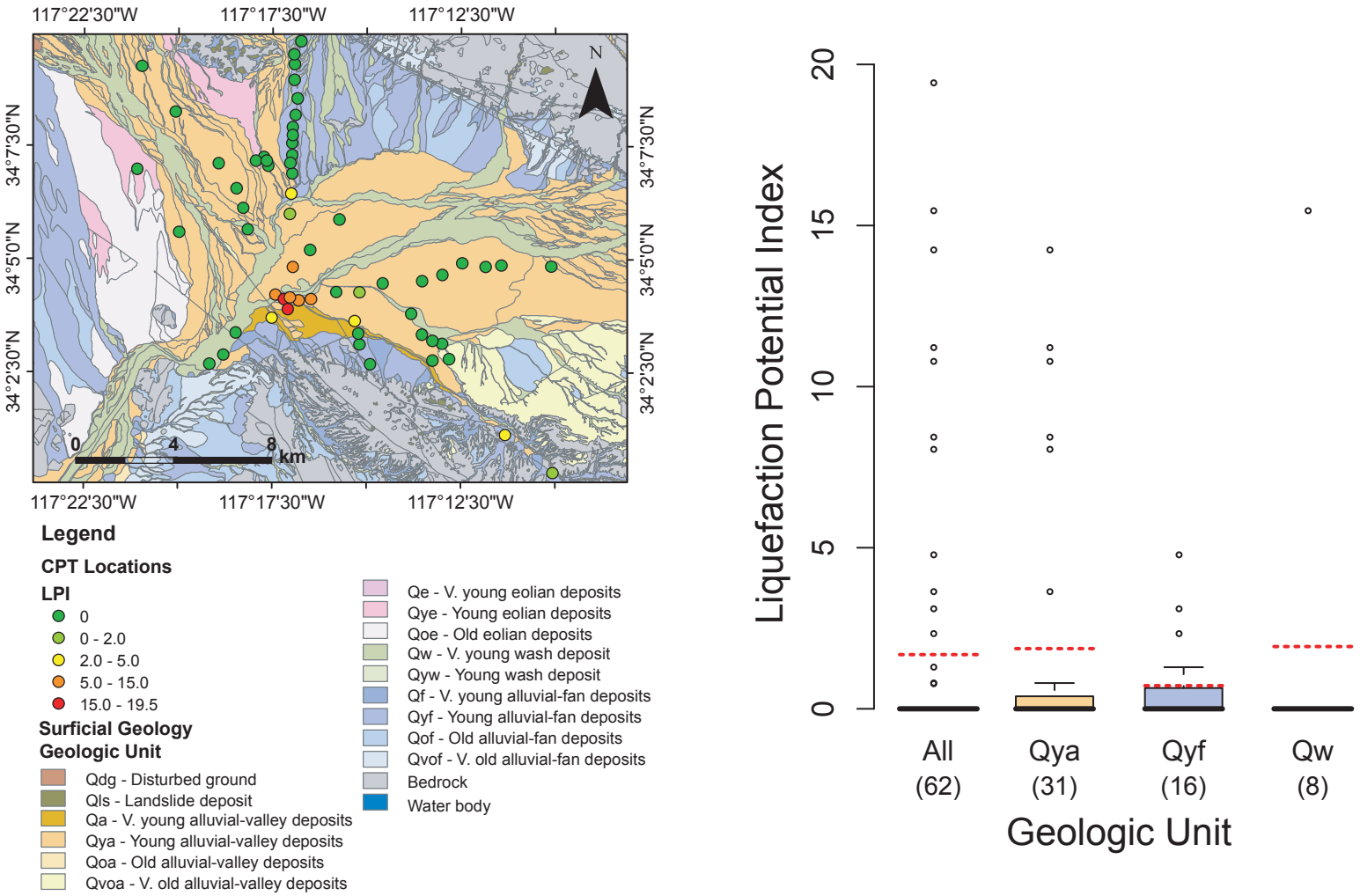


Fig. C.1. CPT-based LPI distributions by geologic unit

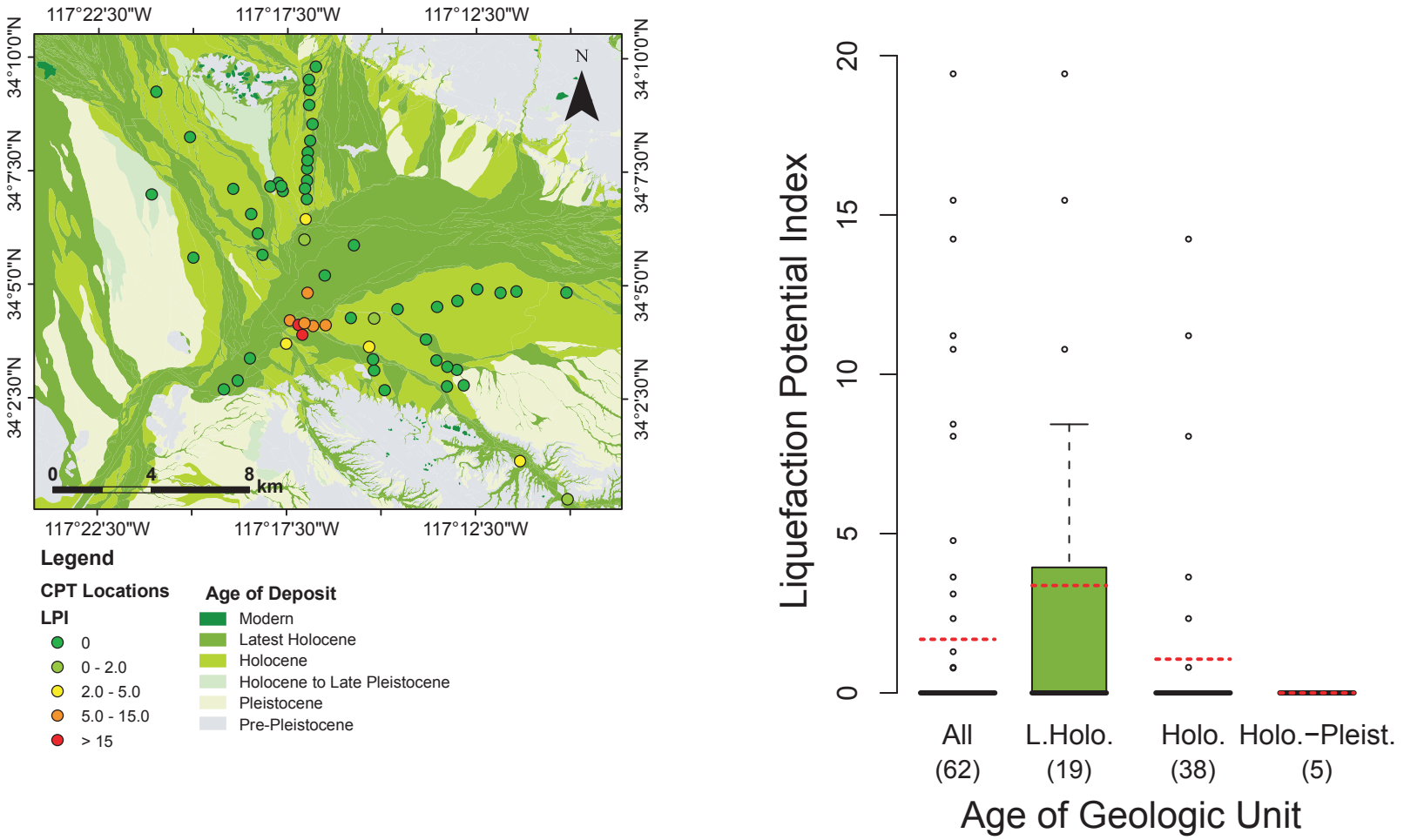


Fig. C.2. CPT-based LPI distributions by age of geologic unit

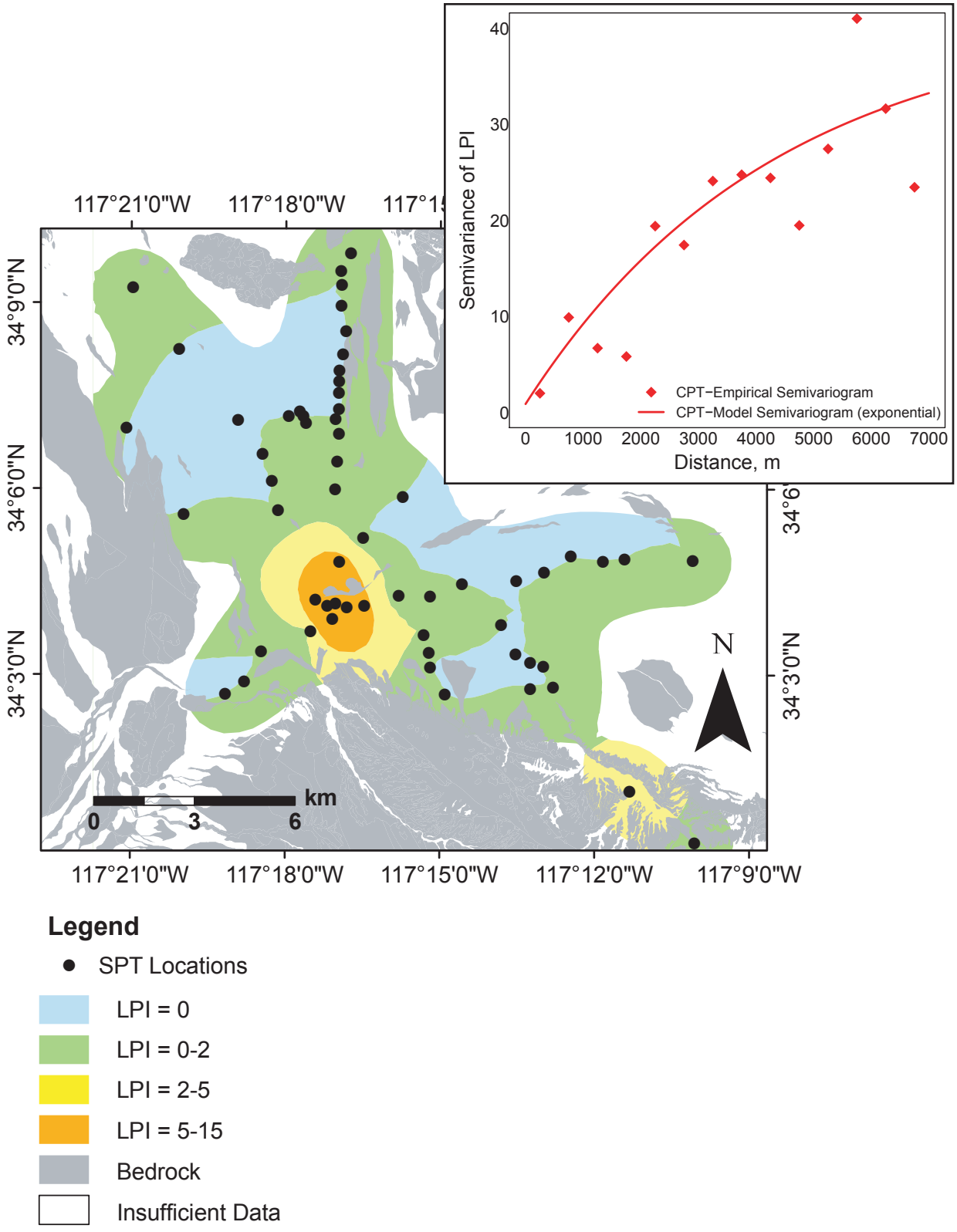


Fig. C.3. Semivariogram and ordinary kriging results for CPT-based LPI

APPENDIX D

Evansville, IN

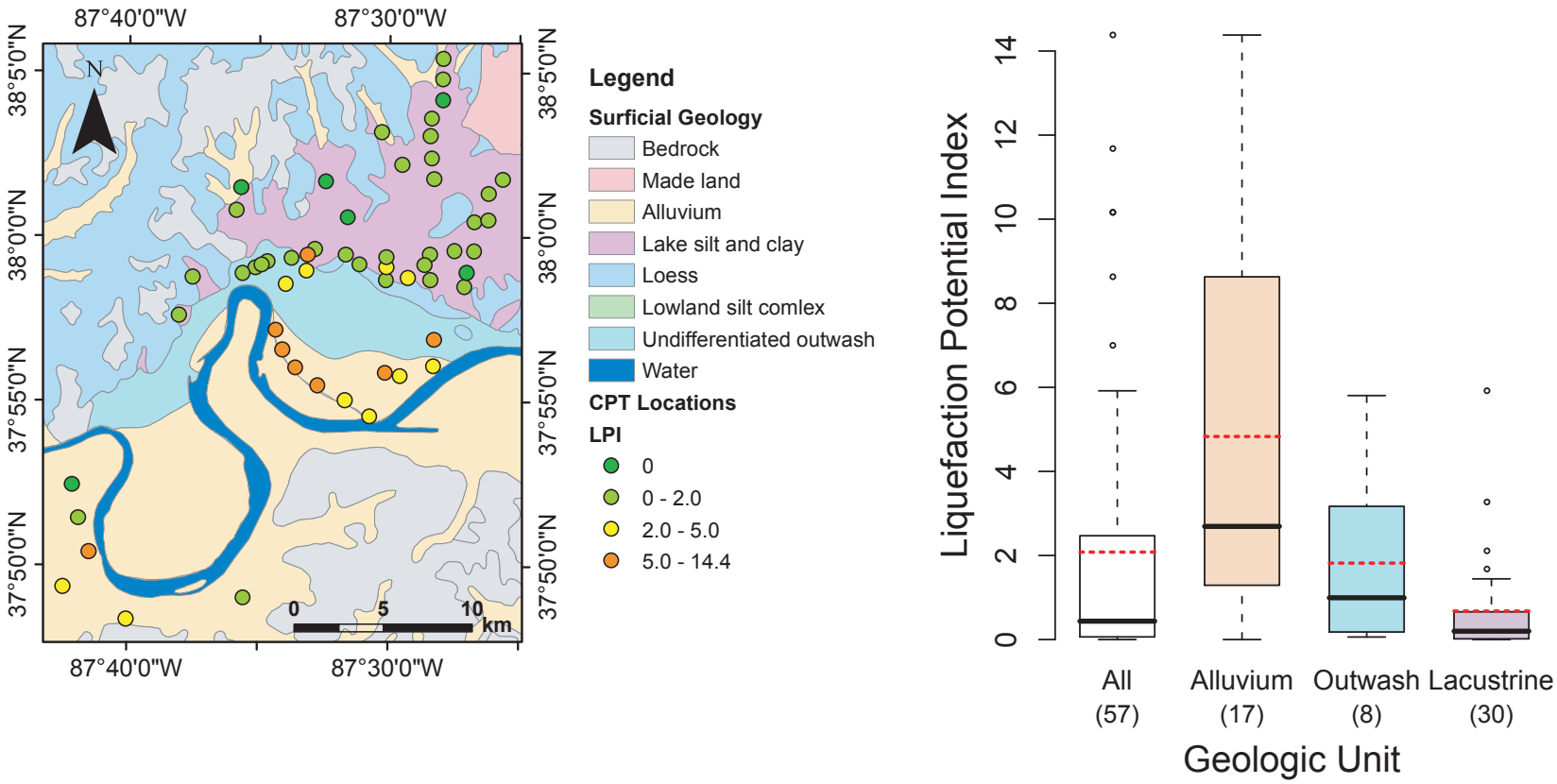


Fig. D.1. CPT-based LPI distributions by geologic unit

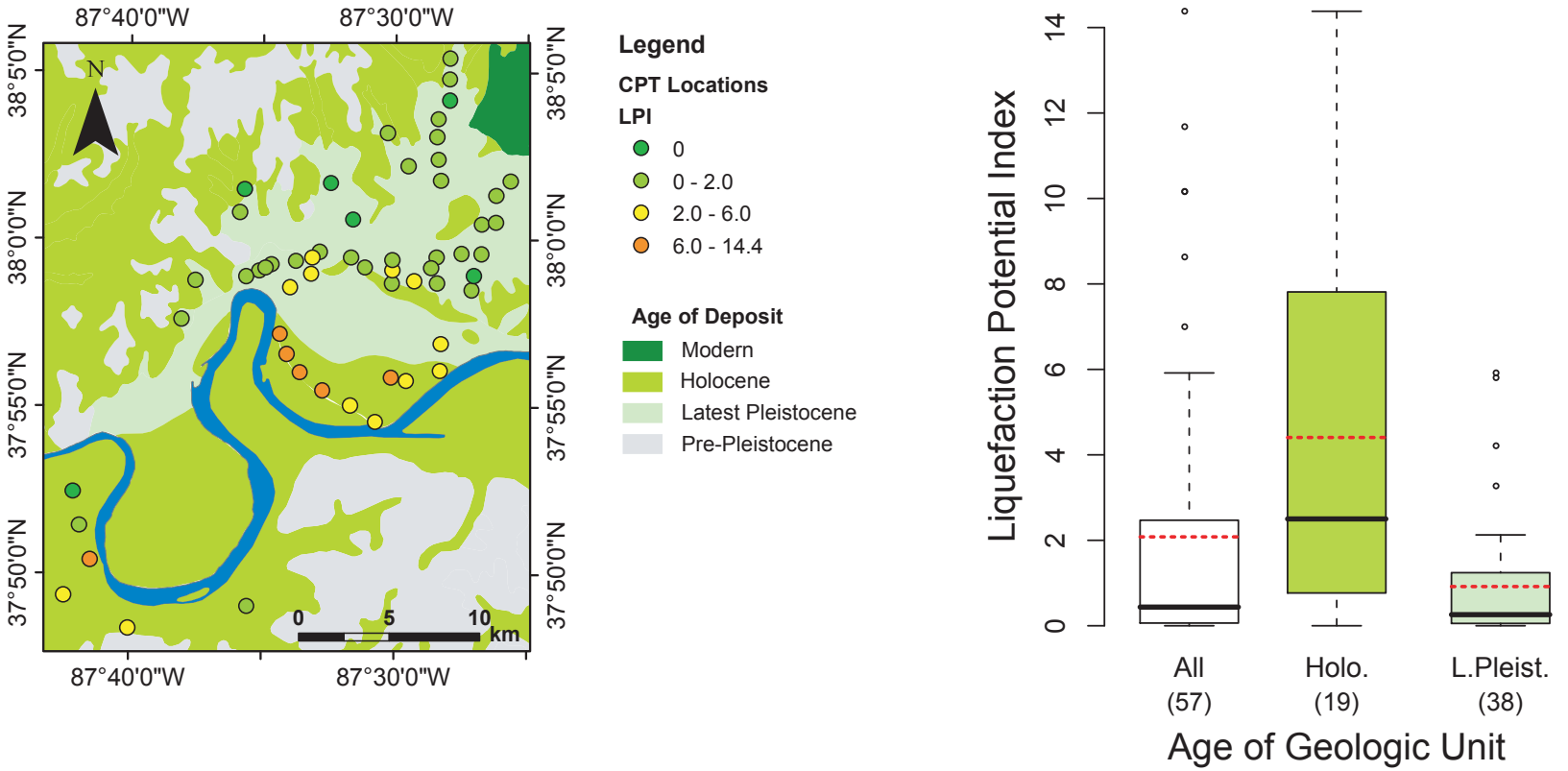


Fig. D.2. CPT-based LPI distributions by age of geologic unit

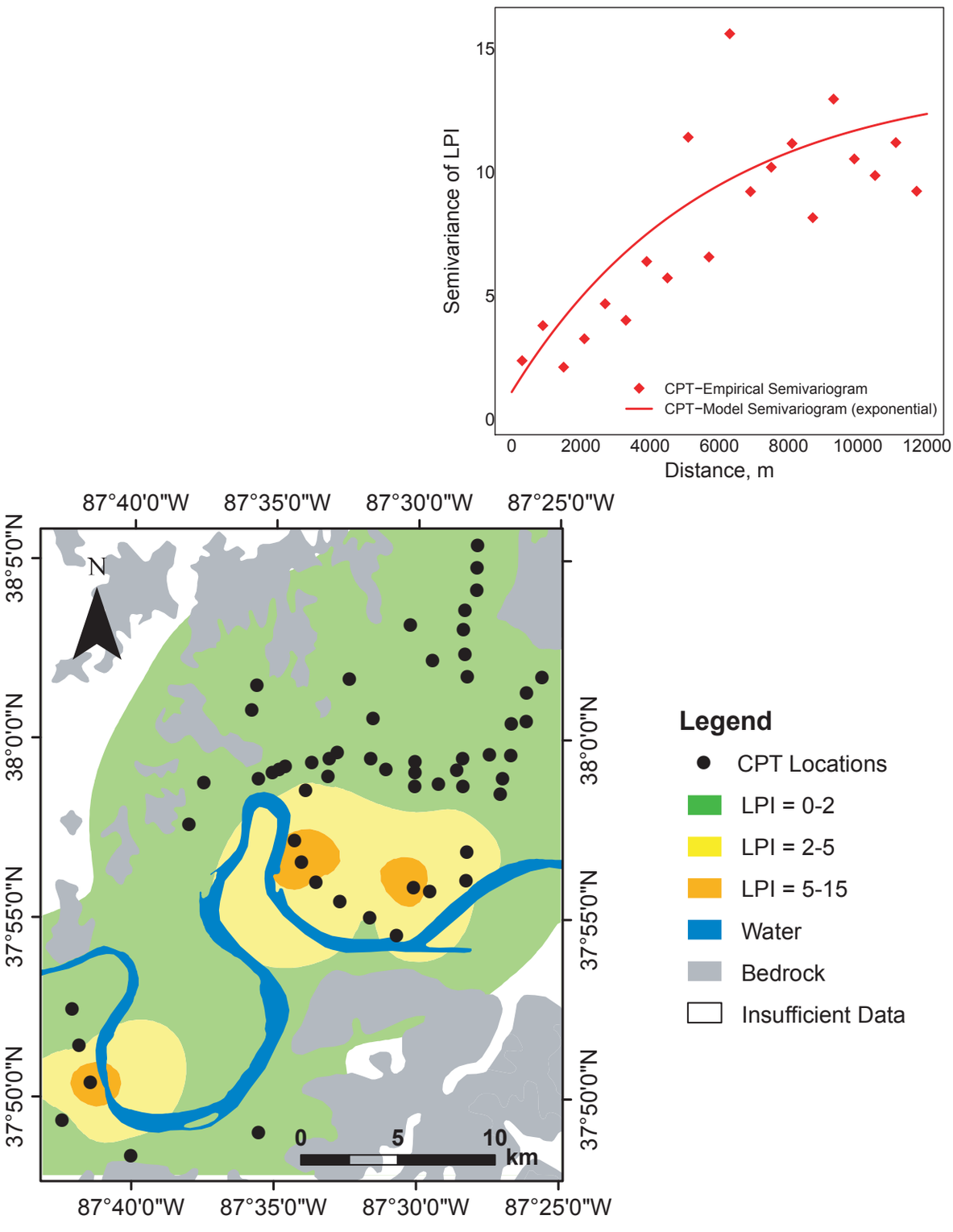


Fig. D.3. Semivariogram and ordinary kriging results for CPT-based LPI

APPENDIX E

Southern San Francisco Bay, CA

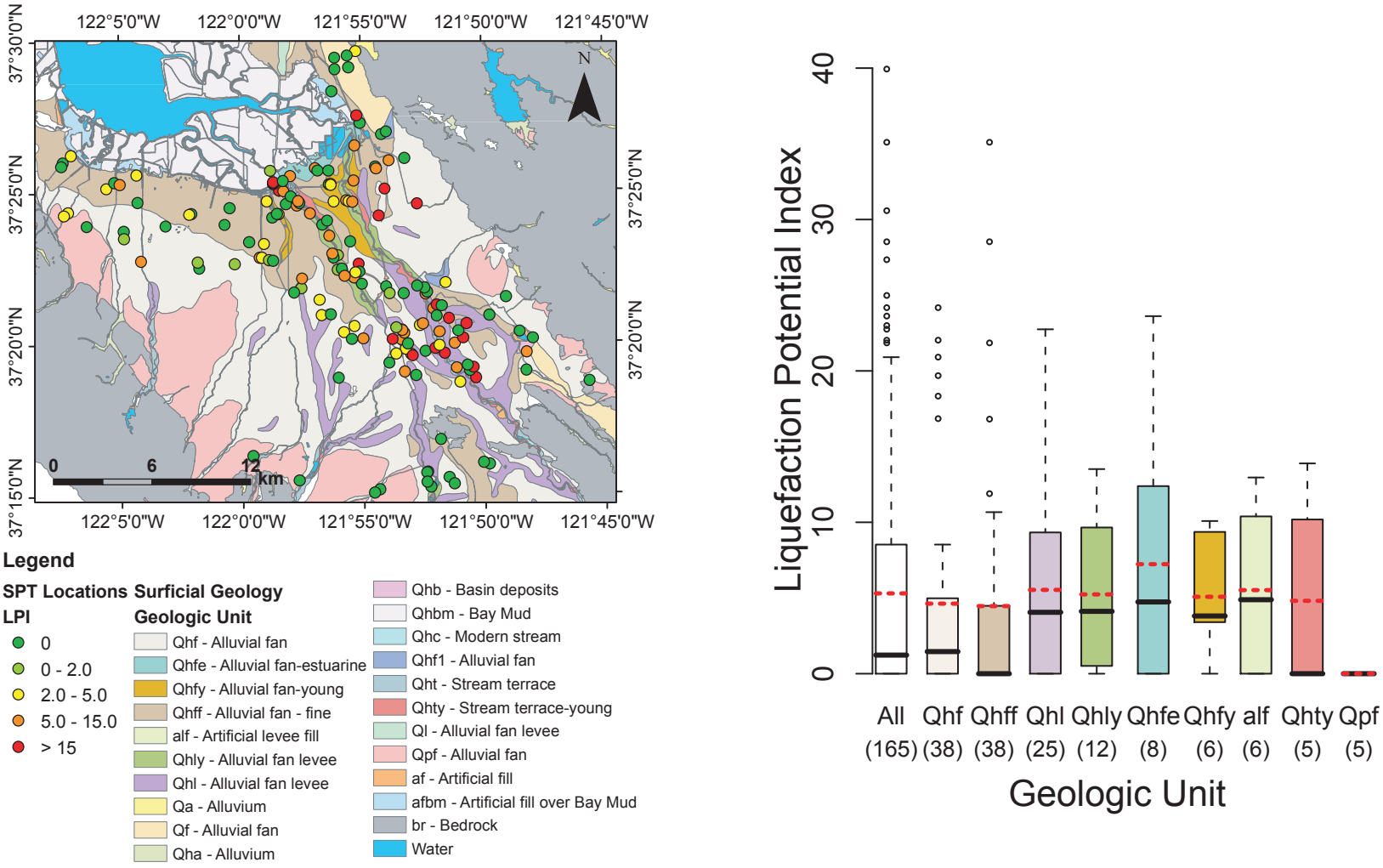


Fig. E.1. SPT-based LPI distributions by geologic unit

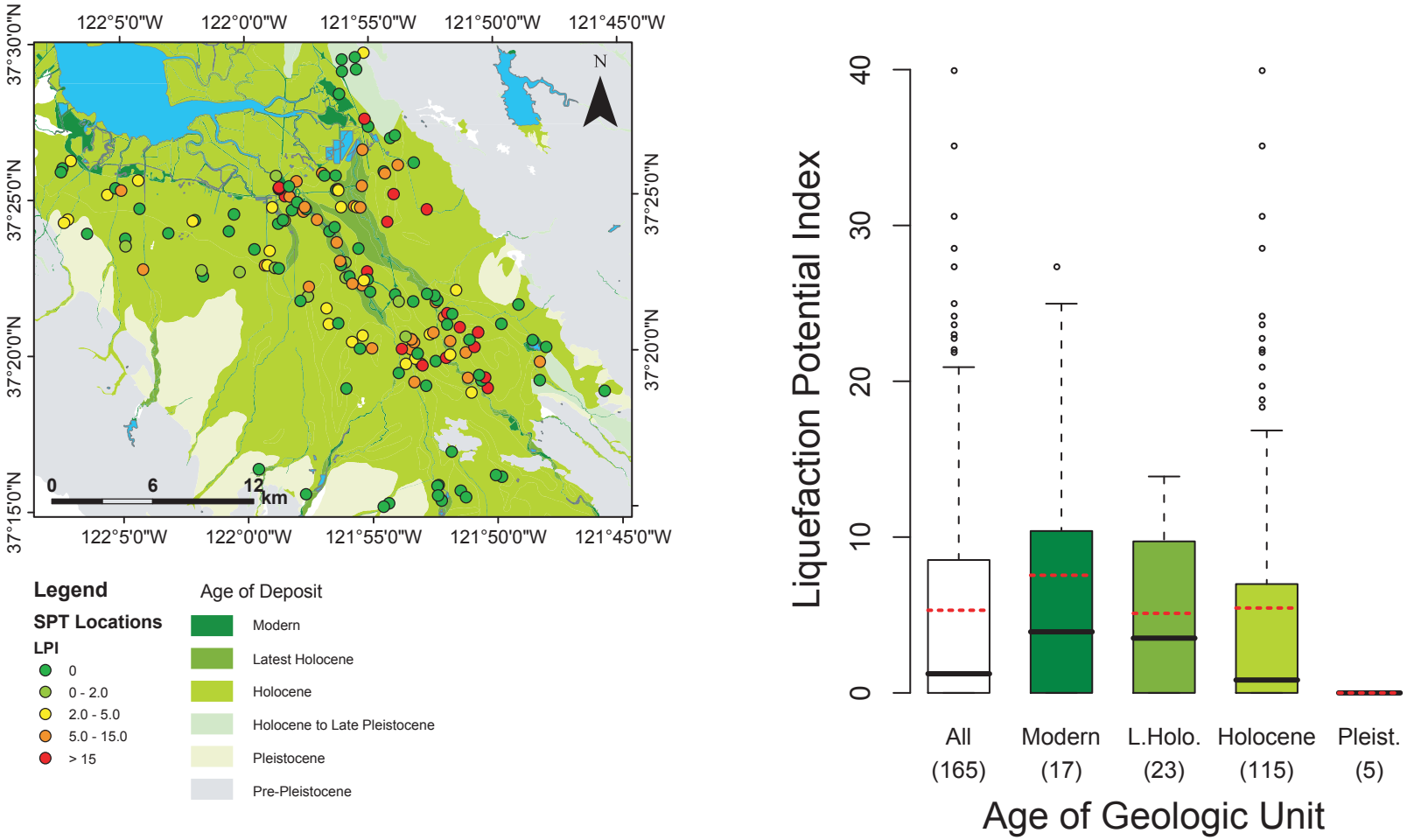


Fig. E.2. SPT-based LPI distributions by age of geologic unit

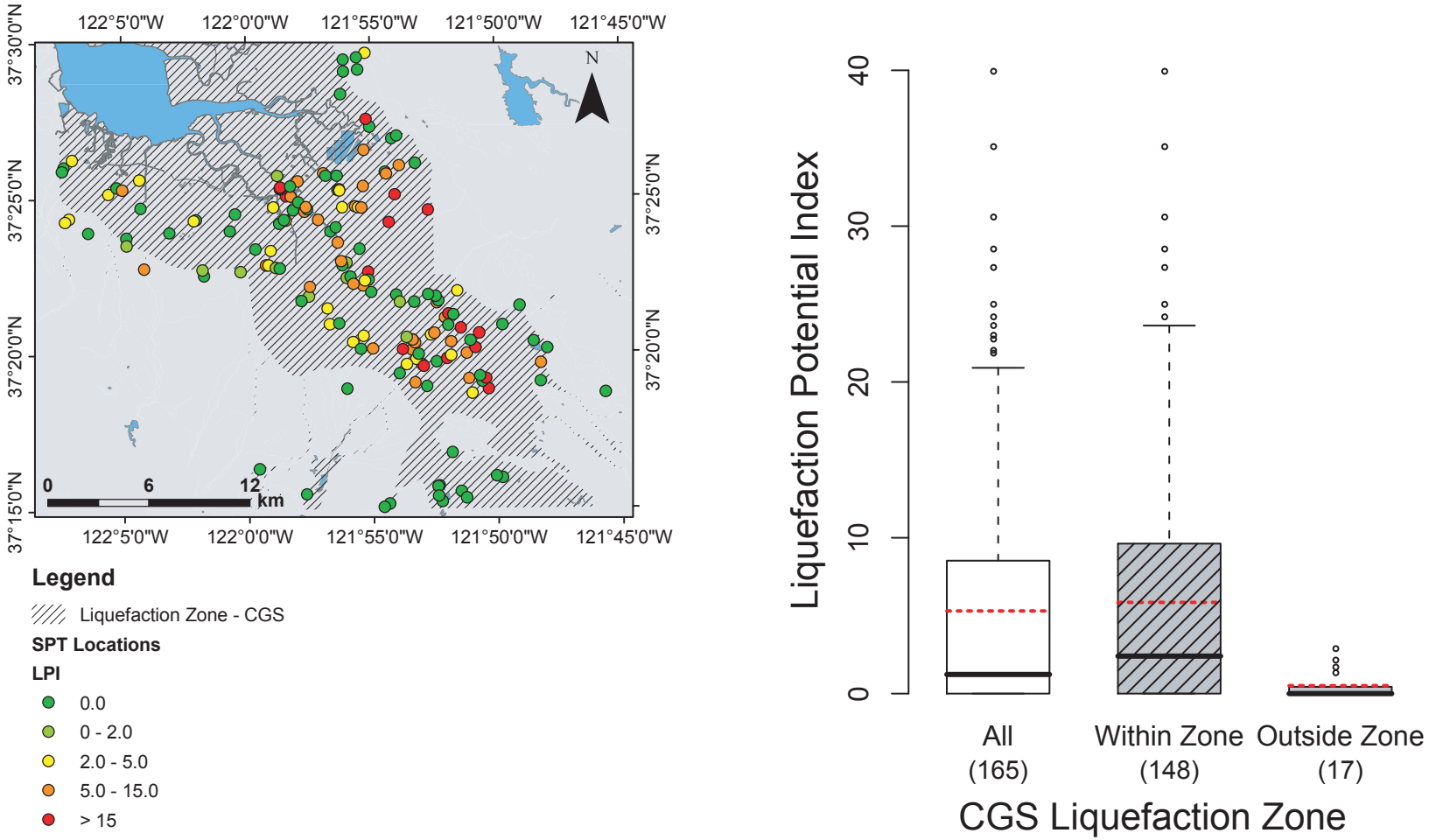


Fig. E.3. SPT-based LPI distributions by California Geological Survey Liquefaction Zone

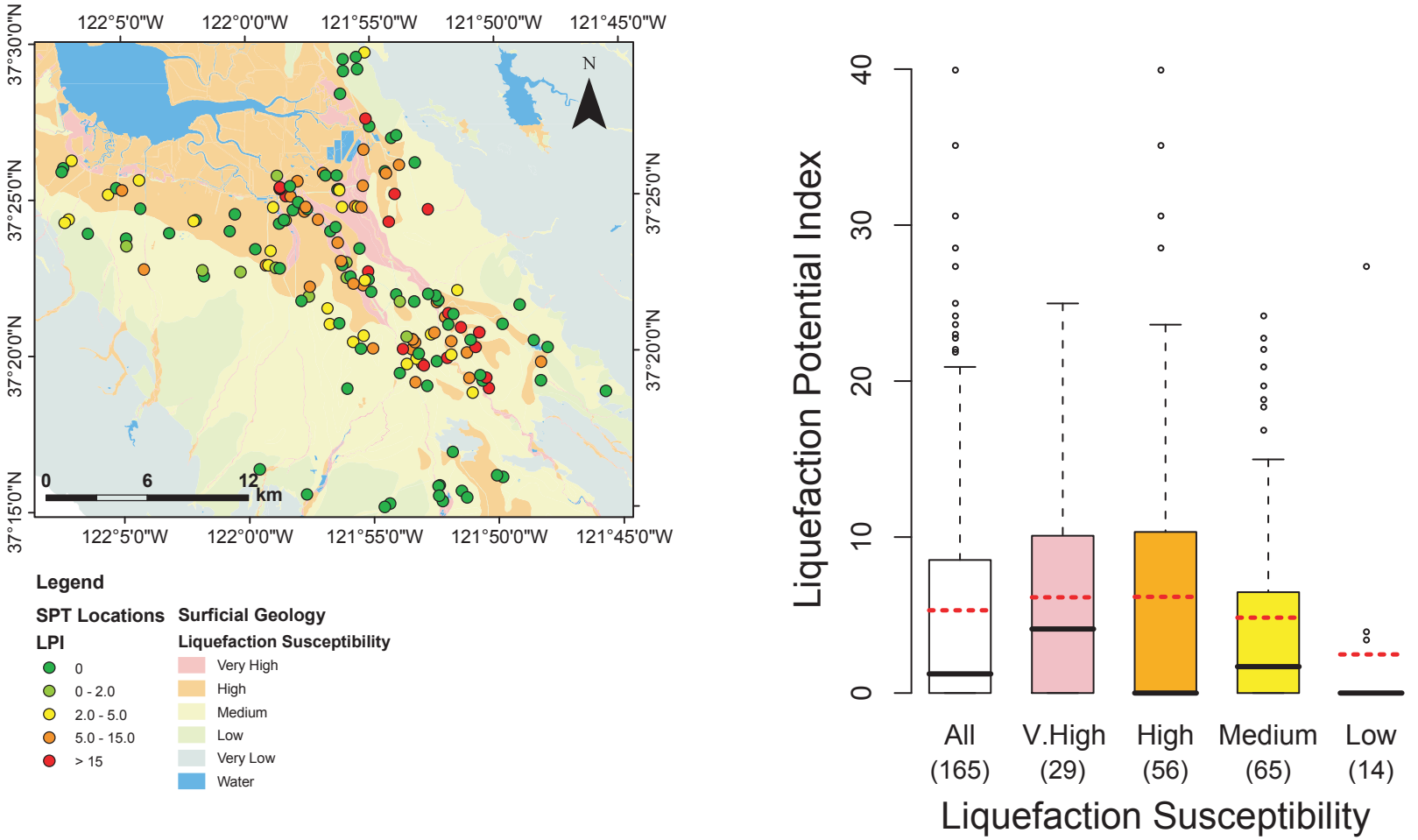


Fig. E.4. SPT-based LPI distributions by liquefaction susceptibility in the Knudsen et al. (2000) geologic maps

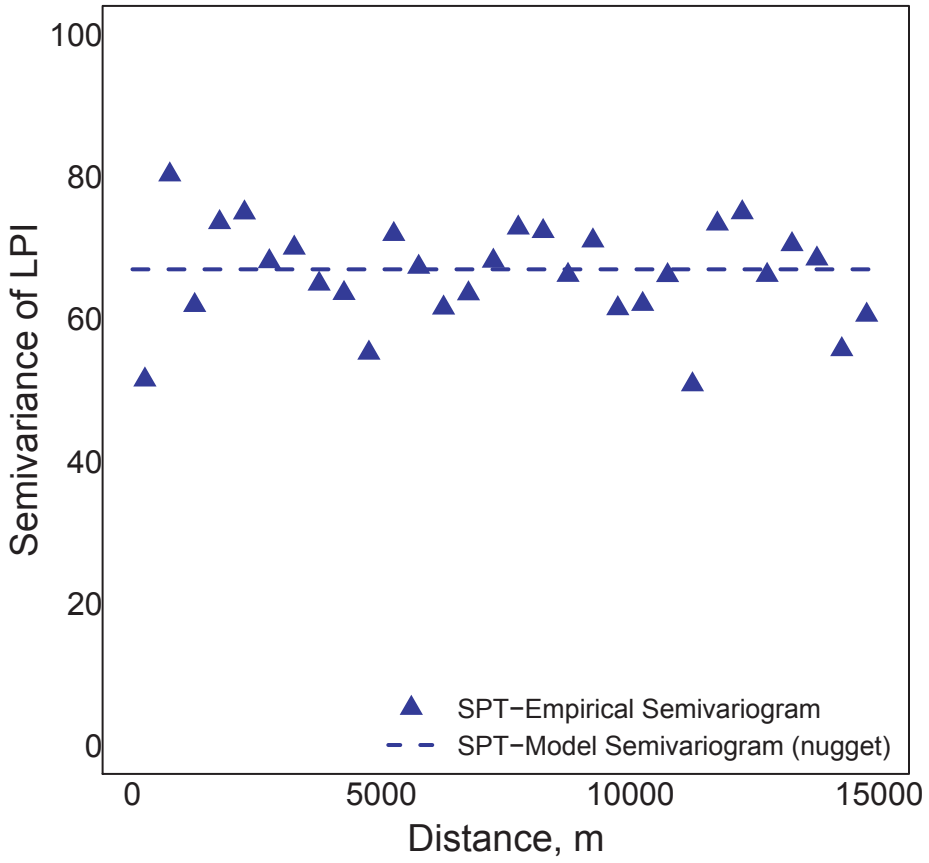
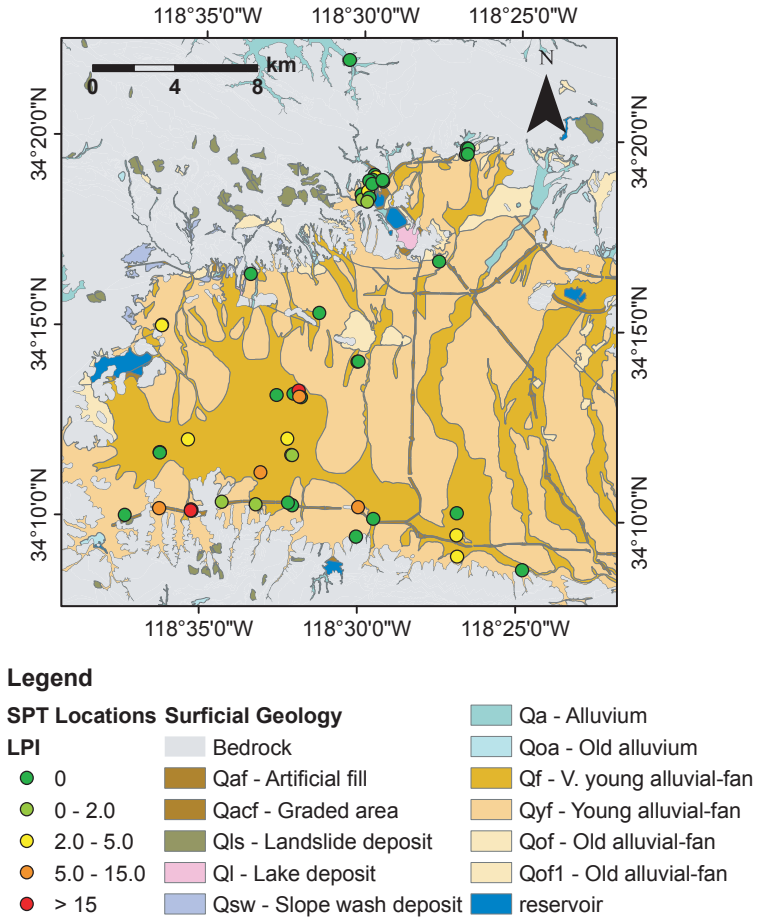


Fig. E.5. Semivariogram for SPT-based LPI

APPENDIX F

San Fernando, CA



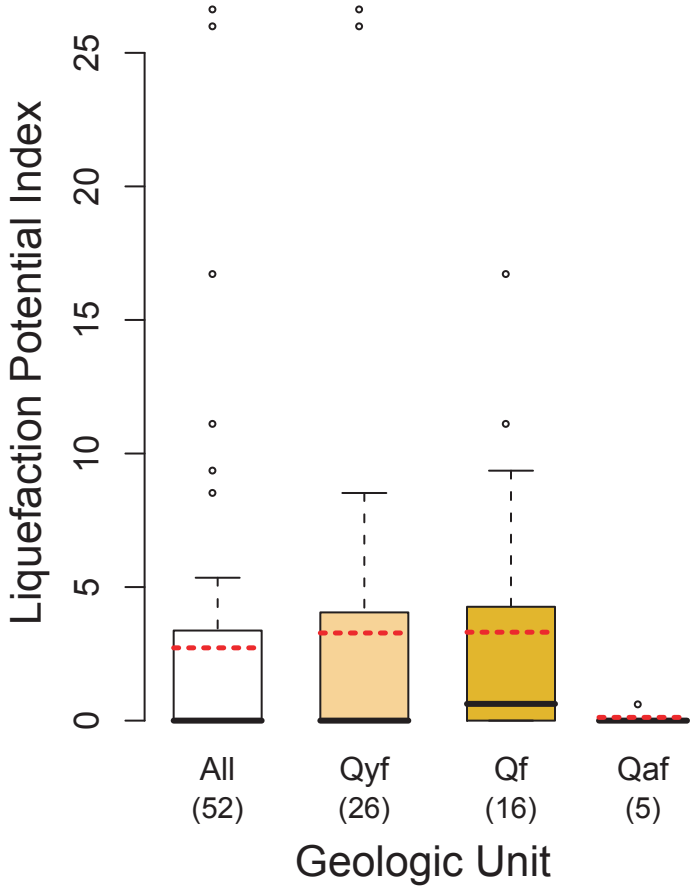


Fig. F.1. SPT-based LPI distributions by geologic unit

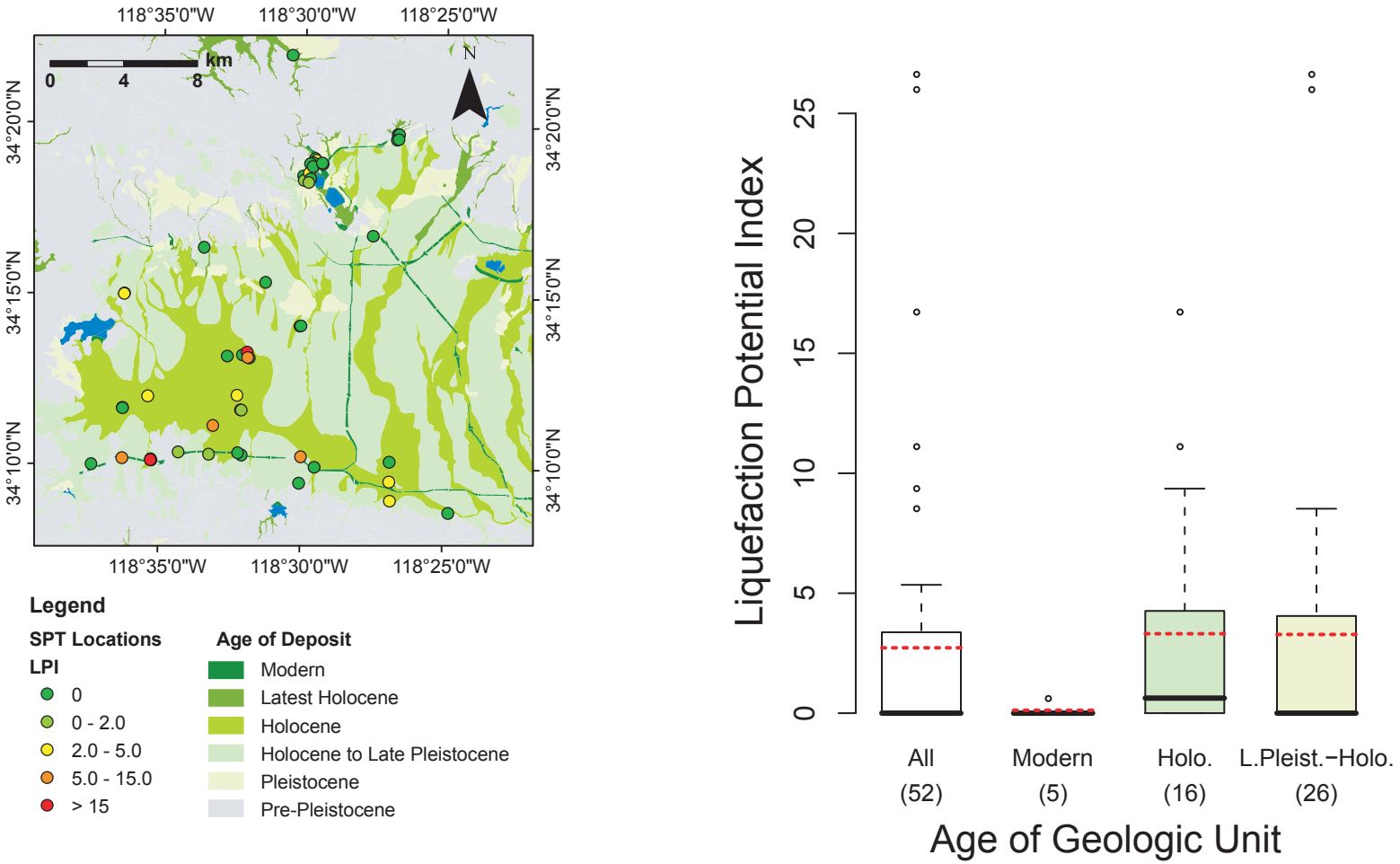


Fig. F.2. SPT-based LPI distributions by age of geologic unit

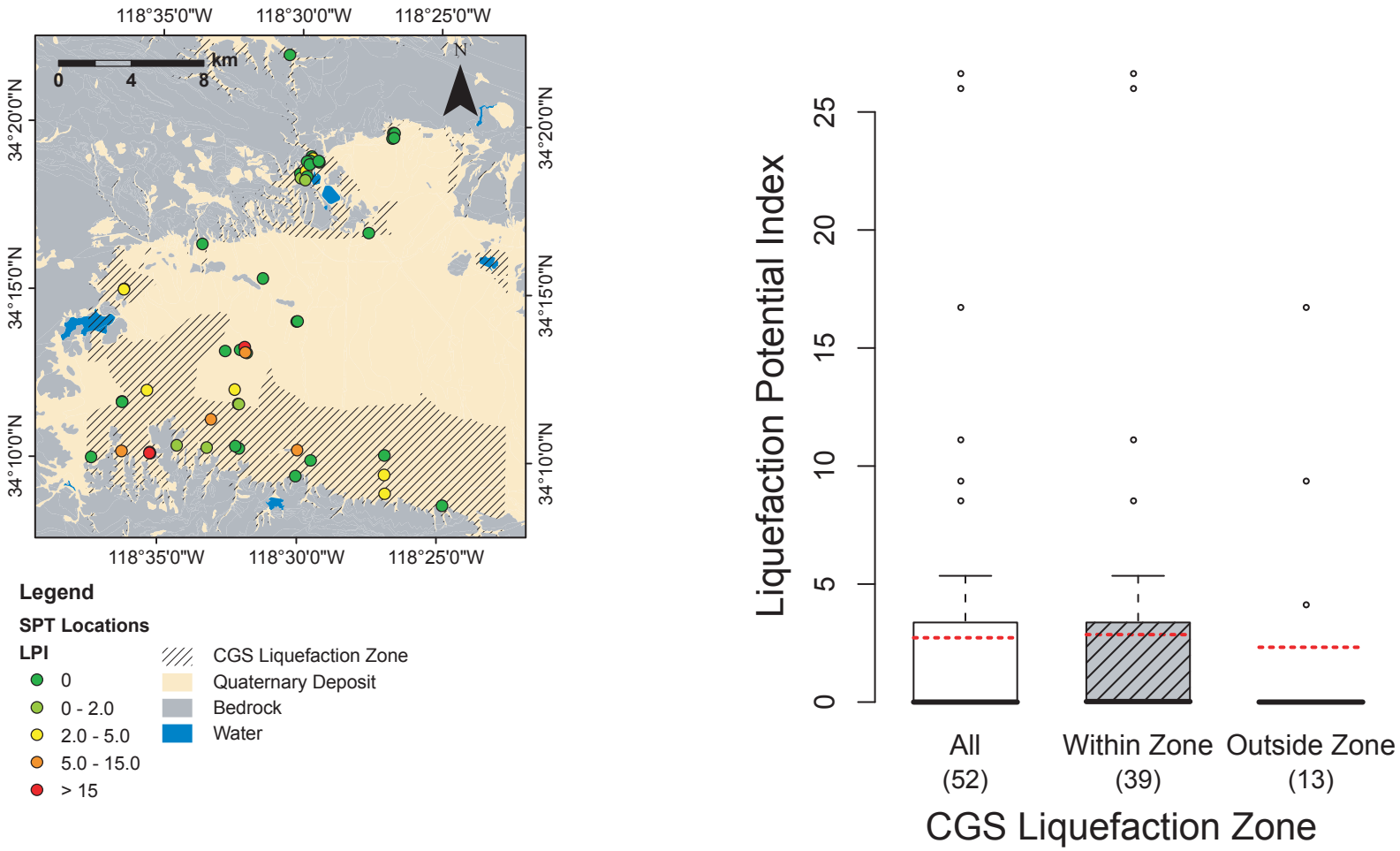


Fig. F.3. SPT-based LPI distributions by California Geological Survey Liquefaction Zone

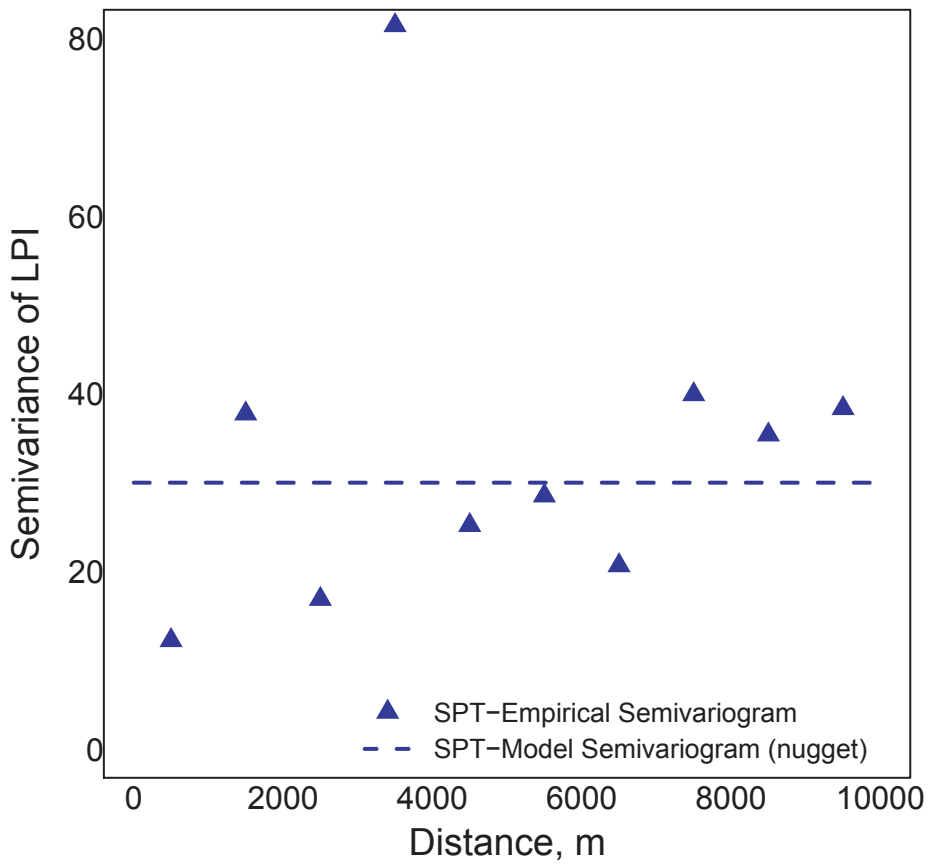


Fig. F.4. Semivariogram for SPT-based LPI

APPENDIX G

Shelby County, TN

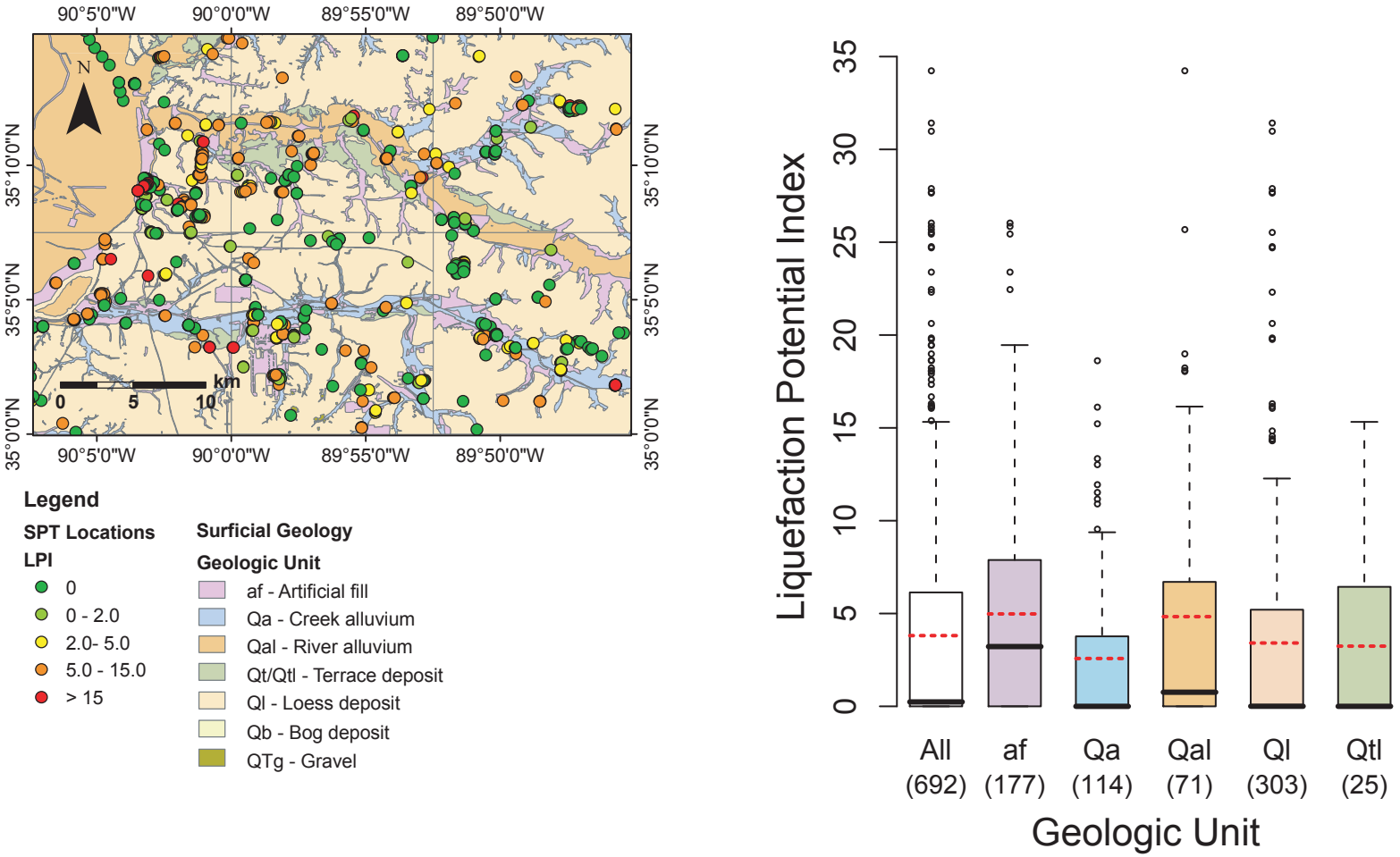
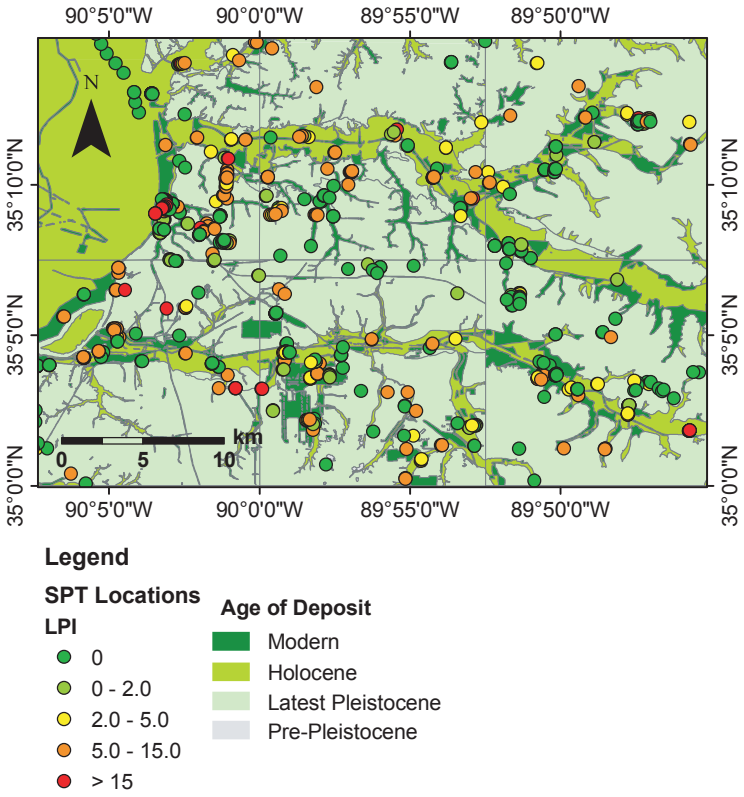


Fig. G.1. SPT-based LPI distributions by geologic unit



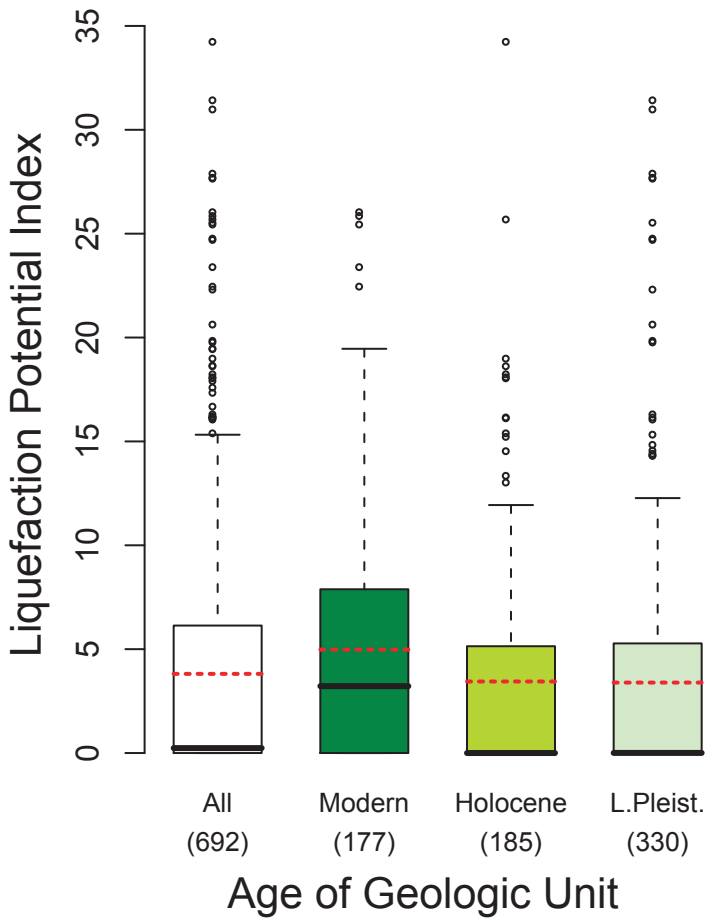


Fig. G.2. SPT-based LPI distributions by age of geologic unit

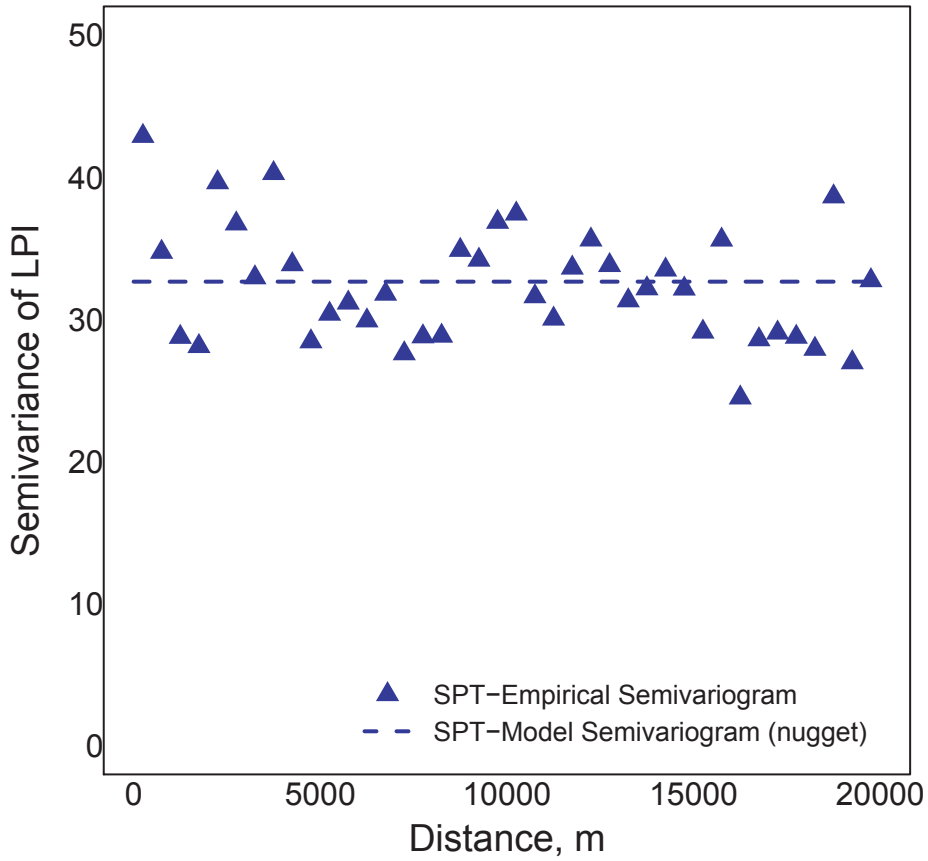


Fig. G.3. Semivariogram for SPT-based LPI

APPENDIX H

St. Louis, IL

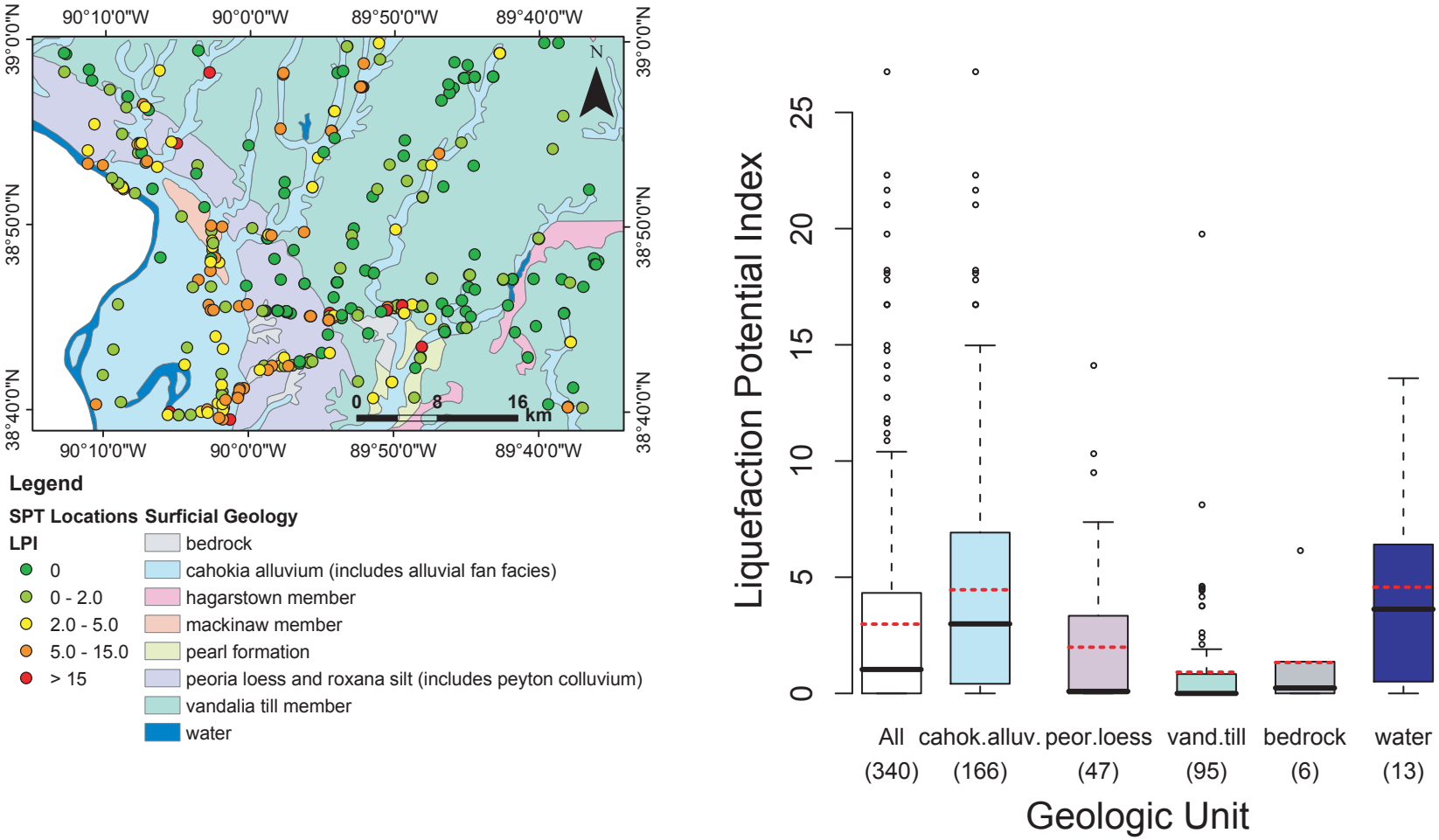


Fig. H.1. SPT-based LPI distributions by geologic unit

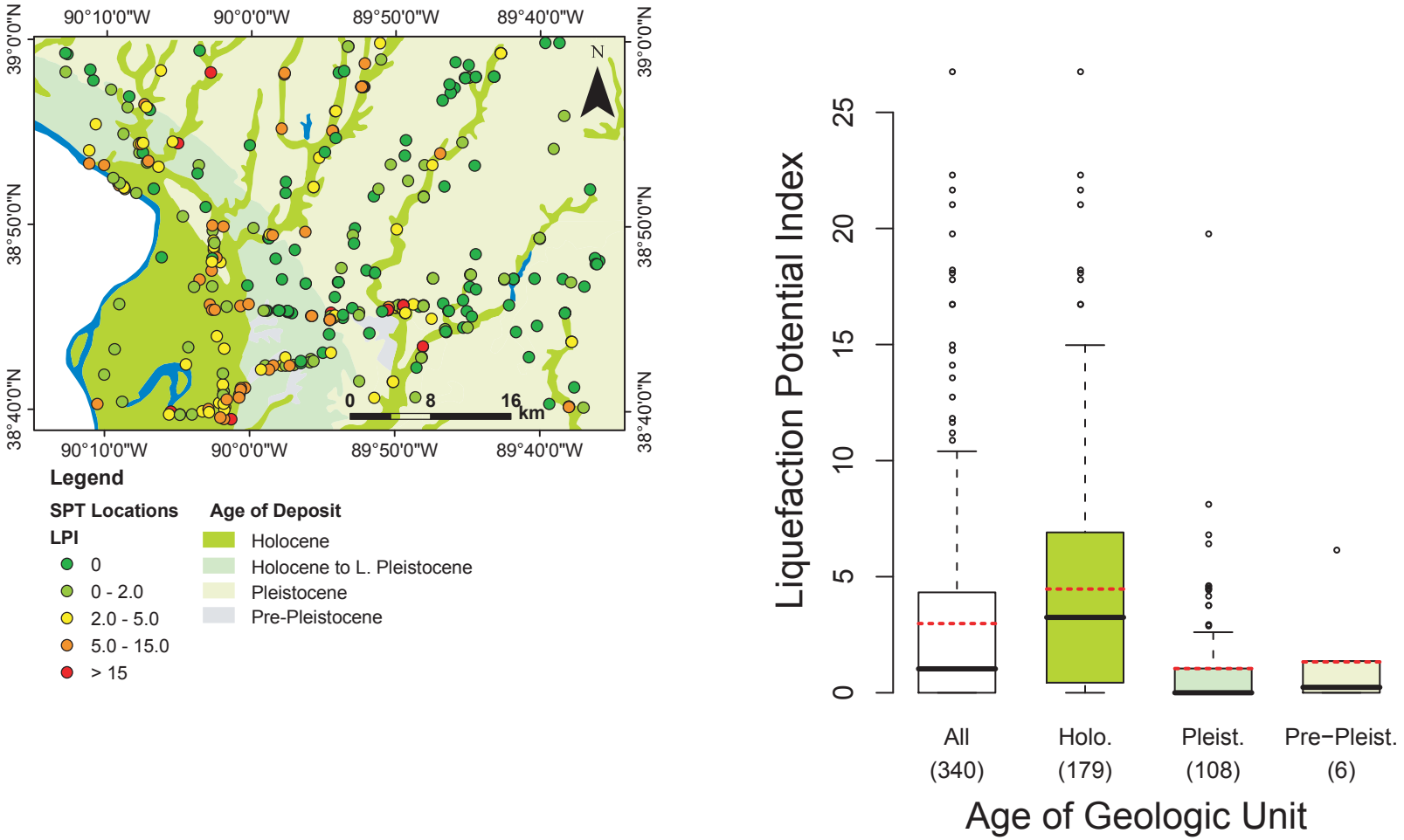
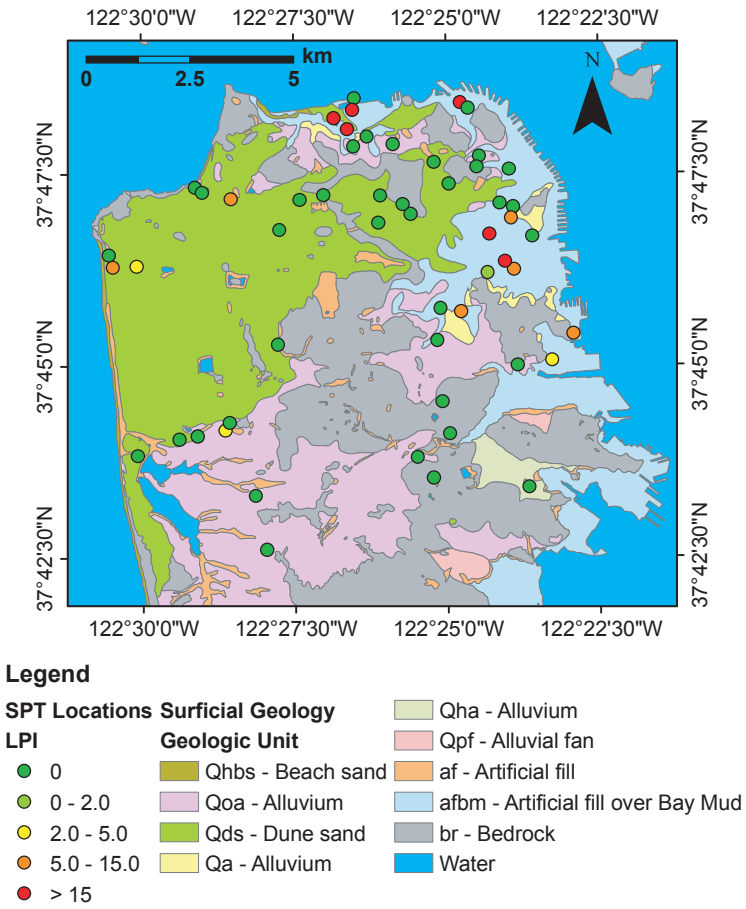


Fig. H.2. SPT-based LPI distributions by age of geologic unit

APPENDIX I

San Francisco, CA



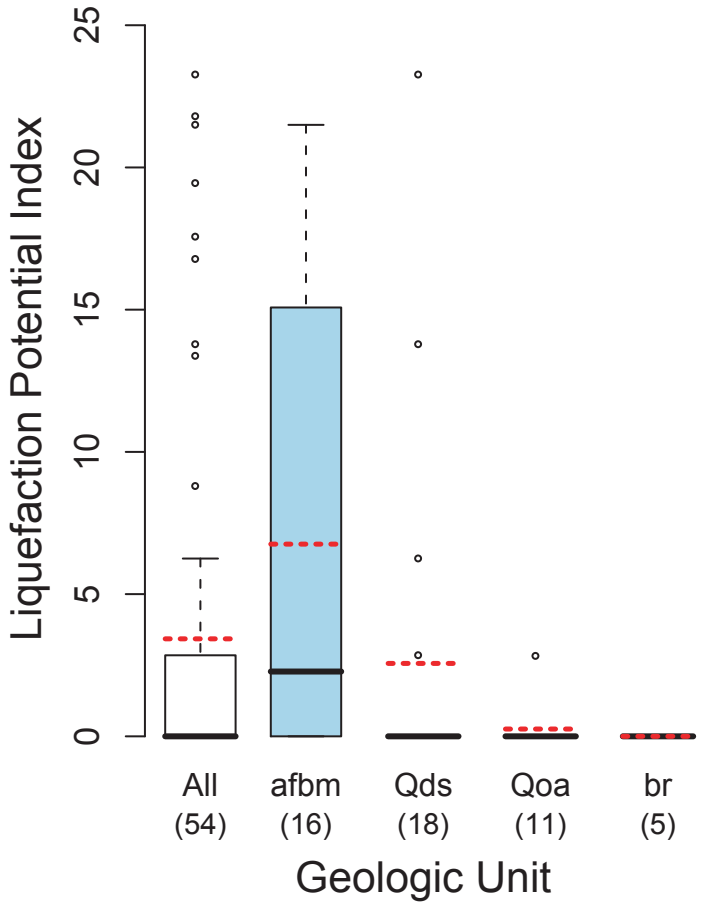


Fig. I.1. SPT-based LPI distributions by geologic unit

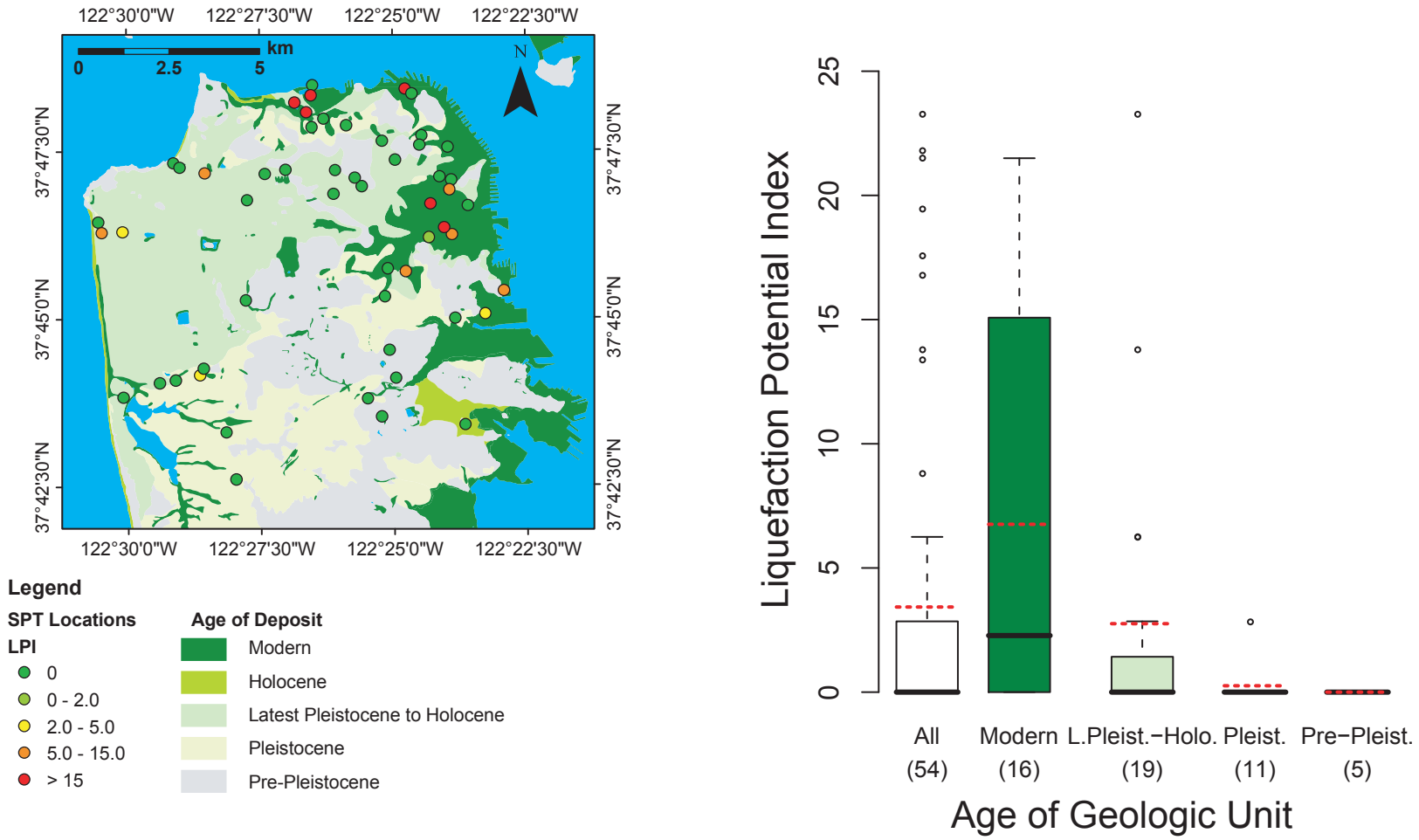


Fig. I.2. SPT-based LPI distributions by age of geologic unit

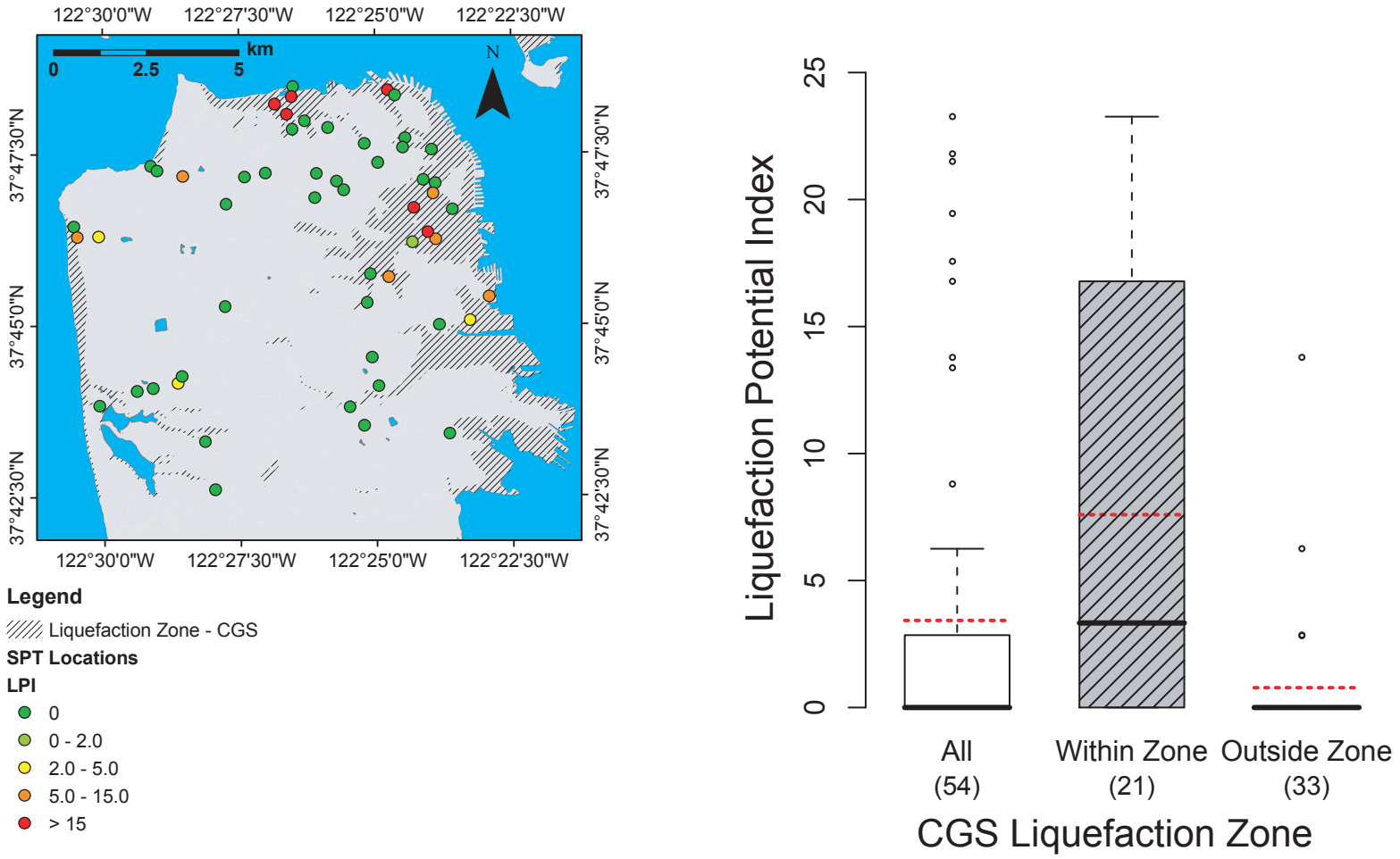


Fig. I.3. SPT-based LPI distributions by California Geological Survey Liquefaction Zone

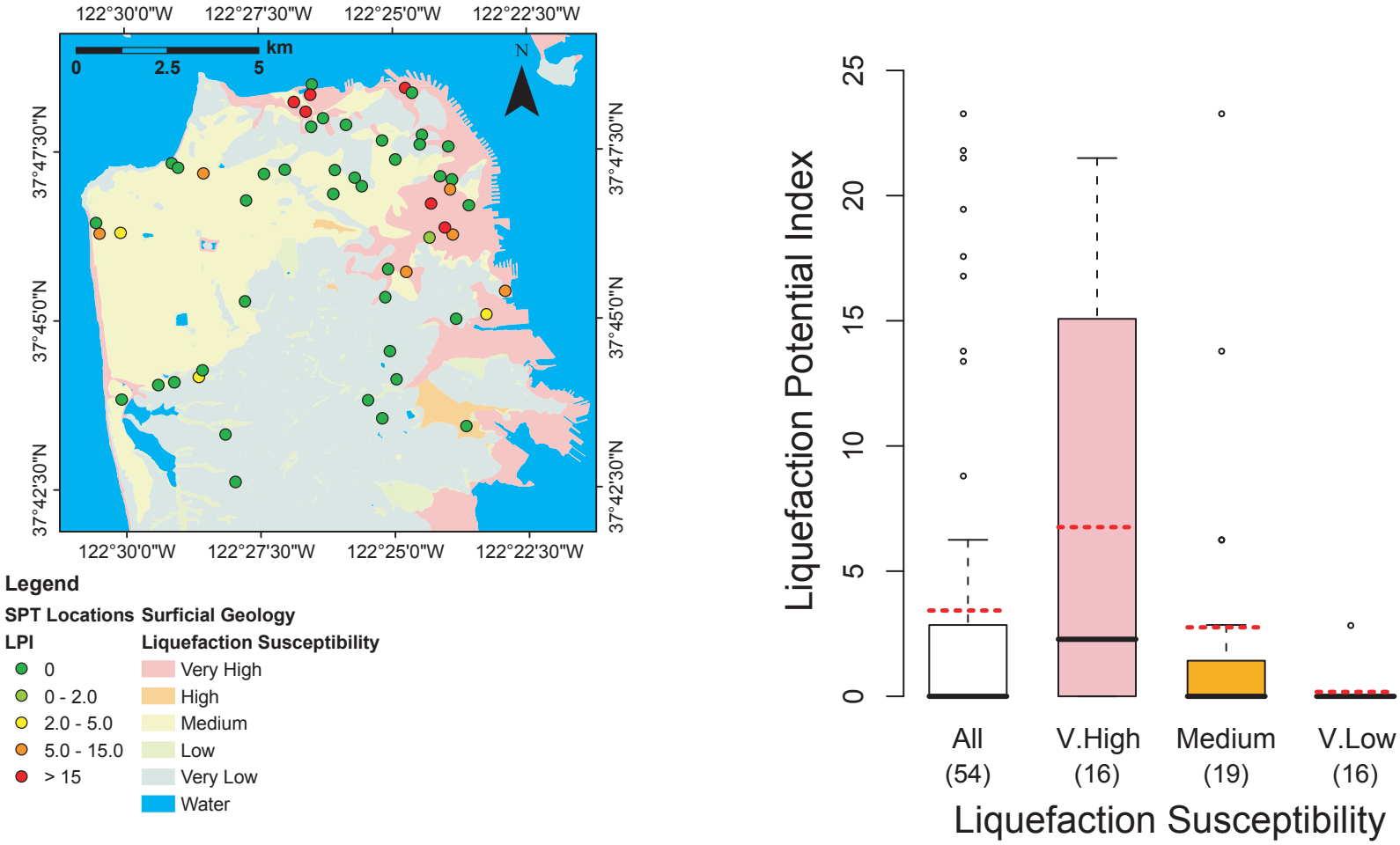


Fig. I.4. SPT-based LPI distributions by liquefaction susceptibility in the Knudsen et al. (2000) geologic maps

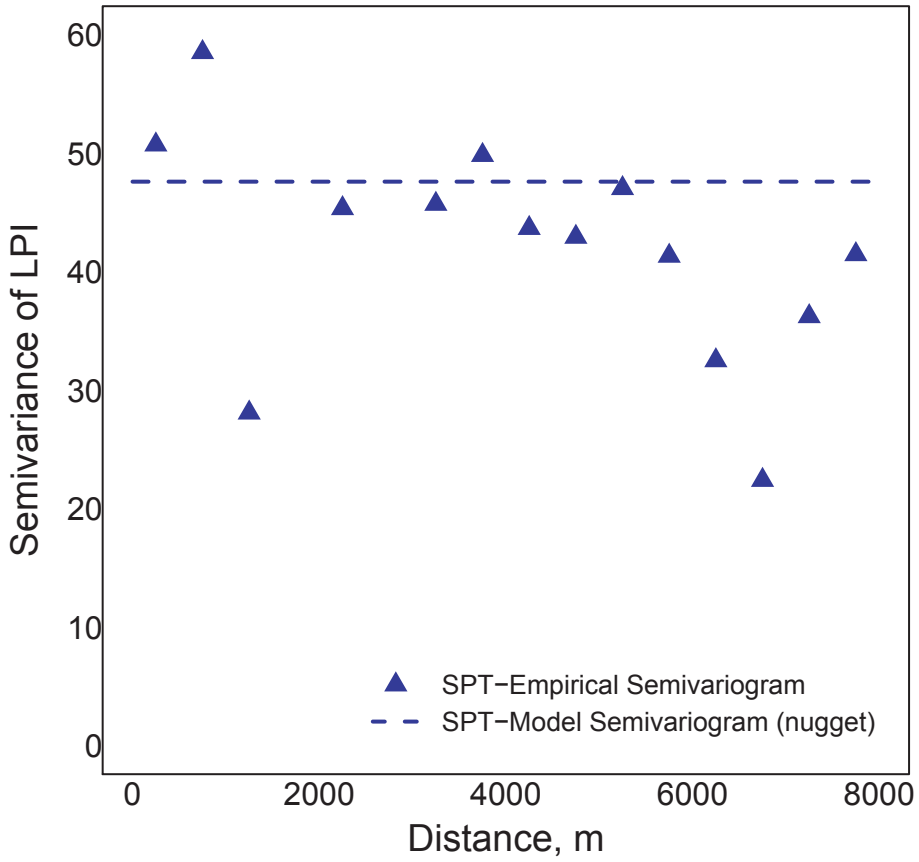


Fig. I.5. Semivariogram for SPT-based LPI